ANALOGUES OF NITROFURAN ANTIBIOTICS ARE POTENT GROEL/ES PRO-DRUG INHIBITORS WITH EFFICACY AGAINST *ENTEROCOCCUS FAECIUM, STAPHYLOCOCCUS AUREUS,* AND *ESCHERICHIA COLI*

Christopher Ryan Howe

Submitted to the faculty of the University Graduate School
in partial fulfillment of the requirements
for the degree
Master of Science
in the Department of Biochemistry and Molecular Biology,
Indiana University

May 2020

Accepted by the Graduate Faculty of Indiana University, in partial fulfillment of the requirements for the degree of Master of Science.

Master's Thesis Committee

_____
Steven M. Johnson, Ph.D., Chair

_____
Quyen Q. Hoang, Ph.D.

_____
Samy O. Meroueh, Ph.D.

DEDICATION

I dedicate this thesis to my parents Terry and Linda, my brother Michael, and my high school calculus teacher Tony Record. I appreciate the impact that you all have made in both my personal and professional lives.

ACKNOWLEDGEMENTS

Following my junior year of college, I began searching for graduate school options. Although my goal has always been to enter industry in a pharmaceutical setting, I realized that additional education would be beneficial to reach my career goals. My determination to enter the workforce in a quick manner led me to pursue local Master's degree programs, as opposed to a PhD route. After hearing positive endorsements from Trent Kunkle, a previous IUSM Biochemistry and Molecular Biology Master's student, I decided to apply to this program among others. After considering my options with family and friends, I ultimately chose to attend this program, during the Fall 2018 semester. The Department's strong track record in research, as well as its access to top-line instrumentation and novel technologies, were too tempting to pass up.

I quickly found that the program's curriculum was rigorous, yet fair. In particular, the Chemical Biology and Cancer Signaling courses were highlights of my graduate experience. They deviated from the generic aspects of first semester courses, allowing me to gain crucial critical thinking skills. In particular, I would like to thank Dr. Johnson and Dr. Quilliam for their in-depth lectures in these courses.

In addition to my coursework, I have greatly enjoyed my thesis work under the tutelage of Dr. Johnson. During my first semester in the program, I was deciding between several labs for the thesis component of my degree. I ultimately chose Dr. Johnson's lab because of his work in small-molecule drug discovery and development, which mirrors my previous experience in undergraduate research and future career aspirations. I also sought to learn more about techniques that are used to analyze compound activity, which was possible in this group. Dr. Johnson's recent experience with assigning Master's students multi-dimensional projects was an additional benefit. When I began my research in January 2019, I discovered how collaborative and interactive this group really was. I was immediately immersed in synthetic chemistry and

compound purification techniques, under the guidance of Dr. Johnson. Also, Dr. Anne-Marie Ray was a tremendous help in training me on protein preparations and purifications for my biochemical assays. Former group member, Alex Washburn, was key in training me on many of the assay types that are included in my thesis. McKayla Stevens, a current PhD candidate in my group, has also been very helpful, particularly in my trainings for cell culture methods and cell viability assays. I would also like to acknowledge another previous Johnson lab member, Siddhi Chitre, for her assistance with acclimating me to the lab. Siddhi was a good friend and colleague who helped guide me through life as a graduate student and the expectations of the lab. All of these individuals have impacted my work in a positive way, providing me with the opportunity to defend my thesis on schedule.

As with any thesis project, faculty committee members are a key factor in project success. My committee members, Dr. Quyen Hoang and Dr. Samy Meroueh, have been instrumental in providing outside guidance on my project.

Graduate school has been a very rewarding opportunity, but it has also come with some challenges. One such difficulty was balancing coursework with extensive hours in the lab, especially considering the diversity of the assays that I was running that required me to be in the lab at various times of the day (or night). While stressful, I found these challenges were well worth the effort as they helped shape me into the dedicated researcher that I am now. Without a great supporting cast, I would not be in this position, thus I bid a final thank you to my lab mates (past and present), PI, committee members, and family. You all have been critical in my drive to develop this exciting research story and obtain my MSc degree.

ANALOGUES OF NITROFURAN ANTIBIOTICS ARE POTENT GROEL/ES PRO-DRUG INHIBITORS WITH EFFICACY AGAINST *ENTEROCOCCUS FAECIUM, STAPHYLOCOCCUS AUREUS,* AND *ESCHERICHIA COLI*

Christopher Ryan Howe

In 2019, the *ESKAPE* pathogens were highlighted by the World Health Organization as some of the most prominent threats to human health, capable of developing significant antibiotic resistance. These pathogens contribute to over 2 million annual infections and ~23,000 annual deaths in the U.S. In addition, various strains of *E. coli* have also shown a proclivity to develop resistance against common drug classes. The prevalence of these infections highlights an urgency to discover new antibiotics that target previously unexploited pathways essential to bacterial survival.

The bacterial GroEL/ES chaperonin system is viewed as a viable antibiotic target. It has been proven essential to bacterial survival and homeostasis under all conditions. Previous studies identified hit GroEL/ES inhibitors with potential antibiotic activity. One promising hit (**1**) was shown to be a moderate but selective GroEL/ES inhibitor with antibacterial effects against Gram-negative pathogens (*K. pneumoniae* and *A. baumannii*). The structural similarity of **1** to known antibiotics – nitroxoline, nifuroxazide, and nitrofurantoin – prompted me to develop two series of hydroxyquinoline and nitrofuran-based analogs. I then assessed these compounds' abilities to inhibit *in vitro* GroEL/ES activity, as well as to selectively target *ESKAPE/E. coli* bacteria over human cells. Initially, I found the nitrofuran analogs were stronger inhibitors of bacterial growth than the hydroxyquinolines, but were weaker at blocking GroEL/ES functions. However, considering nitrofuran-based antibiotics behave as pro-drugs, it was found that they became much more effective GroEL/ES inhibitors when *E.*

coli NfsB nitroreductase was introduced into the GroEL/ES-dMDH refolding assay, metabolizing the nitro groups to their active species. Importantly, lead analogs that potently inhibited bacterial growth exhibited low cytotoxicity to human colon and intestine cells. Although I found *E. coli* were able to generate varying degrees of irreversible resistance to nifuroxazide, nitrofurantoin, and lead inhibitor **17**, perhaps through mutations known to effect NfsA and NfsB nitroreductases, the resulting strains were not necessarily cross-resistant to the other inhibitors. Thus, combination therapy may help bypass these resistance mechanisms.

In summary, this study identified key structure-activity relationships to selectively inhibit GroEL/ES and the growth of several bacterial species. Results from this study will aid future efforts to improve inhibitor potency.

Steven M. Johnson, Ph.D., Chair

TABLE OF CONTENTS

LIST OF TABLES

LIST OF FIGURES

LIST OF SCHEMES

LIST OF ABBREVIATIONS

ADP – Adenosine diphosphate
ATP – Adenosine triphosphate
BHI – Brain heart infusion media
CC_{50} – Cytotoxicity concentration for half-maximal signal in human cell viability assays
CH_3CN– Acetonitrile
Da – Dalton
DMSO – Dimethyl sulfoxide
EC_{50} – Effective concentration for half-maximal signal in bacterial proliferation assays
EDTA – Ethylenediaminetetraacetic acid
HPLC – High-performance liquid chromatography
HSP – Heat shock protein
IC_{50} – Inhibitory concentration for half-maximal signal in biochemical assays
IPTG – Isopropyl β-D-1- thiogalactopyranoside
kDa – Kilodalton
LB – Luria Bertani broth
MDH – Malate dehydrogenase
MeOH – Methanol
MS – Mass spectrometry
NAD^+ – Nicotinamide adenine dinucleotide (oxidized form)
NADH – Nicotinamide adenine dinucleotide (reduced form)
NfsA – *nfsA* nitroreductase gene variant
NfsB – *nfsB* nitroreductase gene variant
NMR – Nuclear magnetic resonance
NTR1 – Nitroreductase 1
NTR2 – Nitroreductase 2
OD – Optical density
PBS – Phosphate buffered saline
Rho – Rhodanese
SAR – Structure activity relationship
TFA – Trifluoroacetic acid

INTRODUCTION

The rise of antibiotic-resistant bacteria

The emergence of antibiotic-resistant bacteria has become a significant threat to human health. A 2019 CDC report titled “Antibiotic Resistance Threats in the United States”[1] touches on the dangers of the *ESKAPE* pathogens, which consist of Gram-positive ***E****nterococcus faecium* and ***S****taphylococcus aureus,* as well as Gram-negative ***K****lebsiella pneumonia,* ***A****cinetobacter baumannii,* ***P****seudomonas aeruginosa, and* ***E****nterobacter* species. These are a subset of bacteria that are prone to developing resistance against commonly used antibiotics. The *ESKAPE* pathogens contribute to approximately two-million infections in the U.S. per year, as well as nearly 23,000 annual deaths.[2] In addition to the *ESKAPE* pathogens, multiple strains of Gram-negative *Escherichia coli* have also shown a tendency to threaten public health through antibiotic resistance. One particular class of *E. coli*, the resistant Shiga-toxin producing (STEC) pathogens, was noted as the chief cause of over 265,000 infections in the U.S., in 2018.[3] It also appears that STEC infections have become more common over the past 20 years, as these pathogens were linked to far fewer (~110,000) U.S. infections in 1999.[4] Although the majority of *E. coli* infections take place in the urinary tract (known as UTIs), these infections can eventually spread to the kidneys and the bloodstream. This can lead to painful symptoms, such as bloody urination and sepsis. The persistence of *ESKAPE* and *E. coli* infections is quite alarming, as it offers the potential for long-term health concerns in the community. Thus, it is crucial that novel antibiotics are developed to combat their proliferation in susceptible populations, which include hospital patients and the immunocompromised, among others.

Current antibiotic classes and a lack of antibiotic variety

In 1928, Sir Alexander Fleming discovered the first known antibiotic drug, penicillin, which provides activity against bacterial cell wall synthesis by inhibiting D,D-transpeptidase, a crosslinking enzyme.[5] At the time of Fleming's initial discovery, penicillin could not be produced for the masses because of a lack of technological means. That changed just 16 years later during World War II. A collaborative effort, headed by the Allied Power pharmaceutical companies, sought to produce larger quantities of penicillin for ailing soldiers. This initiative ultimately led to the production of 2.3 million doses of penicillin for D-Day in Normandy.[5] Not only was this beneficial to the war effort, but it also demonstrated that the world was ready to mass produce antibiotics for public use.

The ability to mass produce penicillin prompted scientists to search for additional classes of antibiotics with different protein targets. For instance, the sulfonamides were discovered in the 1930's.[6] Sulfonamides are known for their ability to mimic *para*-aminobenzoic acid (PABA), an intermediate in the bacterial folic acid synthesis pathway. These antibiotics outcompete PABA for dihydropteroate synthetase, leading to downstream inhibition of folic acid synthesis. In the 1940's and 1950's, tetracyclines and macrolides were developed.[7,8] These classes of antibiotics are primarily linked to inhibition of bacterial peptide synthesis pathways. Tetracyclines bind to the 30S ribosomal subunit to block aminoacyl-tRNA occupation of the A-site, whereas macrolides bind to the 50S subunit to block the ongoing development of the growing peptide chain. In the 1960's, fluoroquinolones came into prominence as strong inhibitors of the major bacterial transcription enzymes Topoisomerase IV and DNA gyrase.[9] The general scaffolds/structures for these antibiotics and their associated mechanisms of action are shown in **Figure 1A-D**.[10-12]

Figure 1 – Mechanisms of action for commonly used antibiotics General mechanisms of action of several current antibiotic classes. Associated "**R**" groups represent a variety of functional groups that are typically attached to these core scaffolds.

A. Sulfonamides mimic PABA, acting as an antagonist of dihydropteroate synthetase. As a result, they inhibit downstream folic acid synthesis in bacteria.

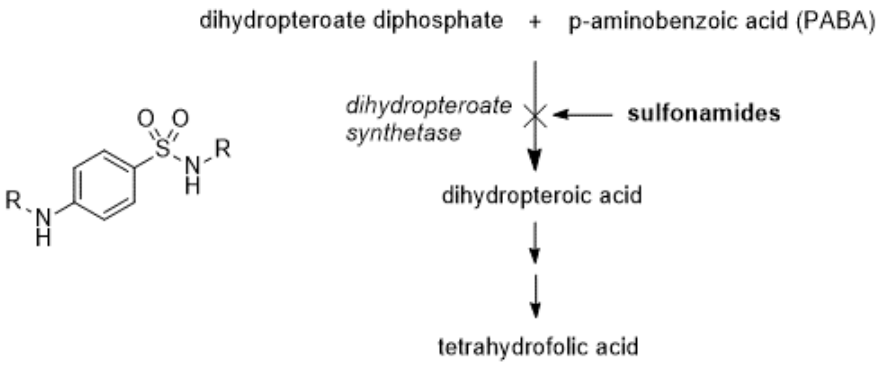

B. Tetracyclines block peptidyl synthesis in bacteria by binding to the ribosomal 30S subunit (occupying the A site). This prevents the delivery of the aminoacyl-tRNA component to the ribosome.[10]

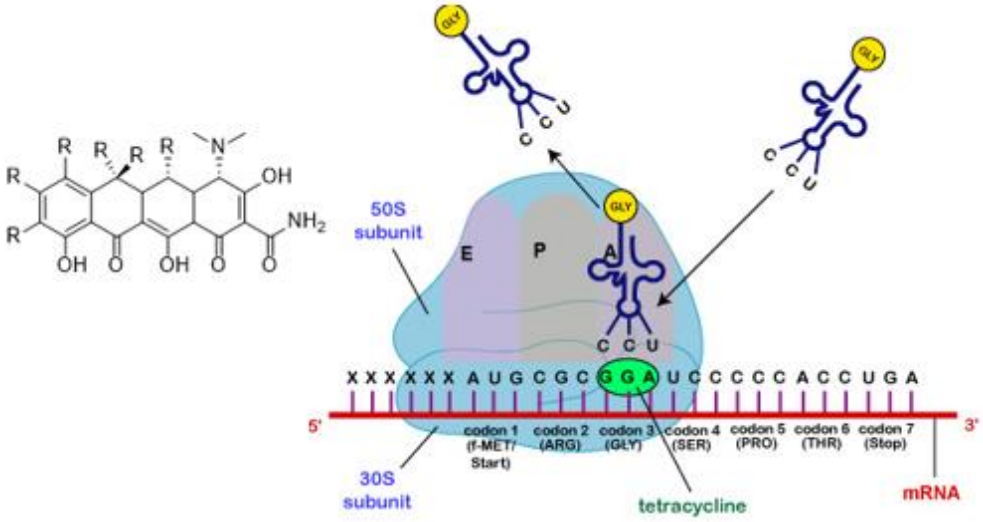

C. Macrolides block peptidyl synthesis in bacteria by binding to the ribosomal 50S subunit (occupying the P site). This disrupts the continuous addition of amino acids to the growing peptide chain.[11]

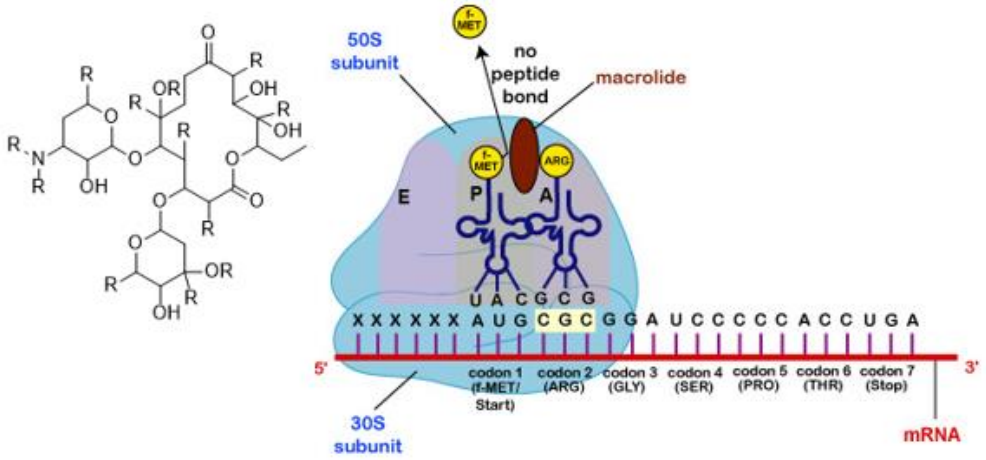

D. Fluoroquinolones inhibit DNA Topoisomerase IV and DNA gyrase enzymes, which are involved in the unwinding of double-stranded, circular bacterial DNA (in preparation for transcription).[12]

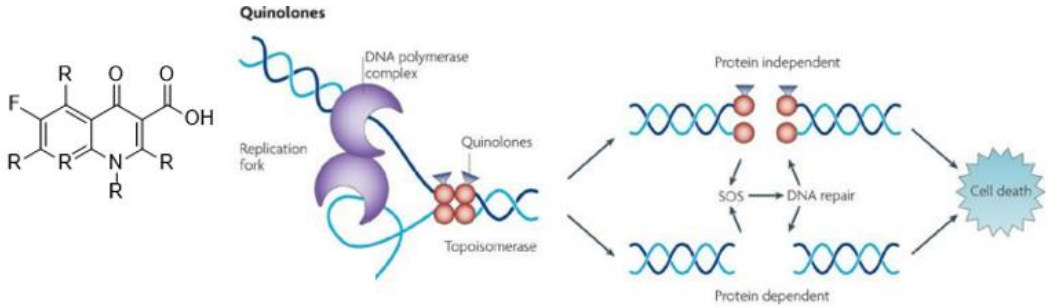

Although these antibiotic classes were initially very effective, they soon experienced resistance in various bacterial species, including the *ESKAPE* pathogens and *E. coli*. For instance, resistance was seen against the sulfonamides in the late 1930's,[6] the penicillins in 1940,[6] the tetracyclines in the mid-1950's,[7] and the macrolides in 1967.[8] Alarmingly, these initial instances of resistance did not occur very long after the respective antibiotic classes had been discovered. A similar trend has been seen in other antibiotic classes, as well. There are many mechanisms through which bacteria

develop antibiotic resistance, many of which are quite common across bacteria and are discussed below.

Mechanisms of resistance in *ESKAPE* pathogens and *E. coli*

The *ESKAPE* pathogens and various strains of *E. coli* are prone to developing antibiotic resistance through a variety of mechanisms. One such mechanism includes synthesis of extended spectrum β-lactamases (e.g. AmpC in *P. aeruginosa* and *E. cloacae*; TEM in *E. coli* and *K. pneumoniae*; CTX-M in *K. pneumoniae, Enterobacter* species, *E. coli*). These specialized enzymes act to hydrolyze drugs with β-lactam rings (penicillins, cephalosporins, etc.), thus rendering them ineffective.[13,14] In addition, pathogens can overexpress efflux pumps (e.g. AcrA-AcrB-TolC in *E. coli*, MexAB-OprM in *P. aeruginosa*, AdeABC in *A. baumannii*), which are membrane-spanning machinery used to remove toxic substances, including antibiotics, from the cytosol.[13,14] Efflux pumps have been linked to fluoroquinolone, tetracycline, macrolide, and β-lactam drug resistance, among others.[13,14] Bacteria can also mutate genes involved in the production of porin structures (e.g. OmpF, OmpC, and PhoE in *E. coli,* as well as OprD in *P. aeruginosa*).[14] Polar antibiotics, such as the β-lactams, tetracyclines, and some fluoroquinolones, require porins to bypass the highly lipophilic cell membrane and enter the bacterial cell. Mutant porins significantly hinder this process, leading to reduced antibiotic efficacy. In addition, bacteria can produce variants of the D,D-transpeptidase enzyme, which typically drives the final cross-linking step in cell wall synthesis (D-Ala^4→mDAP^3, where mDAP (meso-Diaminopimelic acid) is a derivative of lysine with an epsilon-carboxy group substitution). Mutant forms of D,D-transpeptidase can be produced (e.g. PBP2a in *S. aureus*, PBP5 in *E. faecium*)[13,15-16], which typically fold in a manner that shields the enzyme's active site pocket from β-lactam drugs. Even alternative forms of D,D-transpeptidase can be developed (e.g. L,D-transpeptidase in *E.*

faecium, as shown in **Figure 2**), containing different cross-linking substrates altogether (L,D-transpeptidase links mDAP^3→mDAP^3, as opposed to D-Ala^4→mDAP^3).[17]

In addition to acquired resistance, many bacteria are prone to intrinsic resistance. For instance, Gram-negative bacteria are structurally less permeable to drugs than Gram-positive pathogens, owing to their additional lipopolysaccharide (LPS) outer membrane (**Figure 3**).[18-19] The lipopolysaccharide extensions undergo cross-linking, a process that ultimately leads to decreased bacterial membrane fluidity and further reduced cell penetrability (**Figure 3**).[18,20] Several of the pathogens from this current study are Gram-negative (notably *K. pneumonia, A. baumannii, P. aeruginosa, E. cloacae,* and *E. coli*), indicating that they present this additional barrier in drug development.

Figure 2 – L,D-transpeptidase vs. D,D-transpeptidase mechanism of action Illustration of the differences between L,D-transpeptidase (cysteine active site) and D,D-transpeptidase (serine active site) activity. L,D-transpeptidase initiates cross-linking between m-DAP^3 and m-DAP^3, whereas D,D-transpeptidase initiates cross-linking between D-Ala^4 and m-DAP^3. Bacteria can evade the activity of β-lactam antibiotics (which target D,D-transpeptidase), by producing the alternative L,D-transpeptidase form.[13]

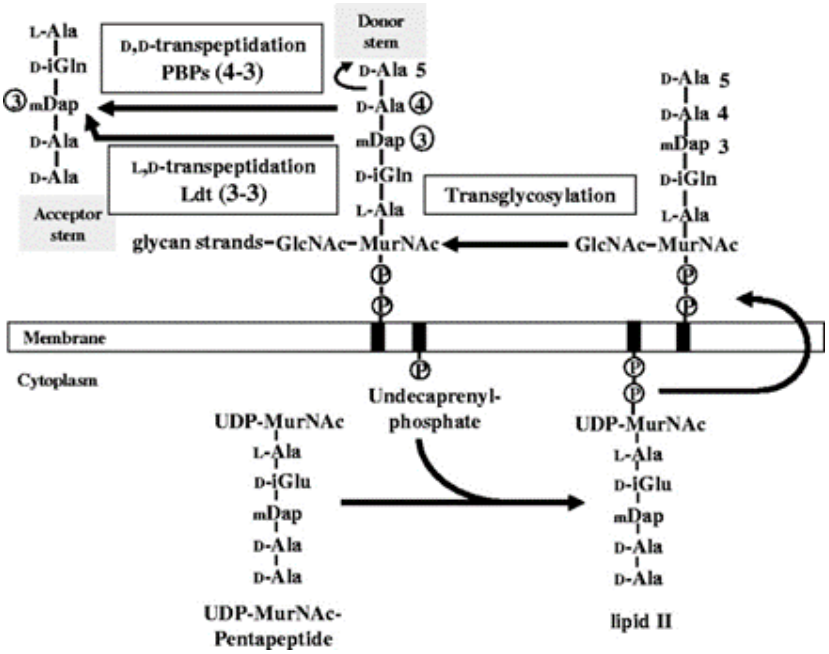

Figure 3 – Gram-positive and Gram-negative bacteria structural differences Structural differences between the cell walls of Gram-positive and Gram-negative bacteria, which promote intrinsic resistance in Gram-negative forms.[18]

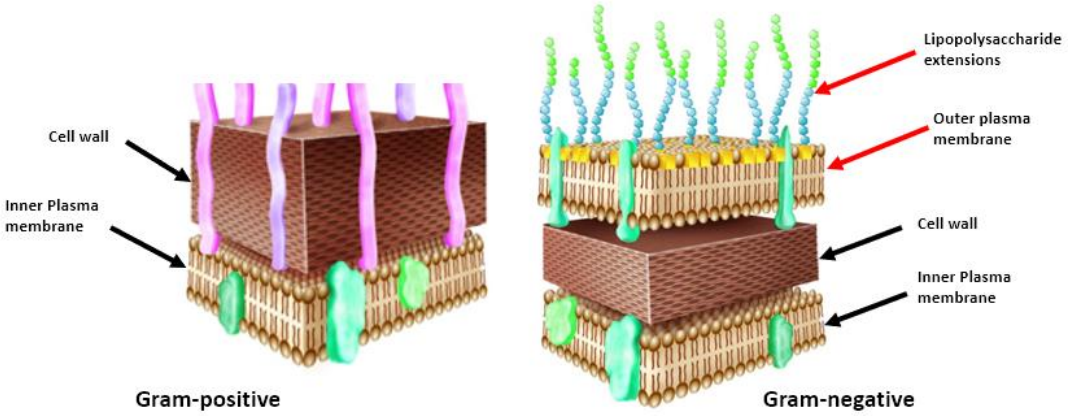

To make matters worse, antibiotics research has continued to decline in recent decades, leading to a depleted drug pipeline. For instance, from 1980-1984, roughly 19 new molecules gained drug status.[21] This dropped to just 6 molecules during the 2010-2014 time frame (**Figure 4**).[21] A perceived lack of monetary incentive has caused pharmaceutical companies to veer away from this area of research in favor of more profitable diseases.[21] The diminished drug pipeline has created a scenario where there are not enough new antibiotics to replace ones that have steadily lost efficacy due to bacterial resistance. This indicates a necessity to develop new antibiotics that can target novel protein systems central to all Gram-positive and Gram-negative species in order to combat a broader spectrum of pathogens.

Figure 4 – Reduction in the antibiotic pipeline The antibiotic pipeline has decreased throughout the past few decades.[21]

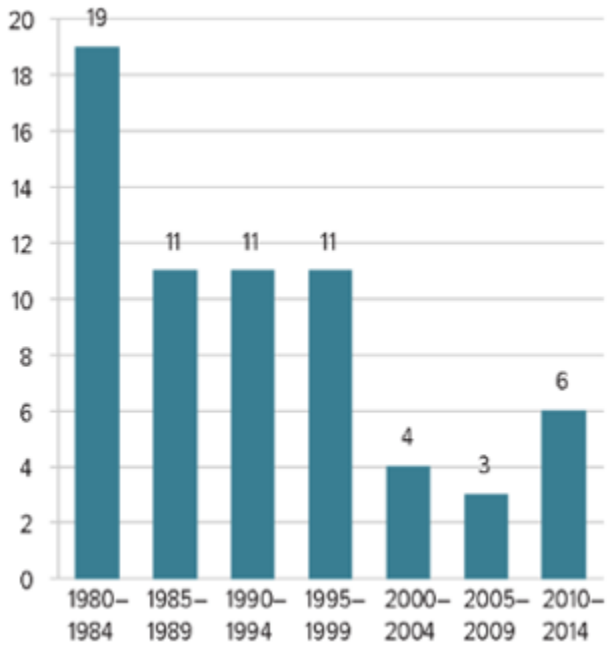

Considerations for GroEL/ES chaperonin systems as antibacterial targets

A promising and largely unexplored class of targets for new antibiotics is the chaperone proteins. These proteins possess two main functions in the cell. The first function is to help fold nascent peptides into functional (native) proteins.[22] The second function is to guide misfolded peptides to the proteasome for degradation, which prevents aggregate formation and associated cell toxicity.[22] In particular, the Johnson lab's focus is on the bacterial GroEL/ES chaperonin system. GroEL consists of two homo-heptameric rings that are stacked back-to-back with each other, which functions with the GroES co-chaperone that acts as a lid to cap off the GroEL folding chambers.[23] Targeting GroEL/ES chaperinin systems offer tremendous potential for developing new antibiotics because they have been shown to be essential to bacterial cell survival under all conditions.[24]

The intricate GroEL/ES folding mechanism is initiated when a nascent peptide binds to the apical domains of one of the GroEL rings. ATP binding to each of the seven

subunits of this *cis*-ring creates an upward conformational shift in the apical domains, allowing them to engage with the GroES co-chaperone.[22] Binding of GroES causes a greater conformational movement that releases the bound polypeptide substrate into the now enclosed GroEL/ES chamber.[22] The polypeptide is allowed to try and refold on its own, sequestered from the outside cytoplasmic milieu, with ATP hydrolysis (~5-10 s) acting as the timing mechanism. ATP hydrolysis in the *cis*-ring sends an allosteric signal for ATP and another unfolded polypeptide substrate to then bind to the GroEL *trans*-ring.[22] This initiates the release of the GroES lid from the *cis*-ring, along with the folded/native protein.[25] If the protein is not in its native state, it can undergo the folding process again or be targeted for degradation. A diagram of the GroEL/ES chaperone structure is illustrated in **Figure 5**,[26] with a diagram depicting the GroEL/ES-mediated polypeptide substrate folding pathway in **Figure 6**.[27]

Figure 5 – GroEL/ES structure The structure of GroEL/ES, shown from both side views and top-down views Two GroEL rings are stacked on top of each other, and each contain an equatorial (blue), intermediate (green), and apical (red) domain. The GroES lid component is mobile and can translocate between GroEL apical domains.[26]

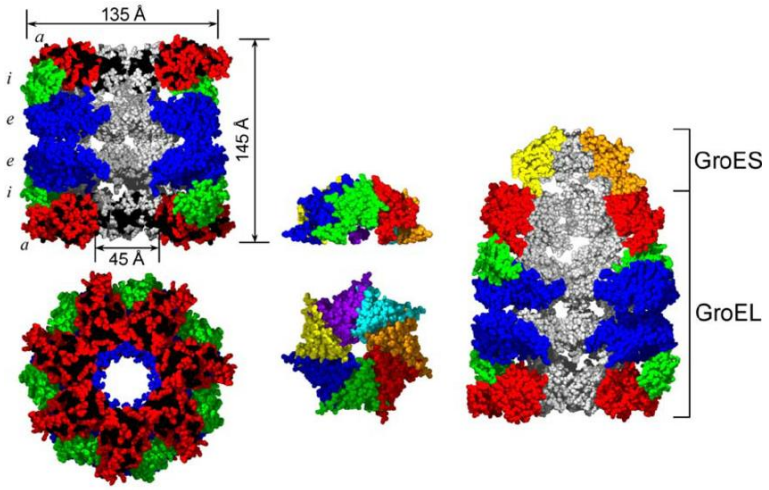

Figure 6 – GroEL/ES refolding pathway steps The functionality of GroEL/ES is shown, including individual steps in the chaperonin-mediated polypeptide substrate folding process. A GroEL *cis*-ring binds a nascent peptide via its apical domain. ATP then binds to the equatorial domain of that ring, creating an upward conformational shift. This conformational shift allows GroES to bind to the GroEL apical domains, which releases the peptide substrate into the chaperone chamber. An ~5-10 second ATP hydrolysis event acts as a timing mechanism for the peptide to fold itself. After ATP hydrolysis in the GroEL *cis*-ring, ATP and another substrate polypeptide then bind to the GroEL *trans*-ring. This causes the GroES lid to be released from the *cis*-ring, along with the potentially folded peptide.[27]

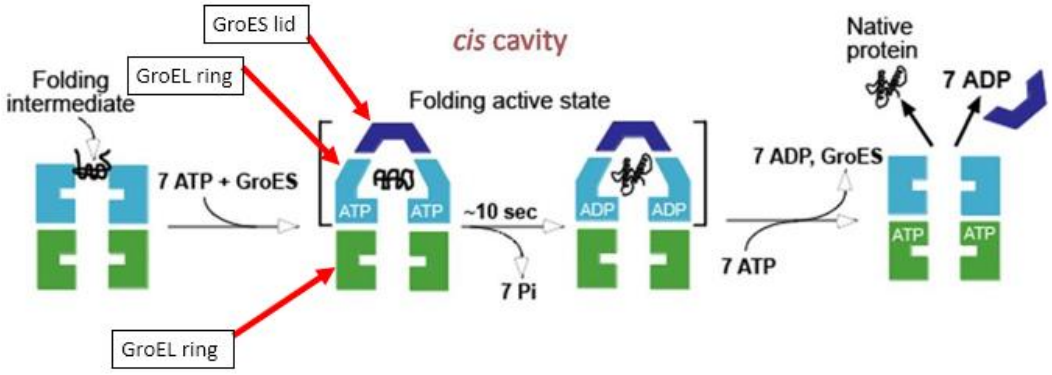

The universal role of GroEL/ES in bacterial cell survival (both Gram-positive and Gram-negative forms) makes it a great target for exploitation by small-molecule inhibitors. A potential caveat for this strategy could be off-target effects against HSP60, the human isoform of bacterial GroEL, which share 48% sequence identity.[28] Despite significant homology between the two chaperones, ongoing studies continue to emphasize the finding that even compounds that inhibit both bacterial GroEL/ES and human HSP60/10 *in vitro* can be viable antibacterial candidates.[28-32] In particular, the Johnson lab has identified numerous known drugs and natural products that can target both GroEL/ES and HSP60/10 *in vitro*, yet show low-to-no toxicity in cells or *in vivo*. For instance, it was discovered that suramin, an antibiotic that has been used to treat *Trypanosoma brucei* infections for over 100 years, is a potent GroEL/ES and HSP60/10 inhibitor in these *in vitro* assays. This is putatively because such inhibitors cannot traverse the highly impermeable mitochondrial membrane to even interact with HSP60/10 in the mitochondrial matrix of human cells.[29]

Previous studies to identify GroEL/ES inhibitors with anti-bacterial effects against the *ESKAPE* pathogens

In 2014, the Johnson lab reported a study that identified 235 GroEL/ES inhibitors from a high-throughput screen of 700,000 compounds.[33] Subsequent screening and med-chem development of two hit-to-lead series, based on scaffolds of **43** and **44** (**Figure 7**), identified lead compounds that were able to potently inhibit the proliferation of *E. faecium* and *S. aureus* bacteria (both Gram-positive), but that were largely ineffective against *E. coli* and the *KAPE* Gram-negative bacteria.[28,31-32] However, from initial antibacterials testing,[28] compound **1** stood out as another hit inhibitor of interest. Despite being only a moderate GroEL/ES inhibitor, **1** demonstrated weak-to-moderate inhibition of two Gram-negative *ESKAPE* pathogens, *K. pneumoniae* and *A. baumannii*.[28] Furthermore, the scaffold of compound **1** resembles other known antibiotics that are active against Gram-negative bacteria. For instance, **1** shares its main hydroxyquinoline group (circled red in **Figure 8**) with nitroxoline, an antibiotic that is currently used to treat *E. coli*-based urinary tract infections (UTI's) and has also demonstrated bioactivity against *A. baumannii, P. aeruginosa*, and *K. pneumoniae*.[34] Furthermore, compound **1** shares its N-acyl hydrazone core component (circled blue in **Figure 8**) with nitrofuran-based antibiotics such as nifuroxazide and nitrofurantoin, which are used to treat *E. coli*-based UTI's.[35] The one aspect nifuroxazide and nitrofurantoin possess that **1** does not, however, is a nitrofuran group (circled green, **Figure 8**), which is known to be key to eliciting antibacterial effects.

Figure 7 – Structures of hit-to-lead inhibitors 43, 44, and 1 The structures of hit-to-lead antibacterial candidates **43, 44**, and **1**.

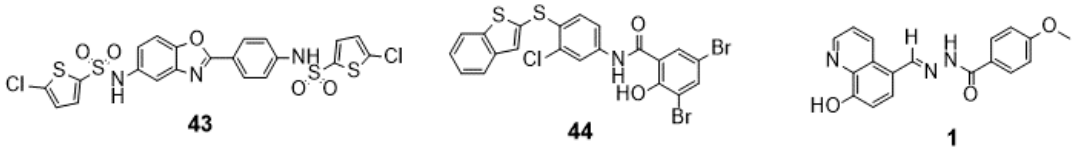

Table 1 – Assay results for high-throughput hits Previously reported biochemical and bacterial growth inhibition results for compounds **43**, **44**, and **1**.[28,31-32] While analogs of **43** and **44** were effective against Gram-positive bacteria (e.g. *E. faecium* and *S. aureus*), they were largely ineffective against Gram-negative bacteria. However, another hit identified from high-throughput screening, compound **1**, showed weak-to-moderate inhibition of *K. pneumonia* and *A. baumannii* (Gram-negative bacteria).

Assay Results for High-Throughput Hits					
Compound #			43	44	1
Chaperone Inhibition Activity IC_{50} (μM)	GroEL/ES-dMDH Refolding		2.4	1.7	31
	HSP60/10-dMDH Refolding		5.9	4.2	>100
Antibacterial Activity EC_{50} (μM)	*E. faecium*		14	0.52	>100
	S. aureus	Sensitive	3.1	0.36	>100
		Resistant	4.6	0.55	56
	K. pneumoniae		>100	>100	95
	A. baumannii		>100	66	32
	P. aeruginosa		>100	>100	>100
	E. cloacae		>100	>100	>100
	E. coli		>100	>100	>100

Based on the similarities of compound **1** with nitroxoline (i.e. hydroxyquinoline) and nifuroxazide/nitrofurantoin (N-acyl hydrazones, albeit with nitrofuran substructures), I compiled a library of analogs that probed the structure-activity relationships (SAR) of the cyclic/aryl substructures on both the right and left-hand sides of the N-acyl hydrazone linker. The left side of these analogues contained either a nitrofuran group (mimicking nifuroxazide and nitrofurantoin) or a hydroxyquinoline group (mimicking **1** and nitroxoline), generating two distinct series of compounds. For each series, 15 right side **R**-groups were assessed that contain a diverse range of substructures including some that were found to be effective with other GroEL/ES inhibitor scaffolds (see **Figure**

8 for the respective substructures). These analogues were tested in a panel of *in vitro* assays for bacterial proliferation inhibition, GroEL/ES inhibition (both substrate folding and ATPase functions), human cell cytotoxicity, and bacterial resistance towards lead analogs. The results from testing analogs in this panel of biochemical and cell-based experiments is presented below, with a discussion on SAR and the potential of these series as GroEL/ES-targeting antibacterial candidates.

Figure 8 – Structural similarity of 1 to known antibiotics and SAR strategy Comparison of the structure of hit GroEL/ES inhibitor **1** with known antibiotics nitroxoline, nifuroxazide, and nitrofurantoin. The hydroxyquinoline group (circled in red) is shared between **1** and the Gram-negative inhibitor nitroxoline. Also, the N-acyl hydrazone core (circled in blue) is shared between **1** and known antibiotics nifuroxazide and nitrofurantoin. The additional nitrofuran group (circled in green) is a component that is unique to nifuroxazide and nitrofurantoin, but not present in **1**. Analogues of compound **1** were synthesized where the N-acyl hydrazine linker was maintained constant, the right-hand **R**-substructures were varied as indicated, and the left-hand aryl substructure consisted of either hydroxyquinoline (mirroring **1** and nitroxoline) or nitrofuran (mirroring nifuroxazide and nitrofurantoin).

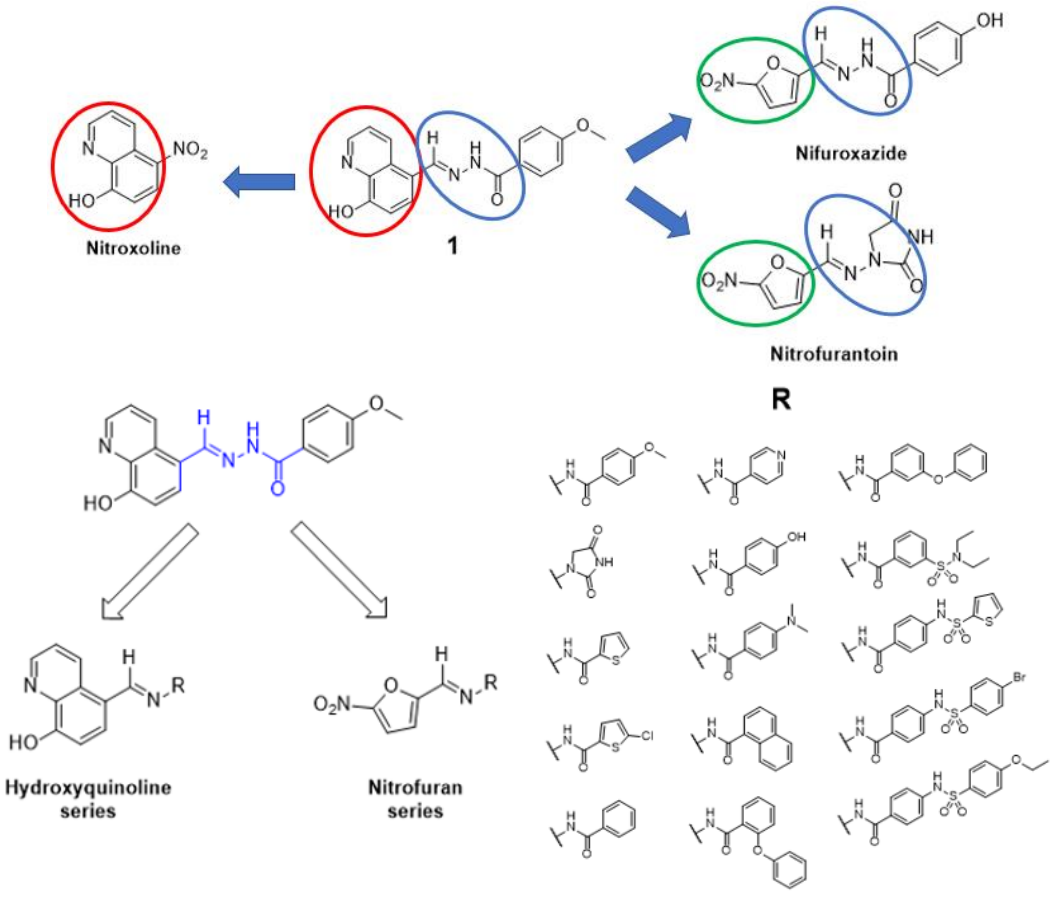

RESULTS AND DISCUSSION

Development of hydroxyquinoline and nitrofuran compound series

As discussed in the introduction, I investigated two primary series of compound **1** analogues in this study: (1) hydroxyquinolines (analogs **1-15**) and (2) nitrofurans (analogs **16-28** and also including nifuroxazide and nitrofurantoin). A third group of analogues (**29-42**) was also investigated to determine which substructures of the hydroxyquinoline and nitrofuran aryls were required for inhibitor potency in the respective assays. Analogues were all synthesized through a one-step coupling reaction between the respective aryl-aldehydes and hydrazides in DMSO, with HCl as a catalyst (**Scheme 1**). After stirring overnight at room temperature, the final Schiff base products were precipitated through the addition of water, and the solids were filtered and dried *in vacuo*. Synthesized analogues were analyzed by RP-HPLC for purity and LC-MS and ^{1}H-NMR for structural confirmation (complete characterization data can be found in the Experimental section). While all compounds were found to be >95% pure using two distinct sets of RP-HPLC conditions, for some analogues (e.g. **3, 4, 6, 9, 10, 17, 23**), we noticed a splitting of peaks in the ^{1}H-NMR spectra. This phenomenon has previously been studied and reported as resulting from hindered rotation around the CO-NH bond, providing rotational isomers (rotamers).[36] Thus, I believe that the purity of these compounds is consistent with HPLC results being >95% pure.

Scheme 1 General protocol for synthesizing compound **1** analogs. Reaction mixtures were stirred overnight at room temperature, then the Schiff-base products were precipitated with water, filtered, and dried *in vacuo*.

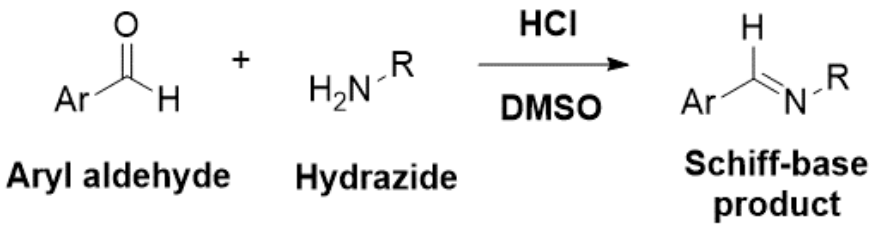

Identifying antibacterial efficacy of compound 1 analogues against the *ESKAPE* pathogens and *E. coli*

Analogues were initially tested for antibacterial activity against representative strains of *E. coli* and the *ESKAPE* bacteria (refer to the Experimental section for strain and vendor information for the respective bacteria). To determine compound efficacy, bacterial proliferation assays were carried out in liquid media culture supplemented with physiological concentrations of free calcium and magnesium cations. For these assays, initial bacterial cultures (OD_{600}=0.01) were exposed to test compounds in 8-point, 3-fold dilution series (100 µM → 46 nM concentration range). After addition of compounds to cultures, the plates were sealed with Breathe-Easy membranes and allowed to incubate/grow to mid-log phase (OD_{600}~0.4-0.6), whereupon final OD_{600} readings were taken to assess for bacterial growth inhibition. An in-depth protocol for this common set of proliferation assays is provided in the Experimental section, and calculated EC_{50} values are reported in **Table 2A** in the Appendix (log-transformed EC_{50} values with standard deviations are presented in **Table 2B**). A heat map portraying inhibitor potencies against the respective bacteria is presented in **Figure 9** for easier visualization of results, with darker cells representing the most potent analogues, and lighter cells least potent inhibitors.

Results from the bacterial proliferation assays indicated that the hydroxyquinoline analogues were largely ineffective against *E. coli* and the *ESKAPE* pathogens, as only a few weak inhibitors (EC_{50} values below the 100 µM threshold) were discovered. This was a disappointing result as, prior to initiating this study, I hypothesized that the metal-chelating properties of the hydroxyquinoline substructure might allow these inhibitors to act as siderophores that could be actively uptaken into bacteria, thus bypassing the potential problems of having to passively diffuse across the impermeable LPS outer membrane.[37] Despite this setback, I was excited to see that many of the nitrofuran-

based analogs were much more effective at inhibiting bacterial growth. In particular, **16-20**, **22-24**, and **26** were moderate to strong inhibitors of the Gram-positive *E. faecium* and *S. aureus* bacteria. It appeared that analogues with bulkier **R**-groups were slightly less effective than those with smaller **R**-groups. While antibacterial effects were limited against the Gram-negative *KAPE* bacteria, what stood out was that several analogs with small **R**-groups (**16-20**) were very potent against *E. coli.* Compounds **16** and **17** were even more potent than nitroxoline, nifuroxazide, and nitrofurantoin, with EC_{50} values <1 μM. This was a significant finding, as previous Johnson group studies had failed to identify lead analogs with significant efficacies against *E. coli*. As evidenced by the results of compound **39**, which has an unsubstituted furan ring, the nitro-group was essential for antibacterial effects. This is putatively because nitrofuran antibiotics are activated to reactive metabolites by nitroreductases in bacteria, which is discussed in greater detail below. Since the Schiff base analogs were largely ineffective against the *KAPE* bacteria, yet the hydroxyquinoline and nitrofuran aldehyde starting materials (**40** and **41**, respectively) were potent inhibitors of nearly all the bacteria (excluding *P. aeruginosa*), it was evident that the imine bonds of the N-acyl hydrazine linkers were not hydrolyzing to give the starting materials. As a result, inhibitor potencies likely owe to the final products.

Figure 9 – Heat map of analogue potencies against *ESKAPE* and *E. coli* bacteria Shown is a heat map displaying relative antibacterial potencies (EC_{50} values) for analogues tested in all bacteria proliferation assays. Cells that are shaded dark blue are most potent, while those that are shaded lighter less potent to inactive (>100 μM). Nitrofurans with small **R**-groups, particularly analogues **16-20**, are potent against *E. faecium* and *S. aureus* (Gram-positive bacteria), as well as *E. coli* (Gram-negative). Associated **R**-groups for the most potent inhibitors are indicated to the right.

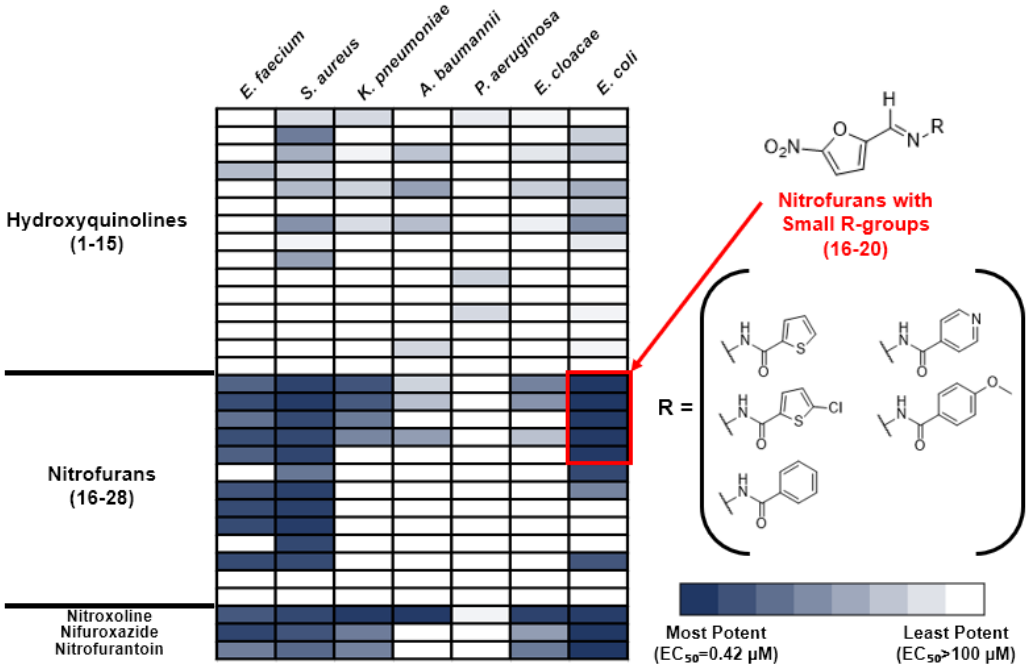

Evaluating analogues for their ability to inhibit GroEL/ES-mediated refolding of substrate polypeptides *in vitro*.

Since I found many potent inhibitors of bacterial growth that merited further investigation, I next proceeded to evaluate their abilities to inhibit GroEL/ES-mediated folding and ATPase functions. All test compounds were first evaluated in standard GroEL/ES-mediated refolding assays that employ malate dehydrogenase (MDH) and Rhodanese (Rho) as the denatured substrate reporter enzymes (detailed descriptions of the assay protocols are presented in the Experimental section, with schematics presented in **Figure 10**). These enzymes are efficiently folded by GroEL/ES in the absence of inhibitors, and thus act as reporter enzymes to determine the degree of

inhibition against the bacterial chaperone. Inhibition was examined in the presence of these two orthogonal substrates in order to support that GroEL/ES inhibitors were on-target. To further support on-target effects against GroEL/ES, I counter-screened for inhibition of the native MDH and Rho enzymatic reporter reactions, where test compounds were added after the denatured MDH and Rho substrate enzymes were completely refolded by GroEL/ES. Previous Johnson lab efforts have found that these series of biochemical assays are highly effective at eliminating false-positives as compounds rarely inhibit both reporter enzymes since their enzymatic read-outs are so different from one another. **Figure 10** presents general schematics for both the GroEL/ES-mediated dMDH and dRho refolding assays and the native MDH and Rho reporter counter-screens, with IC_{50} results presented in **Table 3A** in the Appendix. While GroEL and GroES from *E. coli* were used as surrogates in these assays, I anticipate inhibition results will translate to the chaperonin systems of the other *ESKAPE* bacteria owing to their high sequence similarities: 60.2% with *E. faecium*; 56.8% with *S. aureus*; 96.4% with *K. pneumonia*; 75.5% with *A. baumannii*; 79.6% with *P. aeruginosa*; and 96.2% with *E. cloacae*. My lab is currently in the process of generating recombinant versions of the respective *ESKAPE* bacteria GroEL and GroES proteins and will report on such inhibition results in the future.

Figure 10 – GroEL/ES refolding and native assay schematic General schematics for the GroEL/ES refolding assays and native reporter enzyme counter-screens. In the GroEL/ES-dMDH refolding assay, compounds were added to a solution of GroEL/ES-dMDH, followed by ATP to initiate the refolding cycle. EDTA was added after a short incubation time to quench the refolding cycle followed by the enzymatic reporter reagents (NADH and ketomalonic acid (KMA)). Refolded MDH (i.e. no GroEL/ES inhibition) converts NADH to NAD^+, which was followed by monitoring the absorbance of NADH at 340 nm. To identify false-positives that inhibited the refolded MDH, compounds were added after the EDTA quench step. In the GroEL/ES-dRho refolding assay, compounds were added to a solution of GroEL/ES-dMDH, followed by ATP to initiate the refolding cycle. After a short incubation time to allow the dRho substrate to be refolded, the sodium thiosulfate and potassium cyanide enzymatic reporter reagents were added and incubated for 60 minutes. Then, formaldehyde was added to quench the reporter reaction, followed by the $Fe(NO_3)_3$ developing solution, forming the $Fe(SCN)_3$ complex that was detected at λ=460 nm. To identify false-positives that inhibited the refolded Rho, compounds were added after the refolding incubation period, but prior to addition of the enzymatic reporter and developing reagents.

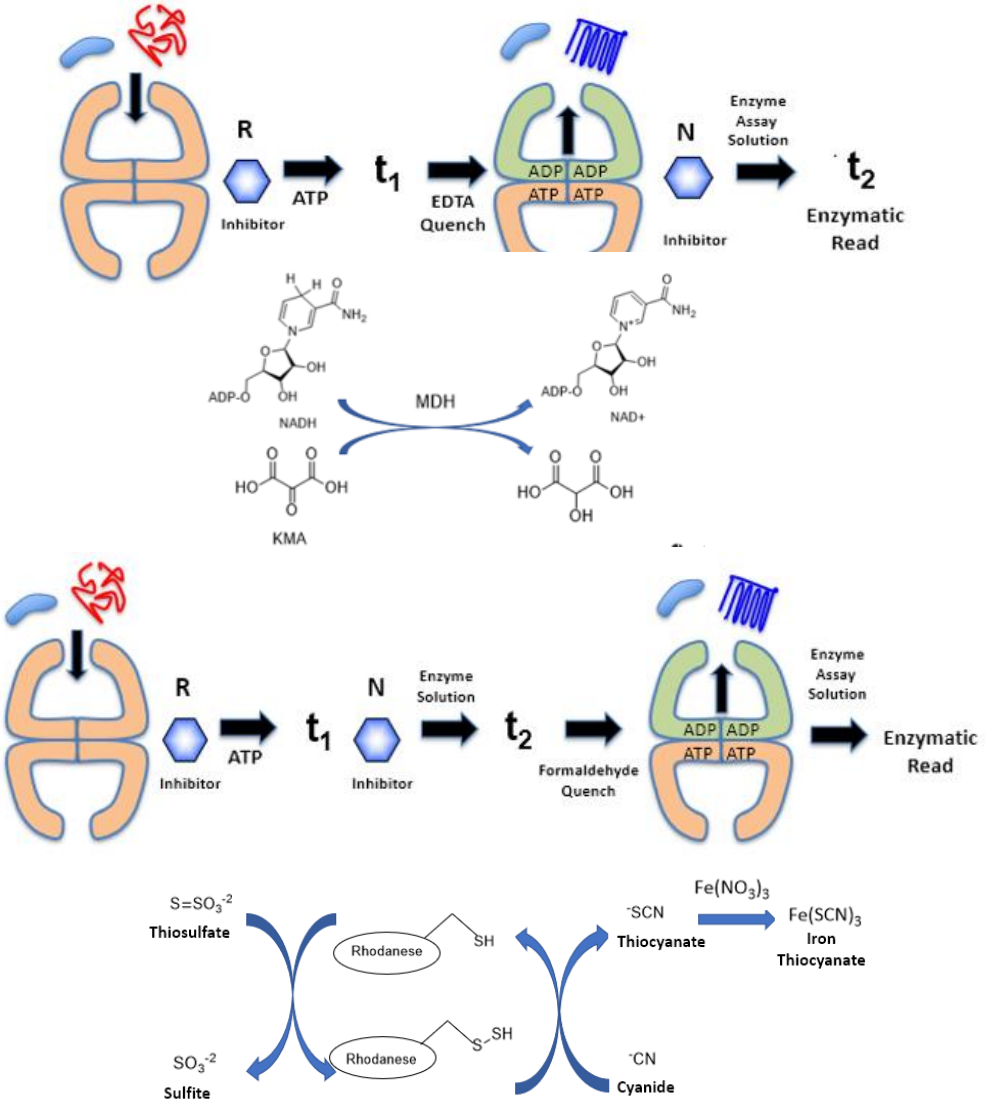

Unfortunately, I found that the nitrofuran analogues were only weak-to-moderate GroEL/ES inhibitors despite their being the most potent at inhibiting bacterial growth (blue circles in **Figure 11A**). Conversely, the hydroxyquinoline analogues (yellow circles in **Figure 11A**) were much stronger GroEL/ES inhibitors, although they were largely inactive against bacteria. SAR indicated that analogues with larger **R**-groups were generally more potent than those with smaller **R**-groups (**Table 3A**), which was a trend generally contradictory to inhibitor potencies against bacteria. While the hydroxyquinolines were slightly more potent in the GroEL/ES-mediated dRho compared to dMDH refolding assays, this was likely because they had the coupled effects of also being weak inhibitors of the native Rho reporter reaction; however, no compounds inhibited native MDH, supporting on-target effects against GroEL/ES. That analogue **6** was more potent in the GroEL/ES-dRho refolding assay is an anomaly since it does not inhibit the native Rho reporter reaction. Since analogs **29-39**, which consist of **R**-groups where various parts of the hydroxyquinoline substructure were pared away, were largely inactive in all biochemical assays indicates the necessity for the complete hydroxyquinoline moiety for inhibition.

Figure 11 – GroEL/ES refolding and native assay results Correlation plots demonstrate *E. coli* GroEL/ES-mediated refolding and native assays, using both MDH and Rho substrates. Single data points represent IC_{50} values for individual analogues. (**A**) Hydroxyquinolines were potent GroEL/ES inhibitors, whereas nitrofurans were weak-to-moderate GroEL/ES inhibitors. The majority of hydroxyquinoline inhibitors appeared to be slightly more potent in the GroEL/ES-mediated dRho assay, as opposed to the dMDH assay (Pearson correlation coefficient for inhibiting in both refolding assays is 0.905, $p < 0.0001$). One analogue, **6**, was potent in the dRho assay but ineffective in the dMDH assay. (**B**) While several compounds were found to be weak inhibitors in the native Rho counter-screen, none inhibited native MDH, supporting on-target effects against GroEL/ES since they were strong inhibitors in the GroEL/ES-dMDH refolding assay.

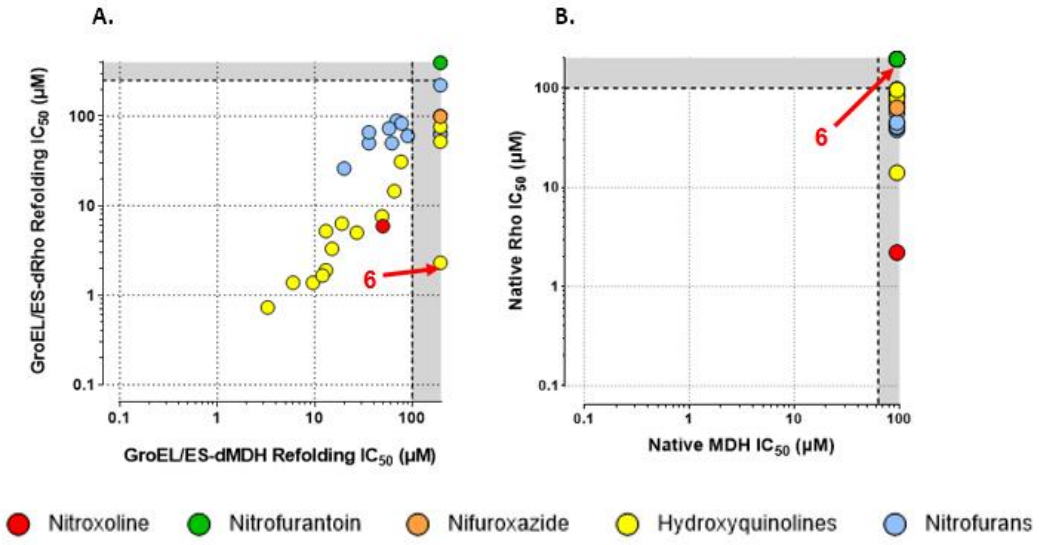

Evaluating whether or not analogues inhibit GroEL ATPase functions.

Since ATPase events are common among many biological processes, inhibiting GroEL/ES by competitively binding to the ATP sites could prove problematic for being able to selectively target the chaperonin system. Thus, I next employed a well-established GroEL ATPase assay using malachite green to monitor inorganic phosphate liberated as ATP gets hydrolyzed by GroEL. Briefly, a solution of GroEL was incubated with test compounds (8-point, 3-fold dilution series) and the assay initiated by addition of ATP. After incubating for 45 minutes, the ATPase reaction was quenched by the addition of EDTA. Malachite green was then added to the assay to bind and detect free phosphates in solution, giving off a green colorimetric reaction (absorbance detection at

λ=600 nm). If analogues inhibited ATPase activity, then there would be no free phosphates for malachite green to bind, leading to a yellow solution color (minimal absorbance at 600 nm). The detailed procedure for this assay is presented in the Experimental section. As indicated in **Figure 12** (and IC_{50} results in **Table 3A** in the Appendix), none of the analogues from either series inhibited the GroEL by blocking ATP hydrolysis. Thus, I believe that these inhibitors bind to sites outside of the ATP pockets. The Johnson lab is currently pursuing studies to identify these unknown binding sites, which will be reported on in the future. While these results alleviate concerns about non-selectively targeting other ATP-dependent proteins (at least as competitive ATP inhibitors), I further assessed for off-target effects through a more definitive approach of evaluating for cytotoxicity of analogues to human cells, as discussed further below.

Figure 12 – GroEL/ES-dMDH refolding vs. ATPase inhibition Correlation plot demonstrates that none of the GroEL/ES inhibitors (hydroxyquinolines or nitrofurans) inhibit the ability of GroEL to hydrolyze ATP.

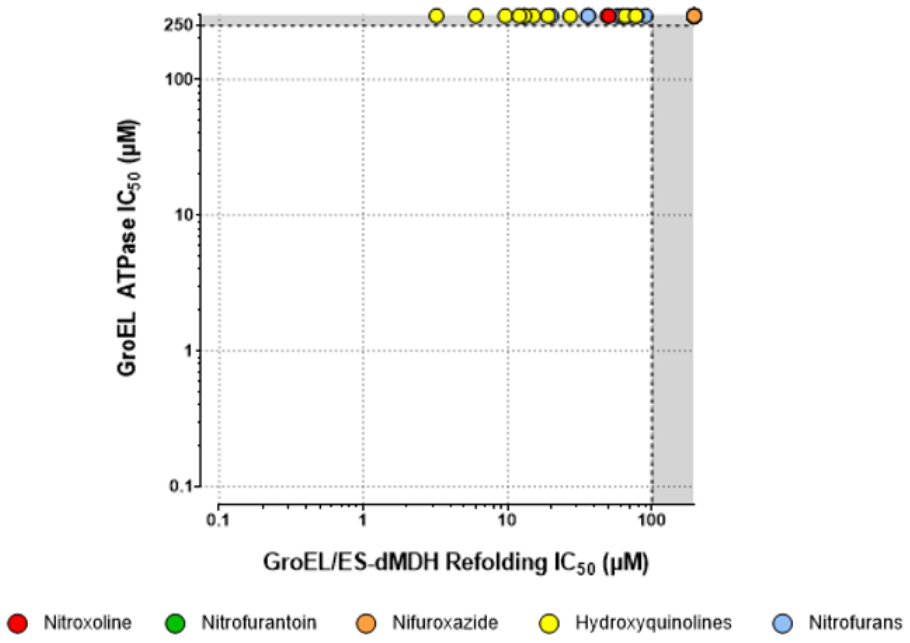

Evaluating the effects of the *E. coli* NfsB type-1 nitroreductase on the ability of test compounds to inhibit GroEL/ES

While in the previous section I discussed how the hydroxyquinolines were shown to be potent GroEL/ES inhibitors, whereas nitrofurans were not, this interpretation is complicated by the fact that nitrofuran-based compounds act as prodrugs *in vivo* – they require metabolism by bacterial nitroreductases to generate reactive metabolites that are associated with their antibacterial effects.[38] Because the standard GroEL/ES-mediated refolding assays and native substrate reporter counter-screens were conducted without nitroreductases present, the nitrofuran analogues were not undergoing bioactivation during these tests. This emphasized the need to re-examine analogues in modified refolding and native assays that included a nitroreductase enzyme to activate the nitrofuran analogs *in situ*.

There are two main classifications of nitroreductase enzymes: Nitroreductase I (NTR1, oxygen-insensitive) and Nitroreductase II (NTR2, oxygen-sensitive).[39] As shown in **Figure 13**, NTR1 functions by performing two-electron reductions on compounds.[40] In this activation pathway, NTR1 initially undergoes consecutive reductions, converting the nitro group to a nitroso group, then the nitroso group to a hydroxylamine intermediate. From there, three separate pathways are possible: (1) reduction into an amine (putatively inert);[41,42] (2) reduction into a nitrenium ion (highly electrophilic and could form covalent adducts);[41,43-45] and (3) a furan ring-opening event that forms either saturated or unsaturated open-chain nitriles (offers potential Michael addition interactions with active site residues).[41,46] Unlike NTR1, NTR2 operates via one-electron reductions and converts the nitrofuran group to a nitro radical anion.[40,45] Since the nitro radical anion is unstable, it oxidizes back to the initial nitro group and creates reactive oxygen species in the process, which can induce cell death at high concentrations.[45]

Figure 13 – NTR1 and NTR2 bioactivation pathways This is a diagram laying out the various pathways of nitrofuran activation that can take place under the influence of NTR1 and NTR2. NTR1 operates via 2-electron reductions, which leads to a hydroxylamine intermediate. From there, three pathways can take place: (1) further reduction to a potentially inert amine; (2) formation of an electrophilic nitrenium ion, which could possibly bind guanine bases in bacterial DNA; (3) nitrofuran ring-opening event that might prompt covalent modification of enzyme active site residues. NTR2 operates via 1-electron reductions. Because the initial reduction leads to an unstable nitro radical anion, it is quickly converted back to the nitro group. In the presence of oxygen, this conversion enables the transfer of a free radical to the oxygen molecule. This generates superoxide, which is a precursor to ROS generation.

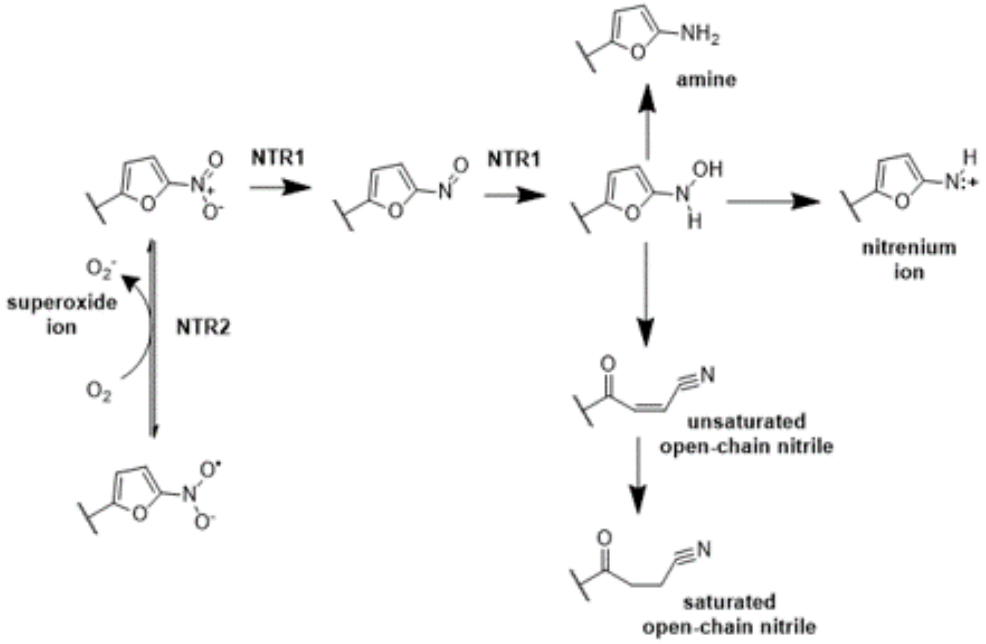

The question then became whether to use NTR1 or NTR2 in the modified GroEL/ES refolding and native assays. Because NTR2 is pertinent to bicyclic/polycyclic nitro drug activation and NTR1 is pertinent to monocyclic nitro drug activation (as seen in the nitrofuran analogues), NTR1 was selected.[47] As an initial test to see whether or not the activated nitrofuran metabolites would be more potent GroEL/ES inhibitors, we purchased the *E. coli* NfsB type 1 nitroreductase (Sigma #N9284) and modified the standard GroEL/ES-dMDH refolding and native MDH counter-screens to generate the reactive metabolites *in situ*. Detailed protocols for these experiments are presented in the Experimental section, with IC_{50} results presented in **Table 4A** in the Appendix, and graphically shown in **Figure 14**. It was exciting to see that in the presence of NfsB, the nitrofuran analogues exhibited dramatically increased inhibition of GroEL/ES refolding

functions. Since the IC_{50} values for the hydroxyquinoline (**1**-**15**) and other analogs without any nitro groups (e.g. **29**-**42**) were nearly identical in the presence and absence of NfsB, this supports that increased inhibition was dependent on the nitrofuran moiety and not other effects from the overall compound scaffold or NfsB itself. Furthermore, that the activated nitrofurans were still inactive in the native MDH reporter counter-screen indicates that the increased inhibitor effects were obtained through selectively targeting GroEL/ES in the refolding assay. While the degree of potency shift varied between the various analogues, eleven shifted to IC_{50} values of less than or equal to 10 μM. As a point of comparison, the most potent nitrofuran analogue in the absence of NfsB had an IC_{50}=20 μM, with three being completely inactive (IC_{50} >100 μM). Significant potency shifts were observed for the most effective antibacterials (**16-20**). This shows that some of the strongest antibacterial compounds were also strong GroEL/ES inhibitors when exposed to a compatible nitroreductase enzyme. While activated nifuroxazide and nitrofurantoin were only moderate GroEL/ES inhibitors in this assay, this is perhaps not surprising as they are reported in the literature to be preferentially activated by the other *E. coli* type 1 nitroreductase, NfsA. As the different nitrofuran analogs would be expected to exhibit varying SAR for activation by NfsA and NfsB, it will be important to test inhibitors in the presence of both to gain a more complete picture of how inhibitors could be function in bacteria. Because of the limitations of employing only NfsB and evaluating such a small number of nitrofuran analogues, it is difficult to ascertain correlations between the nitrofurans inhibiting in the *in situ* NfsB-GroEL/ES-dMDH refolding assay and inhibition of bacterial growth (**Figure 15A-C**). My lab is now in the process of cloning and expressing the *E. coli* NfsA and NfsB nitroreductase variants and developing an expanded panel of nitrofuran-based analogs. Furthermore, investigating the nitroreductases of the various *ESKAPE* bacteria could provide a

stronger rationale for why these compounds are largely inactive against the *KAPE* Gram-negative strains. Associated findings will be reported in future works.

Figure 14 – Chaperone refolding and native MDH enzymatic activity with and without NfsB Correlation plots indicate GroEL/ES inhibition potency shifts in the presence of NfsB. Addition of NfsB causes only the nitrofuran analogues to gain in potency against GroEL/ES.

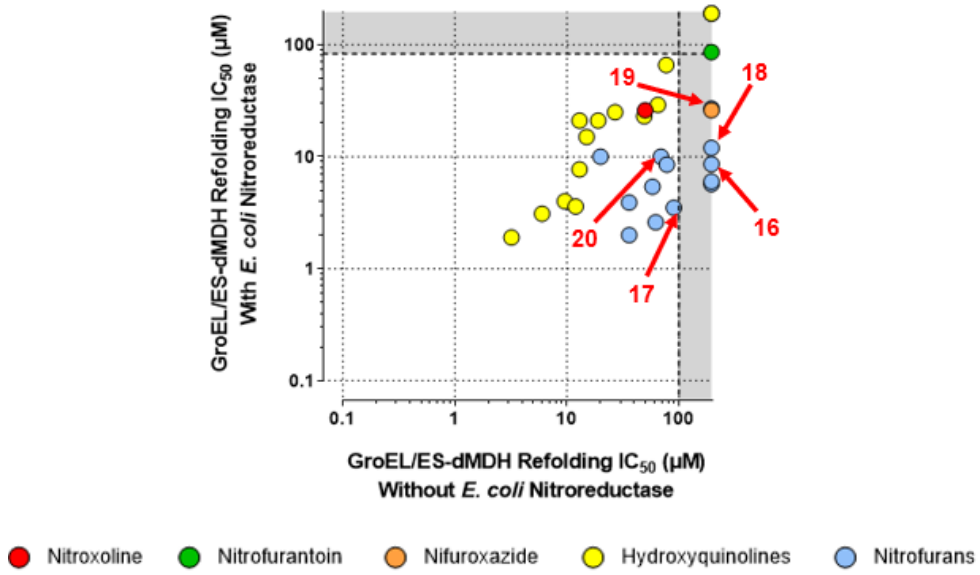

Figure 15 – GroEL/ES-dMDH refolding vs. bacterial growth inhibition Correlation plots to identify potential on-target effects targeting GroEL/ES in *E. faecium* (**A**), *S. aureus* (**B**), and *E. coli* (**C**). While increasing inhibition by the nitrofurans in the *in situ* NfsB-GroEL/ES-dMDH refolding assay may provide more effective inhibition of *S. aureus* growth (an potentially *E. faecium*), more thorough studies will need to be conducted, testing a larger number of nitrofuran analogs in the presence of both NfsA and NfsB, to gain a clearer picture of whether or not compounds may be functioning on-target against GroEL/ES in bacteria.

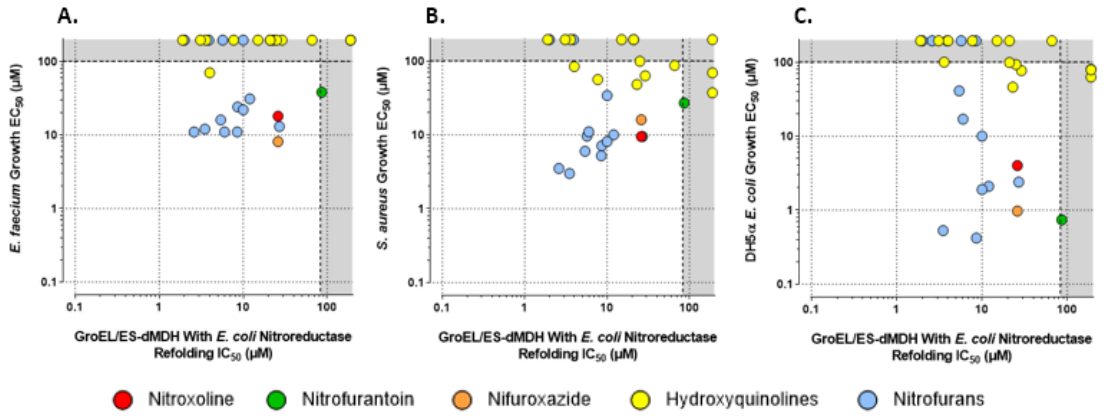

Evaluating analogues for cytotoxicity to human colon and small intestinal cells

While in previous studies, I (as well as previous members) have employed counter-screening with the human HSP60/10 chaperonin system, accumulating results continually reinforce that inhibiting HSP60/10 *in vitro* is a poor indicator of potential off-target toxicity to human cells.[28-32] This is highlighted by the fact that we have identified many known drugs and natural products that are potent HSP60/10 inhibitors *in vitro*, a primary example of which is suramin, which has been safely used for over 100 years as a first-line treatment for *Trypanosoma brucei* infections.[29,48] In addition, as now identified in this study, bioactivation of nitrofuran analogues (and the drug, nifuroxazide) by nitroreductase enzymes greatly increases the degree of inhibition against GroEL/ES refolding activity. This further complicates testing against human HSP60/10, since human cells do not contain nitroreductases. Therefore, I feel the most appropriate initial assessment of potential *in vivo* toxicity is to test compounds for cytotoxicity to human cells in cell culture. Thus, to screen for potential cytotoxic effects, analogues were tested in two Alamar Blue-based cell viability assays using human FHC colon cells and FHs 74 Int small intestinal cells. Briefly, I first grew cells to ~90% confluency, then sub-cultured 1,500 cells per well in the absence of test compounds for 24 h. Test compounds were then added and the cultures were incubated for an additional 48 h, whereupon the Alamar Blue reporter reagents were added and well fluorescence was monitored over time. Alamar Blue contains resazurin (non-fluorescent), which is reduced to resorufin (highly fluorescent) in the presence of healthy, viable cells. A detailed protocol is presented in the Experimental section, with cell cytotoxicity CC_{50} values presented in **Table 5A** in the Appendix. As observed in **Figure 16**, lead nitrofuran inhibitors were able to selectively kill *E. faecium*, *S. aureus*, and *E. coli* bacteria with low-to-no cytotoxicity to human cells (representative results are shown for human FHC colon cells, but FHs 74 Int results are similar). Intriguingly, the nitrofuran analogues were typically less toxic than

their hydroxyquinoline counterparts, putatively because they would need to be metabolized to their active intermediates, yet human cells do not harbor nitroreductases.

Figure 16 – FHC vs. FHS 74 Int cytotoxicity Correlation plots demonstrate differences between compound cytotoxicity to human FHC colon cells and inhibition of the proliferation of *E. faecium* (**A**), *S. aureus* (**B**), and *E. coli* (**C**). It is clear that nitrofuran analogues are selective for inhibiting bacteria over FHC colon cells (results for cytotoxicity to human FHs 74 Int small intestine cells are similar, with CC_{50} values reported in **Table 5A** in the Appendix).

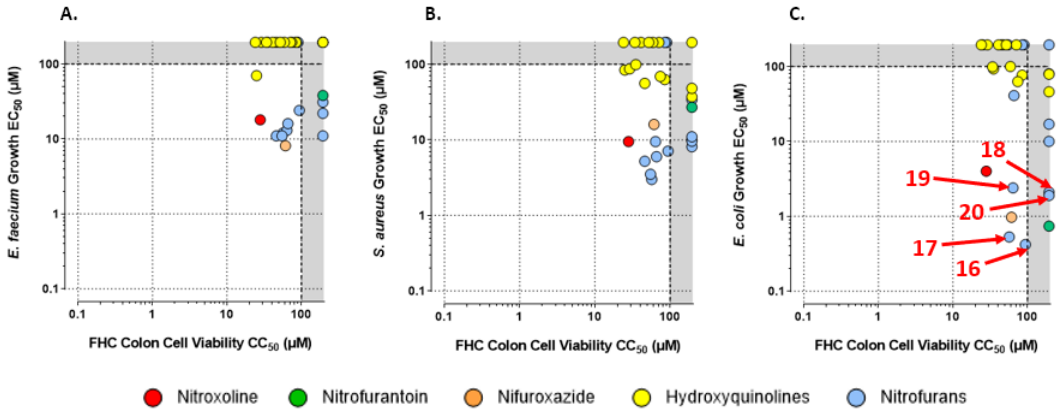

Investigating the ability of *E. coli* to gain resistance to 17, nifuroxazide, and nitrofurantoin

As I discovered several nitrofuran-based analogs that selectively inhibited the growth of *E. faecium*, *S. aureus*, and *E. coli* with minimal toxicity to human cells, I next wanted to explore how easy it would be for bacteria to generate resistance to a lead candidate. I examined the ability of *E. coli* to generate resistance to **17** (with nifuroxazide and nitrofurantoin as controls), since resistance to nitrofuran-based antibiotics has been well-characterized in this bacterium. While **17**, nifuroxazide, and nitrofurantoin were all potent inhibitors of *E. coli* proliferation, **17** was the most potent at inhibiting GroEL/ES in the presence of NfsB, and thus may exhibit greater on-target effects in bacteria. However, there are limitations in the above experiments, as they do not employ the NfsA nitroreductase. To determine if there might be any difference in the ability of *E. coli* to generate resistance to these three compounds with such distinct bioactivity profiles, I

employed a 12 day resistance assay as was previously reported with the biphenylamide compound **44** analogues.[32] A detailed protocol of this assay is presented in the Experimental section. Briefly, a dilute culture of *E. coli* (OD_{600}=0.01) was grown in the presence of inhibitors (tested in dose-response in duplicates) for 24 h, then EC_{50} results were determined from the OD_{600} readings of the wells. Over the course of 12 days, I sequentially sub-cultured bacteria from the respective wells with the highest concentration of inhibitors where bacteria grew to an OD_{600} >0.2, monitoring for increases in EC_{50} values over time.

As shown in **Figure 17**, nifuroxazide and nitrofurantoin were initially more potent than **17**, putatively owing to their preferential activation by NfsA. However, *E. coli* quickly developed intermediate resistance (within 3-5 days) such that all three inhibitors were nearly equipotent in the 20-40 μM range. Literature precedence shows that resistance to nitrofuran antibiotics typically occurs first through mutations affecting NfsA.[49] That EC_{50} values generally plateaued in the 20-40 μM range is consistent with previous reports that NfsB is still able to metabolize the nitrofuran moieties, allowing them to maintain efficacy; however it may further indicate that it is more difficult for bacteria to generate resistance through mutating this second nitroreductase. Thus, inhibitors that are preferentially activated by NfsB, as may be the case for **17**, might be more effective drug candidates with respect to combatting the emergence of drug resistant strains, although this remains to be shown. I note, though, that EC_{50} values continued to slowly increase over time for all three compounds, with a particular jump in resistance seen for replicate 2 of nitrofurantoin.

Figure 17 – *E. coli* resistance generation against lead antibacterials Evaluating the ability of *E. coli* to generate resistance to nifuroxazide (**A**), nitrofurantoin (**B**), and compound **17** (**C**) over time. The time-course plots show the change in EC_{50} values for each compound over the 12-day serial passage resistance assay (compound tested in duplicates, as indicated by the white triangles and black diamonds).

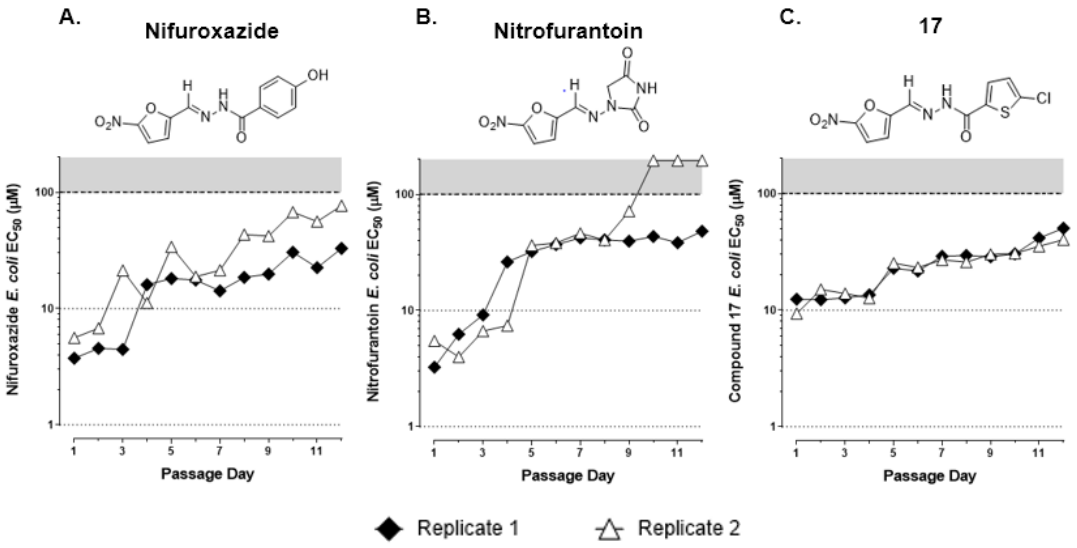

I next confirmed that the resistance generated by the replicate *E. coli* strains was irreversible (i.e. putatively through permanent mutations of NfsA and NfsB, as previously reported) as opposed to transient means (i.e. by up-regulating efflux pumps). To accomplish this, I sub-cultured single colonies obtained from the replicate samples where the bacteria exhibited the greatest degree of resistance to test compounds (day 12 samples for all compound replicates, except replicate 2 for nitrofurantoin, which was taken at day 10), for 4 x 12 h serial passages in fresh media without any test compounds present. I then performed another 24 h follow-up proliferation assay to determine EC_{50} values. As seen in **Figure 18**, the bacterial strains were still resistant to each of the respective inhibitors they were generated from, supporting that resistance was permanent. Previous studies have extensively characterized mutations affecting NfsA and NfsB that *E. coli* acquire to generate resistance mechanisms against nitrofuran antibiotics, and thus genotyping was not performed to further characterize the specific resistance mechanisms for these strains, as they are likely the same.[49]

Figure 18 – *E. coli* permanent resistance against lead antibacterials Dose-response curves for nifuroxazide (**A**), nitrofurantoin (**B**), and compound **17** (**C**) for susceptible parent *E. coli* (shown in blue), the maximally-resistant strains developed to the respective test compounds (shown in orange), and follow-up proliferation assays for resistant strains tested after 4 x 12 h serial passaging in the absence of test compounds to account for possible reversible inhibition mechanisms (shown in purple).

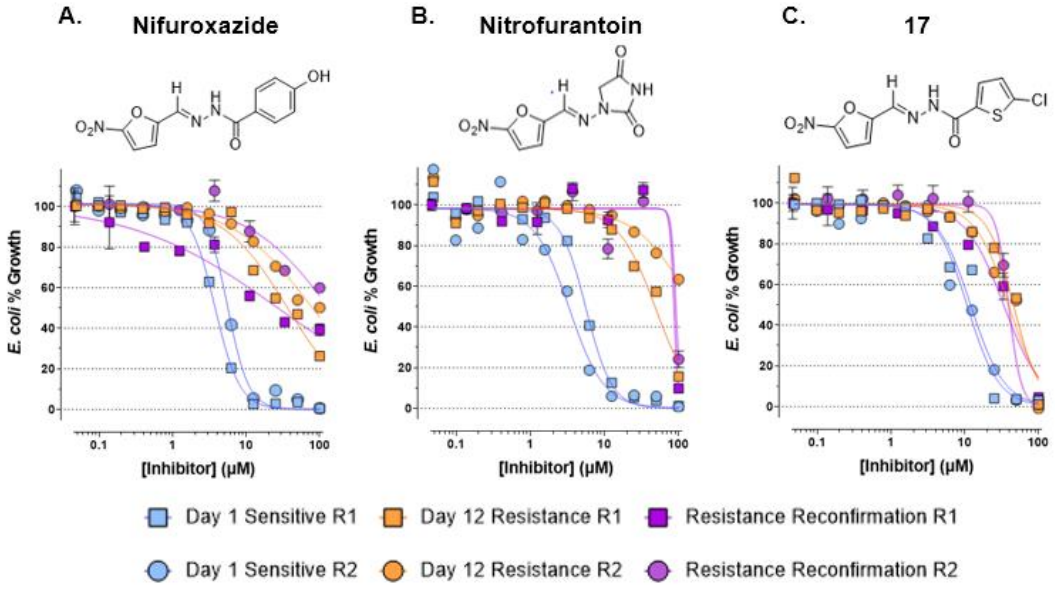

As nifuroxazide, nitrofurantoin, and **17** displayed different inhibition and resistance profiles with one another, I was curious to determine if the respective resistant strains were cross-resistant with each of the other inhibitors. Intriguingly, while the replicate strains that were initially resistant to nifuroxazide were cross-resistant to both nitrofurantoin and **17** (**Figure 19A**), the nitrofurantoin-resistant strains were still sensitive to nifuroxazide and **17** (**Figure 19B**), and the **17**-resistant strains were susceptible to nifuroxazide, but not nitrofurantoin (**Figure 19C**). Thus, it is evident that strains that have generated resistance to one analogue are not necessarily cross-resistant to other analogues. Further studies are warranted to see if combination therapy with 2 or more inhibitor analogues might be synergistic and prevent or prolong the emergence of resistant strains.

Figure 19 – Evaluation of *E. coli* cross-resistance against lead antibacterials Evaluation of cross-resistance between the respective resistant *E. coli* strains with nifuroxazide, nitrofurantoin, and **17**. The three panels show dose-response curves for the three inhibitors tested against strains where resistance was initially generated to nifuroxazide (**A**), nitrofurantoin (**B**), and **17** (**C**). Results indicate that resistance generated to one inhibitor is not necessarily cross-resistant to the other inhibitors, potentially indicating different mechanisms of activation and/or targets.

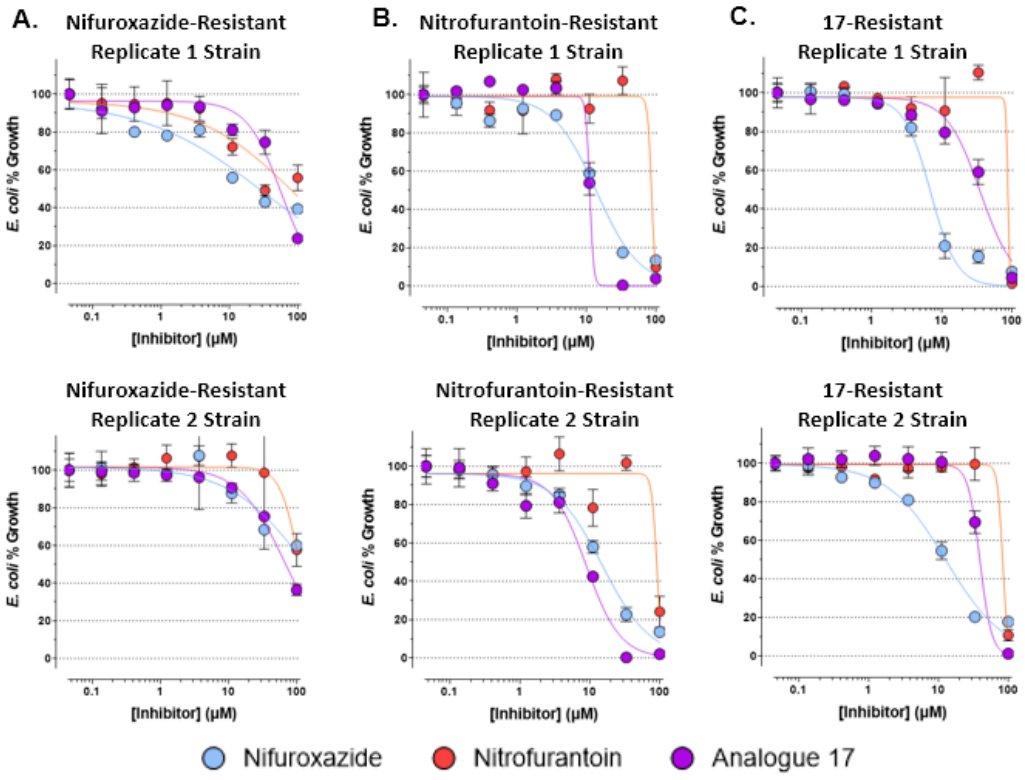

CONCLUSIONS

In a previous high-throughput screen, hit compound **1** was identified as a moderate GroEL/ES inhibitor with weak activity against two Gram-negative bacteria, *K. pneumoniae* and *A. baumannii*. The structure of this hit inhibitor resembles known antibiotics nitroxoline (i.e. shared hydroxyquinoline moiety) and nifuroxazide / nitrofurantoin (i.e. shared N-acyl hydrazone core). The main difference between **1** and nifuroxazide and nitrofurantoin is that the latter two possess a nitrofuran in place of hydroxyquinoline group. With the goal of increasing inhibitor potency against GroEL/ES and *E. coli* and the *ESKAPE* bacteria, while reducing cytotoxicity to human cells, I developed two primary series of hydroxyquinoline and nitrofuran-bearing analogues. These analogues possessed **R**-groups on the distal ends of the scaffolds of varying sizes and chemical compositions to identify SAR profiles.

Results from bacterial proliferation testing demonstrated that the nitrofurans with small **R**-groups (**16-20**) were potent inhibitors of *E. faecium, S. aureus,* and *E. coli* (with maximum efficacy against *E. coli*). Initially, only the hydroxyquinolines were found to be potent GroEL/ES inhibitors in traditional GroEL/ES-mediated substrate refolding assays, whereas nitrofurans were only weak-to-moderate inhibitors. However, subsequent testing in the presence of the *E. coli* NfsB nitroreductase indicated that the nitrofurans act as prodrugs and their reactive metabolites can be potent GroEL/ES inhibitors. Lead nitrofuran antibacterial analogs also exhibited minimal cytotoxicity to human FHC colon and FHs 74 Int small intestinal cells. When evaluating *E. coli* resistance generation against lead antibacterials (**17**, nifuroxazide, and nitrofurantoin), it was evident that all three compounds experienced resistance, albeit to varying degrees. Nifuroxazide and nitrofurantoin were shown to be most effective initially, however, they were found to generate resistance in *E. coli* more rapidly than compound **17** did. This could potentially be attributed to the two drugs being more reliant on NfsA for bioactivation than **17** (as

previous literature has pointed to NfsA mutations being a primary cause of early nitrofuran drug resistance), or because **17** is a more potent inhibitor of GroEL/ES. Resistance to each compound was revealed to be permanent in nature, as opposed to transient (i.e. up-regulation of efflux pumps). Upon further examination, strains that were able to generate resistance against one of the lead antibacterials were not necessarily cross-resistant to the other inhibitors, which could indicate diverging mechanisms of activation and/or targets. This may indicate that combination therapy with structurally distinct analogs could prove synergistic and delay the onset of bacterial resistance.

EXPERIMENTAL

General synthetic methods

Unless otherwise stated, all chemicals were purchased from commercial suppliers and used without further purification. Reaction progress was monitored by thin-layer chromatography on silica gel 60 F254 coated glass plates (EM Sciences). Flash chromatography was performed using a Biotage Isolera One flash chromatography system and eluting through Biotage KP-Sil Zip or Snap silica gel columns for normal-phase separations (hexanes:EtOAc gradients), or Snap KP-C18-HS columns for reverse-phase separations (H_2O:MeOH gradients). Reverse-phase high-performance liquid chromatography (RP-HPLC) was performed using a Waters 1525 binary pump, 2489 tunable UV/Vis detector (254 and 280 nm detection), and 2707 autosampler. For preparatory HPLC purification, samples were chromatographically separated using a Waters XSelect CSH C18 OBD prep column (part number 186005422, 130 Å pore size, 5 µm particle size, 19x150 mm), eluting with a H_2O:CH_3CN gradient solvent system. Linear gradients were run from either 100:0, 80:20, or 60:40 A:B to 0:100 A:B (A = 95:5 H_2O:CH_3CN, 0.05% TFA; B = 5:95 H_2O:CH_3CN, 0.05% TFA. Products from normal-phase separations were concentrated directly, and reverse-phase separations were concentrated, diluted with H_2O, frozen, and lyophilized. For primary compound purity analyses (HPLC-1), samples were chromatographically separated using a Waters XSelect CSH C18 column (part number 186005282, 130 Å pore size, 5 µm particle size, 3.0x150 mm), eluting with the above H_2O:CH_3CN gradient solvent systems. For secondary purity analyses (HPLC-2) of final test compounds, samples were chromatographically separated using a Waters XBridge C18 column (part number 186003132, 130 Å pore size, 5.0 µm particle size, 3.0x100 mm), eluting with a H_2O:MeOH gradient solvent system. Linear gradients were run from either 100:0, 80:20, 60:40, or 20:80 A:B to 0:100 A:B (A = 95:5 H_2O:MeOH, 0.05% TFA; B = 5:95

H_2O:MeOH, 0.05% TFA). Test compounds were found to be >95% in purity from both RP-HPLC analyses. Mass spectrometry data were collected using either Agilent LC 1200-MS 6130 or Agilent LC 1290-MS 6545 Q-TOF analytical LC-MS instruments at the IU Chemical Genomics Core Facility (CGCF). ^{1}H-NMR spectra were recorded on a Bruker 300 MHz spectrometer at the IU CGCF. Chemical shifts are reported in parts per million and calibrated to the d_6-DMSO solvent peaks at 2.50 ppm.

.....

1-(((8-hydroxyquinolin-5-yl)methylene)amino)imidazolidine-2,4-dione (2).

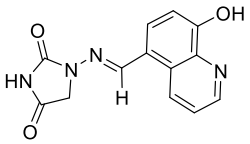

^{1}H-NMR (300 MHz, d_6-DMSO) δ 11.30 (s, 1H), 9.66 (dd, *J* = 8.7, 1.3 Hz, 1H), 8.99 (dd, *J* = 4.4, 1.4 Hz, 1H), 8.21 (s, 1H), 7.92 (d, *J* = 8.2 Hz, 1H), 7.86 (dd, *J* = 8.8, 4.5 Hz, 1H), 7.27 (d, *J* = 8.1 Hz, 1H), 4.46 (s, 2H); MS (ESI) $C_{13}H_{11}N_4O_3$ $[MH]^+$ *m/z* expected = 271.1, observed = 271.0. HPLC-1 = 98%, HPLC-2 = 98%.

.....

***N'*-((8-hydroxyquinolin-5-yl)methylene)thiophene-2-carbohydrazide (3).**

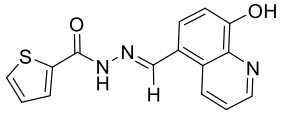

^{1}H-NMR (300 MHz, d_6-DMSO) δ 11.86 (s, 0.6H), 11.74 (s, 0.3H), 10.46 (br s, 0.8H), 9.57 (d, *J* = 8.4 Hz, 0.6H), 8.94 (dd, *J* = 4.1, 1.4 Hz, 1.3H), 8.79 (s, 0.7H), 8.71 (s, 0.3H), 7.65-8.11 (m, 4H), 7.12-7.31 (m, 2H) – Putatively mixture of ~2:1 rotamers; MS (ESI) $C_{15}H_{12}N_3O_2S$ $[MH]^+$ *m/z* expected = 298.1, observed = 298.0; HPLC-1 = 99%;

.....

5-chloro-*N′*-((8-hydroxyquinolin-5-yl)methylene)thiophene-2-carbohydrazide (4).

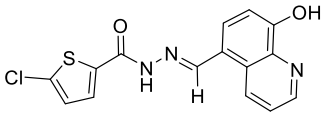

^{1}H-NMR (300 MHz, d_6-DMSO) δ 9.55 (d, *J* = 8.1 Hz, 0.5H), 8.93 (dd, *J* = 4.0, 1.2 Hz, 1H), 8.84 (d, *J* = 8.6 Hz, 0.5H), 8.74 (d, *J* = 9.4 Hz, 1H), 8.02 (d, *J* = 8.1 Hz, 0.5H), 7.89 (d, *J* = 4.1 Hz, 0.5H), 7.76-7.85 (m, 0.9H), 7.66-7.75 (m, 1.1H), 7.12-7.32 (m, 2H) – Putatively mixture of ~1:1 rotamers; MS (ESI) $C_{15}H_{11}ClN_3O_2S$ $[MH]^+$ *m/z* expected = 332.1, observed = 332.0; HPLC-1 = 97%; HPLC-2 = 98%.

.....

***N′*-((8-hydroxyquinolin-5-yl)methylene)benzohydrazide (5).**

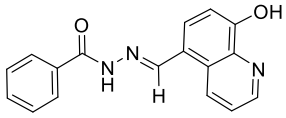

^{1}H-NMR (300 MHz, d_6-DMSO) δ 11.84 (s, 1H), 9.61 (dd, *J* = 8.7, 1.4 Hz, 1H), 8.94 (dd, *J* = 4.1, 1.4 Hz, 1H), 8.83 (s, 1H), 7.90-8.00 (m, 2H), 7.78 (d, *J* = 8.2 Hz, 1H), 7.74 (dd, *J* = 8.8, 4.2 Hz, 1H), 7.50-7.65 (m, 3H), 7.17 (d, *J* = 8.1 Hz, 1H); MS (ESI) $C_{17}H_{14}N_3O_2$ $[MH]^+$ *m/z* expected = 292.1, observed = 292.1; HPLC-1 = 98%; HPLC-2 = 99%.

.....

***N′*-((8-hydroxyquinolin-5-yl)methylene)isonicotinohydrazide (6).**

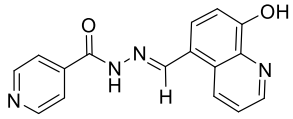

^{1}H-NMR (300 MHz, d_6-DMSO) δ 12.14 (s, 0.8H), 12.08 (s, 0.1H), 9.74 (dd, *J* = 8.7, 1.4 Hz, 0.8H), 9.00 (dd, *J* = 4.3, 1.5 Hz, 1H), 8.82-8.90 (m, 2.8H), 8.48 (s, 0.1H), 7.90-7.98 (m, 1.8H), 7.77-7.90 (m, 1.9H), 7.69-7.74 (m, 0.1H), 7.49-7.57 (m, 0.2H), 7.25 (d, *J* = 8.1 Hz, 0.9H), 7.13-7.20 (m, 0.1H) – Putatively mixture of ~9:1 rotamers; MS (ESI)

$C_{16}H_{13}N_4O_2$ $[MH]^+$ *m/z* expected = 293.1, observed = 293.1; HPLC-1 = 98%, HPLC-2 = >99%.

.....

4-hydroxy-*N'*-((8-hydroxyquinolin-5-yl)methylene)benzohydrazide (7).

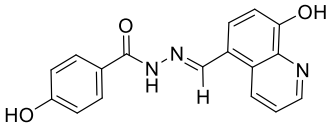

^{1}H-NMR (300 MHz, d_6-DMSO) δ 11.61 (s, 1H), 10.22 (br s, 1H), 9.60 (d, *J* = 8.5 Hz, 1H), 8.92 (d, *J* = 2.9 Hz, 1H), 8.80 (s, 1H), 7.79-7.91 (m, 2H), 7.65-7.78 (m, 2H), 7.14 (d, *J* = 8.0 Hz, 1H), 6.82-6.93 (m, 2H); MS (ESI) $C_{17}H_{14}N_3O_3$ $[MH]^+$ *m/z* expected = 308.1, observed = 308.0; HPLC-1 = 98%; HPLC-2 = >99%.

.....

***N'*-((8-hydroxyquinolin-5-yl)methylene)-4-methoxybenzohydrazide (1).**

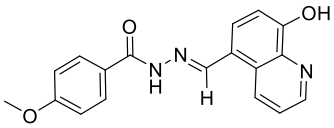

^{1}H-NMR (300 MHz, d_6-DMSO) δ 11.70 (s, 1H), 10.44 (br s, 1H), 9.61 (d, *J* = 8.6 Hz, 1H), 8.94 (d, *J* = 2.8 Hz, 1H), 8.81 (s, 1H), 7.90-8.01 (m, 2H), 7.68-7.82 (m, 2H), 7.17 (d, *J* = 8.1 Hz, 1H), 7.04-7.13 (m, 2H), 3.85 (s, 3H); MS (ESI) $C_{18}H_{16}N_3O_3$ $[MH]^+$ *m/z* expected = 322.1, observed = 322.1; HPLC-1 = 99%; HPLC-2 = 99%.

.....

4-(dimethylamino)-*N'*-((8-hydroxyquinolin-5-yl)methylene)benzohydrazide (8).

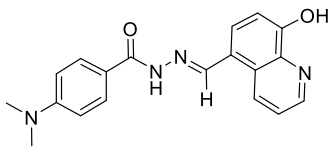

^{1}H-NMR (300 MHz, d_6-DMSO) δ 11.52 (s, 1H), 10.36 (br s, 1H), 9.60 (d, *J* = 8.0 Hz, 1H), 8.93 (dd, *J* = 4.1, 1.6 Hz, 1H), 8.80 (s, 1H), 7.81-7.91 (m, 2H), 7.67-7.78 (m, 2H), 7.16

(d, *J* = 8.0 Hz, 1H), 6.72-6.82 (m, 2H), 3.00 (s, 6H); MS (ESI) $C_{19}H_{19}N_4O_2$ $[MH]^+$ *m/z* expected = 335.2, observed = 335.1; HPLC-1 = >99%; HPLC-2 = 98%.

.....

***N'*-((8-hydroxyquinolin-5-yl)methylene)-1-naphthohydrazide (9).**

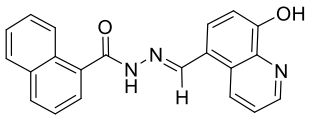

^{1}H-NMR (300 MHz, d_6-DMSO) δ 11.99 (s, 0.3H), 11.97 (s, 0.6H), 10.45 (br s, 0.9H), 9.66 (dd, *J* = 8.7, 1.5 Hz, 0.7H), 8.96 (dd, *J* = 4.1, 1.6 Hz, 0.7H), 8.72 (s, 0.7H), 8.64-8.69 (m, 0.3H), 8.23-8.35 (m, 1.0H), 7.99-8.16 (m, 2.3H), 7.87-7.93 (m, 0.3H), 7.73-7.83 (m, 2.1H), 7.49-7.68 (m, 3.4H), 7.42-7.49 (m, 0.3H), 7.18 (d, *J* = 8.1 Hz, 0.7H), 6.96-7.03 (m, 0.3H), 6.75-6.84 (m, 0.3H) – Putatively mixture of ~7:3 rotamers; MS (ESI) $C_{21}H_{10}N_3O_2$ $[MH]^+$ *m/z* expected = 342.1, observed = 342.1; HPLC-1 = >99%; HPLC-2 = 99%.

.....

***N'*-((8-hydroxyquinolin-5-yl)methylene)-2-phenoxybenzohydrazide (10).**

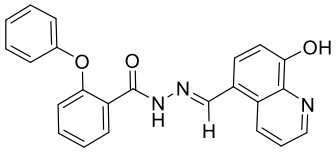

^{1}H-NMR (300 MHz, d_6-DMSO) δ 11.73 (s, 0.4H), 11.70 (s, 0.6H), 10.39 (br s, 0.8H), 9.57 (dd, *J* = 8.7, 1.5 Hz, 0.6H), 8.92 (dd, *J* = 4.1, 1.5 Hz, 0.6H), 8.78-8.89 (m, 0.8H), 8.65 (s, 0.6H), 8.31 (s, 0.4H), 7.66-7.78 (m, 1.8H), 7.47-7.58 (m, 1.7H), 7.35-7.45 (m, 1.3H), 7.20-7.34 (m, 1.4H), 7.10-7.19 (m, 2H), 7.03-7.10 (m, 1.6H), 6.93-7.03 (m, 1.4H), 6.82-6.89 (m, 0.8H) – Putatively mixture of ~3:2 rotamers; MS (ESI) $C_{23}H_{18}N_3O_3$ $[MH]^+$ *m/z* expected = 384.1, observed = 384.2; HPLC-1 = >99%; HPLC-2 = 99%.

.....

***N'*-((8-hydroxyquinolin-5-yl)methylene)-3-phenoxybenzohydrazide (11).**

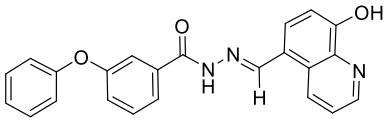

^{1}H-NMR (300 MHz, d_6-DMSO) δ 11.83 (s, 1H), 10.46 (br s, 1H), 9.59 (dd, *J* = 8.7, 1.4 Hz, 1H), 8.94 (dd, *J* = 4.1, 1.5 Hz, 1H), 8.81 (s, 1H), 7.68-7.82 (m, 3H), 7.53-7.64 (m, 2H), 7.39-7.50 (m, 2H), 7.13-7.28 (m, 3H), 7.03-7.13 (m, 2H); MS (ESI) $C_{23}H_{18}N_3O_3$ $[MH]^+$ *m/z* expected = 384.1, observed = 384.1; HPLC-1 = >99%; HPLC-2 = >99%.

.....

***N,N*-diethyl-3-(2-((8-hydroxyquinolin-5-yl)methylene)hydrazine-1-carbonyl)benzenesulfonamide (12).**

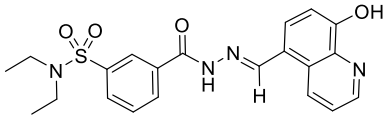

^{1}H-NMR (300 MHz, d_6-DMSO) δ 12.06 (s, 1H), 10.50 (br s, 1H), 9.62 (dd, *J* = 8.7, 1.5 Hz, 1H), 8.95 (dd, *J* = 4.0, 1.5 Hz, 1H), 8.85 (s, 1H), 8.36 (s, 1H), 8.24 (d, *J* = 7.8 Hz, 1H), 8.02 (d, *J* = 8.0 Hz, 1H), 7.71-7.84 (m, 3H), 7.18 (d, *J* = 8.0 Hz, 1H), 3.22 (q *J* = 7.1 Hz, 4H), 1.06 (t, *J* = 7.1 Hz, 6H); MS (ESI) $C_{21}H_{23}N_4O_4S$ $[MH]^+$ *m/z* expected = 427.1, observed = 427.2; HPLC-1 = 99%; HPLC-2 = 99%.

.....

***N*-(4-(2-((8-hydroxyquinolin-5-yl)methylene)hydrazine-1-carbonyl)phenyl)thiophene-2-sulfonamide (13).**

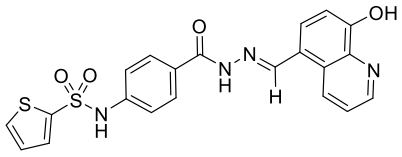

^{1}H-NMR (300 MHz, d_6-DMSO) δ 11.71 (s, 1H), 10.90 (s, 1H), 10.44 (br s, 1H), 9.58 (d, *J* = 8.7 Hz, 1H), 8.93 (d, *J* = 2.7 Hz, 1H), 8.77 (s, 1H), 7.94 (dd, *J* = 5.0, 1.3 Hz, 1H), 7.81-

7.91 (m, 2H), 7.69-7.81 (m, 2H), 7.67 (dd, *J* = 3.7, 1.3 Hz, 1H), 7.23-7.35 (m, 2H), 7.08-7.20 (m, 2H); MS (ESI) $C_{21}H_{15}N_4O_4S_2$ $[M-H]^-$ *m/z* expected = 451.1, observed = 451.0; HPLC-1 = 99%; HPLC-2 = 99%.

.....

4-bromo-*N*-(4-(2-((8-hydroxyquinolin-5-yl)methylene)hydrazine-1-carbonyl)phenyl)benzenesulfonamide (14).

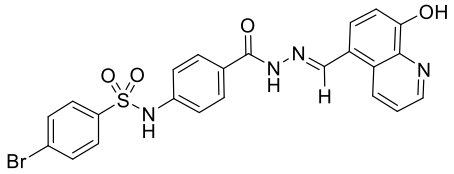

^{1}H-NMR (300 MHz, d_6-DMSO) δ 11.71 (s, 1H), 10.86 (s, 1H), 10.44 (br s, 1H), 9.57 (d, *J* = 8.6 Hz, 1H), 8.93 (d, *J* = 2.7 Hz, 1H), 8.78 (s, 1H), 7.66-7.91 (m, 8H), 7.23 (d, *J* = 8.6 Hz, 2H), 7.09-7.18 (m, 1H), 8.96 (s, 1H); MS (ESI) $C_{23}H_{16}BrN_4O_4S$ $[M-H]^-$ *m/z* expected = 523.0, observed = 522.9; HPLC-1 = 99%; HPLC-2 = 99%.

.....

4-ethoxy-*N*-(4-(2-((8-hydroxyquinolin-5-yl)methylene)hydrazine-1-carbonyl)phenyl)benzenesulfonamide (15).

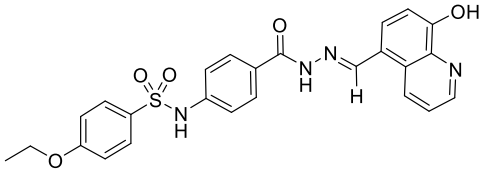

^{1}H-NMR (300 MHz, d_6-DMSO) δ 11.67 (s, 1H), 10.63 (s, 1H), 10.43 (br s, 1H), 9.57 (d, *J* = 7.8 Hz, 1H), 8.93 (d, *J* = 2.8 Hz, 1H), 8.76 (s, 1H), 7.67-7.86 (m, 6H), 7.22 (d, *J* = 8.8 Hz, 2H), 7.15 (d, *J* = 8.0 Hz, 1H), 7.06 (d, *J* = 8.9 Hz, 2H), 4.06 (q, *J* = 6.9 Hz, 2H), 1.30 (t, *J* = 6.9 Hz, 3H); MS (ESI) $C_{25}H_{21}N_4O_5S$ $[M-H]^-$ *m/z* expected = 489.1, observed = 489.0; HPLC-1 = 98%; HPLC-2 = 98%.

.....

***N′*-((5-nitrofuran-2-yl)methylene)thiophene-2-carbohydrazide (16).**

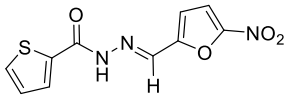

^{1}H-NMR (300 MHz, d_6-DMSO) δ 12.26 (s, 1H), 8.35 (br s, 1H), 7.96 (br s, 2H), 7.81 (d, *J* = 4.0 Hz, 1H), 7.28 (d, *J* = 4.0 Hz, 1H), 7.24 (dd, *J* = 4.9, 3.9 Hz, 1H); MS (ESI) $C_{10}H_8N_3O_3S$ $[MH]^+$ *m/z* expected = 266.0, observed = 266.1; HPLC-1 = 98%; HPLC-2 = 98%.

.....

5-chloro-*N′*-((5-nitrofuran-2-yl)methylene)thiophene-2-carbohydrazide (17).

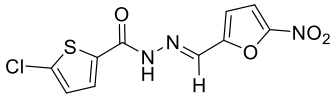

^{1}H-NMR (300 MHz, d_6-DMSO) δ 12.38 (s, 1H), 8.34 (br s, 0.3H), 8.03 (br s, 0.7H), 7.89 (br s, 0.7H), 7.80 (d, *J* = 3.9 Hz, 1.3H), 7.24-7.33 (m, 2.2H) – Putatively mixture of ~2:1 rotamers; MS (ESI) $C_{10}H_7N_3O_4S$ $[MH]^+$ *m/z* expected = 300.0, observed = 300.0; HPLC-1 = 98%; HPLC-2 = 98%.

.....

***N′*-((5-nitrofuran-2-yl)methylene)benzohydrazide (18).**

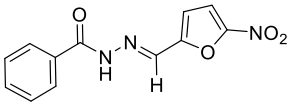

^{1}H-NMR (300 MHz, d_6-DMSO) δ 12.25 (s, 1H), 8.40 (br s, 1H), 7.91 (d, *J* = 7.2 Hz, 2H), 7.80 (d, *J* = 3.9 Hz, 1H), 7.59-7.67 (m, 1H), 7.50-7.59 (m, 2H), 7.28 (d, *J* = 3.6 Hz, 1H); MS (ESI) $C_{12}H_{10}N_3O_4$ $[MH]^+$ *m/z* expected = 260.0, observed = 260.1; HPLC-1 = >99%; HPLC-2 = 98%.

.....

***N′*-((5-nitrofuran-2-yl)methylene)isonicotinohydrazide (19).**

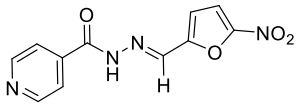

^{1}H-NMR (300 MHz, d_6-DMSO) δ 12.44 (s, 1H), 8.81 (d, *J* = 5.6 Hz, 2H), 8.41 (s, 1H), 7.75-7.89 (m, 3H), 7.33 (d, *J* = 3.8 Hz, 1H); MS (ESI) $C_{11}H_9N_4O_4$ $[MH]^+$ *m/z* expected = 261.1, observed = 261.1; HPLC-1 = 99%; HPLC-2 = 99%.

.....

4-methoxy-*N′*-((5-nitrofuran-2-yl)methylene)benzohydrazide (20).

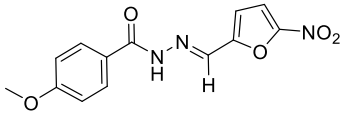

^{1}H-NMR (300 MHz, d_6-DMSO) δ 12.12 (s, 1H), 8.39 (br s, 1H), 7.88-7.96 (m, 2H), 7.80 (d, *J* = 4.0 Hz, 1H), 7.26 (d, *J* = 3.9 Hz, 1H), 7.05-7.12 (m, 2H), 3.84 (s, 3H); MS (ESI) $C_{13}H_{10}N_3O_5$ $[M-H]^-$ *m/z* expected = 288.1, observed = 288.0; HPLC-1 = >99%; HPLC-2 = >99%.

.....

4-(dimethylamino)-*N′*-((5-nitrofuran-2-yl)methylene)benzohydrazide (21).

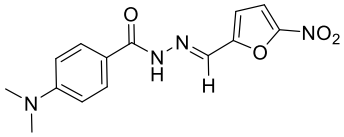

^{1}H-NMR (300 MHz, d_6-DMSO) δ 11.95 (s, 1H), 8.38 (s, 1H), 7.77-7.85 (m, 3H), 7.22 (d, *J* = 3.9 Hz, 1H), 6.73-6.81 (m, 2H), 3.01 (s, 6H); MS (ESI) $C_{14}H_{15}N_4O_4$ $[MH]^+$ *m/z* expected = 303.1, observed = 303.1; HPLC-1 = >99%; HPLC-2 = 99%.

.....

***N'*-((5-nitrofuran-2-yl)methylene)-1-naphthohydrazide (22).**

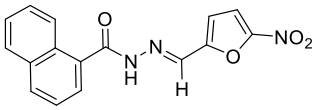

^{1}H-NMR (300 MHz, d_6-DMSO) δ 12.26 (s, 1H), 8.30 (s, 1H), 8.18-8.25 (m, 1H), 8.13 (d, *J* = 8.2 Hz, 1H), 7.99-8.08 (m, 1H), 7.76-7.86 (m, 2H), 7.57-7.67 (m, 3H), 7.30 (d, *J* = 3.9 Hz, 1H); MS (ESI) $C_{16}H_{12}N_3O_4$ $[M-H]^-$ *m/z* expected = 310.1, observed = 310.0; HPLC-1 = >99%; HPLC-2 = 98%.

.....

***N'*-((5-nitrofuran-2-yl)methylene)-2-phenoxybenzohydrazide (23).**

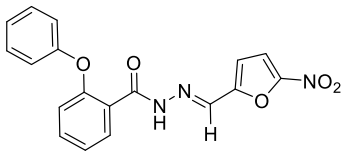

^{1}H-NMR (300 MHz, d_6-DMSO) δ 12.17 (s, 1H), 8.26 (s, 0.7H), 7.92 (s, 0.3H), 7.78 (d, *J* = 3.8 Hz, 0.7H), 7.70-7.75 (m, 0.4H), 7.67 (d, *J* = 7.3 Hz, 0.7H), 7.34-7.58 (m, 2.9H), 6.94-7.33 (m, 7.0H), 6.893-6.91 (m, 0.4H) – Putatively mixture of ~2:1 rotamers; MS (ESI) $C_{18}H_{14}N_3O_5$ $[MH]^+$ *m/z* expected = 352.1, observed = 352.1; HPLC-1 = >99%; HPLC-2 = 98%.

.....

***N'*-((5-nitrofuran-2-yl)methylene)-3-phenoxybenzohydrazide (24).**

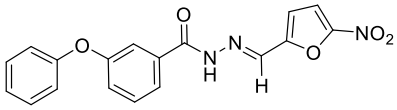

^{1}H-NMR (300 MHz, d_6-DMSO) δ 12.25 (s, 1H), 8.39 (s, 1H), 7.80 (d, *J* = 3.9 Hz, 1H), 7.70 (d, *J* = 7.6 Hz, 1H), 7.51-7.61 (m, 2H), 7.38-7.48 (m, 2H), 7.23-7.32 (m, 2H), 7.15-7.23 (m, 1H), 7.04-7.12 (m, 2H); MS (ESI) $C_{18}H_{14}N_3O_5$ $[MH]^+$ *m/z* expected = 352.1, observed = 352.1; HPLC-1 = >99%; HPLC-2 = 98%.

.....

***N,N*-diethyl-3-(2-((5-nitrofuran-2-yl)methylene)hydrazine-1-carbonyl)benzenesulfonamide (25).**

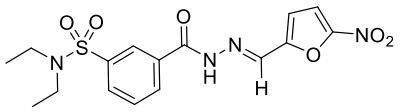

^{1}H-NMR (300 MHz, d_6-DMSO) δ 12.45 (s, 1H), 8.43 (s, 1H), 8.31 (s, 1H), 8.20 (d, *J* = 7.2 Hz, 1H), 8.03 (d, *J* = 7.7 Hz, 1H), 7.74-7.85 (m, 2H), 7.31 (d, *J* = 3.4 Hz, 1H), 3.20 (q, *J* = 7.1 Hz, 4H), 1.05 (t, *J* = 7.1 Hz, 6H); MS (ESI) $C_{16}H_{19}N_4O_6S$ $[MH]^+$ *m/z* expected = 395.1, observed = 395.1; HPLC-1 = >99%; HPLC-2 = >99%.

.....

***N*-(4-(2-((5-nitrofuran-2-yl)methylene)hydrazine-1-carbonyl)phenyl)thiophene-2-sulfonamide (26).**

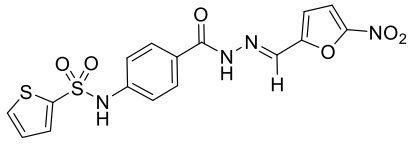

^{1}H-NMR (300 MHz, d_6-DMSO) δ 12.06 (s, 1H), 10.87 (s, 1H), 8.27 (s, 1H), 7.85 (dd, *J* = 5.0, 1.4 Hz, 1H), 7.69-7.79 (m, 3H), 7.58 (dd, *J* = 3.8, 1.4 Hz, 1H), 7.15-7.25 (m, 3H), 7.06 (dd, *J* = 4.9, 3.8 Hz, 1H); MS (ESI) $C_{16}H_{13}N_4O_6S_2$ $[MH]^+$ *m/z* expected = 421.0, observed = 421.1; HPLC-1 = 98%; HPLC-2 = 99%.

.....

4-bromo-*N*-(4-(2-((5-nitrofuran-2-yl)methylene)hydrazine-1-carbonyl)phenyl)benzenesulfonamide (27).

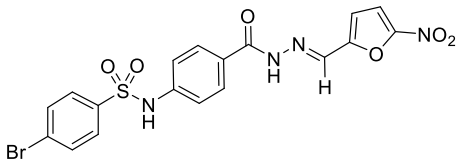

^{1}H-NMR (300 MHz, d_6-DMSO) δ 12.11 (s, 1H), 10.89 (s, 1H), 8.34 (s, 1H), 7.70-7.87 (m, 7H), 7.18-7.31 (m, 3H); MS (ESI) $C_{18}H_{14}BrN_4O_6S$ $[MH]^+$ *m/z* expected = 495.0, observed = 494.9; HPLC-1 = 98%; HPLC-2 = 97%.

.....

4-ethoxy-*N*-(4-(2-((5-nitrofuran-2-yl)methylene)hydrazine-1-carbonyl)phenyl)benzenesulfonamide (28).

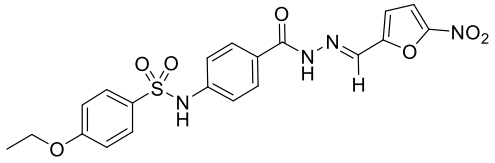

^{1}H-NMR (300 MHz, d_6-DMSO) δ 12.09 (s, 1H), 10.68 (s, 1H), 8.34 (s, 1H), 7.68-7.86 (m, 5H), 7.17-7.29 (m, 3H), 7.01-7.10 (m, 2H), 4.06 (q, *J* = 7.0 Hz, 2H), 1.30 (t, *J* = 1.3 Hz, 3H); MS (ESI) $C_{20}H_{19}N_4O_7S$ $[MH]^+$ *m/z* expected = 459.1, observed = 459.0; HPLC-1 = 97%; HPLC-2 = 97%.

.....

***N'*-((4-hydroxynaphthalen-1-yl)methylene)-4-methoxybenzohydrazide (29).**

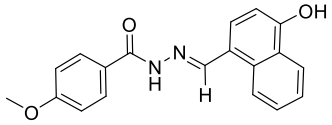

^{1}H-NMR (300 MHz, d_6-DMSO) δ 11.57 (s, 1H), 10.75 (s, 1H), 8.82-8.99 (m, 2H), 8.20 (d, *J* = 8.1 Hz, 1H), 7.84-7.99 (m, 2H), 7.69 (d, *J* = 7.8 Hz, 1H), 7.61 (t, *J* = 7.5 Hz, 1H), 7.50 (t, *J* = 7.5 Hz, 1H), 6.99-7.11 (m, 2H), 6.93 (d, *J* = 7.9 Hz, 1H), 3.81 (s, 3H); MS (ESI)

$C_{19}H_{17}N_2O_3$ $[M-H]^-$ *m/z* expected = 321.1, observed = 321.1; HPLC-1 = 99%; HPLC-2 = 99%.

.....

***N'*-((4-hydroxynaphthalen-1-yl)methylene)benzohydrazide (30).**

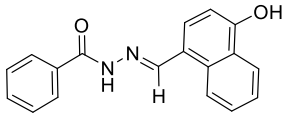

^{1}H-NMR (300 MHz, d_6-DMSO) δ 11.72 (s, 1H), 10.81 (s, 1H), 8.89-9.02 (m, 2H), 8.24 (d, *J* = 8.1 Hz, 1H), 7.95 (d, *J* = 7.2 Hz, 2H), 7.74 (d, *J* = 8.1 Hz, 1H), 7.48-7.70 (m, 5H), 6.97 (d, *J* = 7.9 Hz, 1H); MS (ESI) $C_{18}H_{15}N_2O_2$ $[MH]^+$ *m/z* expected = 291.1, observed = 291.1; HPLC-1 = 99%; HPLC-2 = 98%.

.....

4-methoxy-*N'*-(quinolin-5-ylmethylene)benzohydrazide (31).

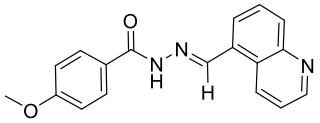

^{1}H-NMR (300 MHz, d_6-DMSO) δ 11.91 (s, 1H), 9.45 (d, *J* = 8.3 Hz, 1H), 8.98 (d, *J* = 3.9 Hz, 2H), 8.10 (d, *J* = 8.1 Hz, 1H), 7.91-8.02 (m, 3H), 7.80-7.89 (m, 1H), 7.68 (dd, *J* = 8.1, 3.7 Hz, 1H), 7.10 (d, *J* = 8.8 Hz, 2H), 3.85 (s, 3H); MS (ESI) $C_{18}H_{16}N_3O_2$ $[MH]^+$ *m/z* expected = 306.1, observed = 306.1; HPLC-1 = 99%; HPLC-2 = 99%.

.....

***N'*-(quinolin-5-ylmethylene)benzohydrazide (32).**

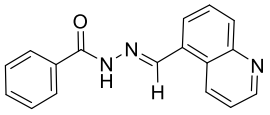

^{1}H-NMR (300 MHz, d_6-DMSO) δ 12.05 (s, 1H), 9.45 (d, *J* = 8.5 Hz, 1H), 8.93-9.06 (m, 2H), 8.10 (d, *J* = 8.2 Hz, 1H), 7.97 (t, *J* = 7.5 Hz, 3H), 7.80-7.89 (m, 1H), 7.69 (dd, *J* =

8.7, 4.0 Hz, 1H), 7.50-7.64 (m, 3H); MS (ESI) $C_{17}H_{14}N_3O$ $[MH]^+$ *m/z* expected = 276.1, observed = 276.1; HPLC-1 = >99%; HPLC-2 = >99%.

.....

4-methoxy-*N′*-(naphthalen-1-ylmethylene)benzohydrazide (33).

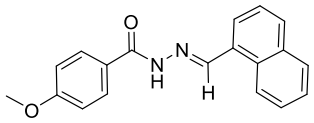

^{1}H-NMR (300 MHz, d_6-DMSO) δ 11.83 (s, 1H), 9.10 (s, 1H), 8.87 (d, *J* = 8.2 Hz, 1H), 8.02 (d, *J* = 7.9 Hz, 2H), 7.89-7.99 (m, 3H), 7.57-7.72 (m, 3H), 7.06-7.13 (m, 2H), 3.85 (s, 3H); MS (ESI) $C_{19}H_{17}N_2O_2$ $[MH]^+$ *m/z* expected = 305.1, observed = 305.1; HPLC-1 = f>99%; HPLC-2 = >99%.

.....

***N′*-(naphthalen-1-ylmethylene)benzohydrazide (34).**

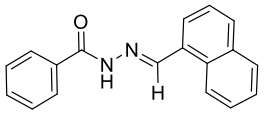

^{1}H-NMR (300 MHz, d_6-DMSO) δ 11.96 (s, 1H), 9.12 (s, 1H), 8.88 (d, *J* = 8.3 Hz, 1H), 8.03 (dd, *J* = 7.7, 3.2 Hz, 2H), 7.91-8.00 (m, 3H), 7.52-7.73 (m, 6H); MS (ESI) $C_{18}H_{15}N_2O$ $[MH]^+$ *m/z* expected = 275.1, observed = 275.0; HPLC-1 = >99%; HPLC-2 = >99%.

.....

***N′*-(4-hydroxybenzylidene)-4-methoxybenzohydrazide (35).**

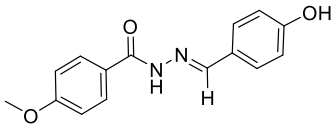

^{1}H-NMR (300 MHz, d_6-DMSO) δ 11.53 (s, 1H), 9.93 (s, 1H), 8.33 (s, 1H), 7.89 (d, *J* = 8.8 Hz, 2H), 7.50-7.59 (m, 2H), 7.00-7.09 (m, 2H), 6.83 (d, *J* = 8.5 Hz, 2H), 3.83 (s, 3H); MS (ESI) $C_{15}H_{15}N_2O_3$ $[MH]^+$ *m/z* expected = 271.1, observed = 271.1; HPLC-1 = 95%; HPLC-2 = 99%.

.....

***N′*-(4-hydroxybenzylidene)benzohydrazide (36).**

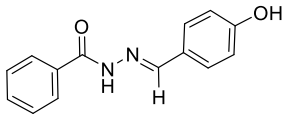

^{1}H-NMR (300 MHz, d_6-DMSO) δ 11.65 (s, 1H), 9.95 (s, 1H), 8.34 (s, 1H), 7.89 (d, *J* = 6.8 Hz, 2H), 7.44-7.64 (m, 5H), 6.84 (d, *J* = 8.6 Hz, 2H); MS (ESI) $C_{14}H_{13}N_2O_2$ $[MH]^+$ *m/z* expected = 241.1, observed = 241.1; HPLC-1 = 95%; HPLC-2 = 98%.

.....

***N′*-benzylidene-4-methoxybenzohydrazide (37).**

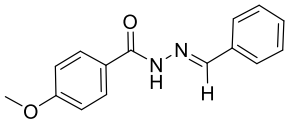

^{1}H-NMR (300 MHz, d_6-DMSO) δ 11.74 (s, 1H), 8.45 (s, 1H), 7.87-7.96 (m, 2H), 7.67-7.77 (m, 2H), 7.39-7.51 (m, 3H), 7.02-7.11 (m, 2H), 3.83 (s, 3H); MS (ESI) $C_{15}H_{15}N_2O_2$ $[MH]^+$ *m/z* expected = 255.1, observed = 255.1; HPLC-1 = 99%; HPLC-2 = 99%.

.....

***N′*-benzylidenebenzohydrazide (38).**

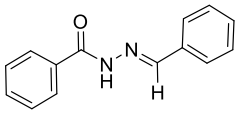

^{1}H-NMR (300 MHz, d_6-DMSO) δ 11.87 (s, 1H), 8.47 (s, 1H), 7.92 (d, *J* = 7.0 Hz, 2H), 7.69-7.78 (m, 2H), 7.41-7.64 (m, 6H); MS (ESI) $C_{14}H_{13}N_2O$ $[MH]^+$ *m/z* expected = 225.1, observed = 225.1; HPLC-1 = >99%; HPLC-2 = >99%.

.....

***N'*-(furan-2-ylmethylene)-4-methoxybenzohydrazide (39).**

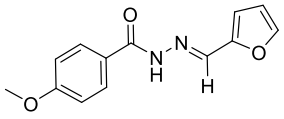

^{1}H-NMR (300 MHz, d_6-DMSO) δ 11.68 (s, 1H), 8.33 (s, 1H), 7.86-7.92 (m, 2H), 7.84 (s, 1H), 7.02-7.10 (m, 2H), 6.91 (d, *J* = 3.1 Hz, 1H), 6.63 (dd, *J* = 3.3, 1.7 Hz, 1H), 3.83 (s, 3H); MS (ESI) $C_{13}H_{13}N_2O_3$ $[MH]^+$ *m/z* expected = 245.1, observed = 245.1; HPLC-1 = 98%; HPLC-2 = 98%.

General materials and methods for biochemical and cell-based experiments

NEB 5-alpha (a derivative of DH5α *E. coli*) and BL21 (DE3) *E. coli* cells were purchased from New England Biolabs, and Rosetta™ 2 (DE3) *E. coli* cells were purchased from EMD Millipore. The human cell viability assays used FHC colon cells (CRL-1831) and FHs 74 Int small intestine cells (CCL-241) obtained from the ATCC. Ampicillin was used at a concentration of 50 μg/mL, when appropriate.

NOTE: While the following experimental protocols have been reported in previous studies, detailed descriptions are included in an effort to maintain rigor, reproducibility, and transparency throughout these studies.[28,31,33,50-51]

***E. coli* GroEL and GroES purification**

E. coli GroEL was expressed from a trc-promoted and Amp(+) resistance marker plasmid in NEB 5-alpha *E. coli* cells. GroES was expressed from a T7-promoted and Amp(+) resistance plasmid in *E. coli* BL21 (DE3) cells. Transformed colonies were plated onto Ampicillin-treated LB agar and incubated overnight at 37°C. A single colony was selected and grown in LB media treated with Ampicillin for 16 hours at 37°C at 200

rpm. Cells were then sub-cultured in scaled-up Ampicillin-treated LB medium and grown at 37°C at 230 rpm until an OD_{600} of 0.5 was reached, then were induced with 0.8 mM IPTG and continued to grow for ~2.5 h at 37°C. The cultures were centrifuged at 8,000 rpm at 4°C and the cell pellets were collected and re-suspended in Buffer A (50 mM Tris-HCl, pH 7.4, and 20 mM NaCl) supplemented with EDTA-free complete protease inhibitor cocktail (Roche). The combined suspension was lysed by sonication, the lysate was centrifuged at 14,000 rpm at 4°C, and the clarified lysate was passed through a 0.45 µm filter (Millipore).

Anion exchange purification of GroEL: The filtered lysate was loaded onto a GE HiScale Anion exchange column (Q Sepharose fast flow anion exchange resin) that was equilibrated with 2 column volumes of Buffer A. The loaded column was washed with 3 column volumes of Buffer A containing 28% of Buffer B (50 mM Tris-HCl, pH 7.4, and 1 M NaCl), then bound protein was eluted with a 28-60% gradient elution of Buffer B over 3 column volumes. Protein-containing fractions, as identified by SDS-PAGE, were collected, spin concentrated using a 10 kDa Amicon Ultra-15 centrifugal filter (EMD Millipore), and dialyzed overnight with 10 kDa SnakeSkin™ dialysis tubing (Thermo Scientific) at 4°C in 50 mM Tris-HCl, pH 7.4, and 150 mM NaCl solution.

Size exclusion chromatography of GroEL: The dialyzed protein was loaded onto a Superdex 200 size exclusion column (HiLoad 26/600, GE) that was equilibrated with 2 column volumes of 50 mM Tris-HCl, pH 7.4, and 150 mM NaCl solution. The loaded column was eluted with 1 column volume of 50 mM Tris-HCl, pH 7.4, and 150 mM NaCl solution. Protein-containing fractions, as identified by SDS-PAGE, were collected, spin concentrated using a 10 kDa Amicon Ultra-15 centrifugal filter (EMD Millipore), and dialyzed overnight with 10 kDa SnakeSkin™ dialysis tubing (Thermo Scientific) at 4°C in

50 mM Tris-HCl, pH 7.4, and 150 mM NaCl solution. The final protein concentration was determined by Coomassie Protein Assay Kit (Thermo Scientific). Batches of GroEL protein for testing were stored at 4°C for up to one month, then discarded.

Anion exchange purification of GroES: The filtered lysate was loaded onto a GE HiScale anion exchange column (Q Sepharose fast flow anion exchange resin) that was equilibrated with 2 column volumes of Buffer A. The loaded column was washed with 3 column volumes of Buffer A containing 10% of Buffer B (50 mM Tris-HCl, pH 7.4, and 1 M NaCl), then bound protein was eluted with a 10-50% gradient elution of Buffer B over 3 column volumes. Protein-containing fractions, as identified by SDS-PAGE, were collected, spin concentrated using a 10 kDa Amicon Ultra-15 centrifugal filter (EMD Millipore), and dialyzed overnight with 10 kDa SnakeSkin™ dialysis tubing (Thermo Scientific) at 4°C in 50 mM Tris-HCl, pH 7.4, and 150 mM NaCl solution.

Size exclusion chromatography of GroES: The dialyzed protein was loaded onto a Superdex 200 size exclusion column (HiLoad 26/600, GE) that was equilibrated with 2 column volumes of 50 mM Tris-HCl, pH 7.4, and 150 mM NaCl solution. The loaded column was eluted with 1 column volume of 50 mM Tris-HCl, pH 7.4, and 150 mM NaCl solution. Protein-containing fractions, as identified by SDS-PAGE, were collected, spin concentrated using a 10 kDa Amicon Ultra-15 centrifugal filter (EMD Millipore), and dialyzed overnight with 10 kDa SnakeSkin™ dialysis tubing (Thermo Scientific) at 4°C in 50 mM Tris-HCl, pH 7.4, and 150 mM NaCl solution. The final protein concentration was determined by Coomassie Protein Assay Kit (Thermo Scientific). Batches of GroES protein for testing were stored at 4°C for up to one month, then discarded.

Evaluation of compounds in the GroEL/ES-mediated dMDH refolding assays

Reagent preparation: For these assays, four primary reagent stocks were prepared: 1) GroEL/ES-dMDH binary complex stock; 2) ATP initiation stock; 3) EDTA quench stock; 4) MDH enzymatic assay stock. Denatured MDH (dMDH) was prepared by 2-fold dilution of MDH (5 mg/ml, soluble pig heart MDH from Roche, product #10127248001) with denaturant buffer (7 M guanidine-HCl, 200 mM Tris, pH 7.4, and 50 mM DTT). MDH was completely denatured by incubating at room temperature for >45 min. The binary complex solutions were prepared by slowly adding the dMDH stock to a stirring stock with GroEL and GroES in folding buffer (50 mM Tris-HCl, pH 7.4, 50 mM KCl, 10 mM $MgCl_2$, and 1 mM DTT). The binary complex stocks were prepared immediately prior to dispensing into the assay plates and had final protein concentrations of 83.3 nM GroEL, 100 nM GroES, and 20 nM dMDH in folding buffer. For the ATP initiation stock, ATP solid was diluted into folding buffer to a final concentration of 2.5 mM. Quench solution contained 600 mM EDTA (pH 8.0). The MDH enzymatic assay stock consisted of 20 mM sodium mesoxalate and 1.6 mM NADH in reaction buffer (50 mM Tris-HCl, pH 7.4, 50 mM KCl, and 1 mM DTT).

Assay Protocol: First, 30 µL aliquots of the GroEL/ES-dMDH binary complex stocks were dispensed into clear, 384-well polystyrene plates. Next, 0.5 µL of the compound stocks (10 mM to 4.6 µM, 3-fold dilutions series in DMSO) were added by pin-transfer (V&P Scientific). The chaperonin-mediated refolding cycles were initiated by addition of 20 µL of ATP stock (reagent concentrations during refolding cycle: 50 nM GroEL, 60 nM GroES, 12 nM dMDH, 1 mM ATP, and compounds of 100 µM to 46 nM, 3-fold dilution series) and the refolding reactions were incubated at 37°C. The incubation time was determined from refolding time-course control experiments until they reached ~90% completion of the refolding of dMDH – generally ~20-40 min. Next, the assay was

quenched by addition of 10 µL of the EDTA stock to give a final concentration of 100 mM in the wells. Enzymatic activity of the refolded MDH was initiated by addition of 20 µL MDH enzymatic assay stock, and followed by measuring the NADH absorbance in each well at 340 nm using a Molecular Devices SpectraMax Plus384 microplate reader (NADH absorbs at 340 nm, while NAD^+ does not). $A_{340\ nm}$ measurements were recorded at 0.5 minutes (start point) and at successive time points until the amount of NADH consumed reached ~90% (end point, generally between 20-35 minutes). The ratio between start and end point A_{340} values were used to calculate the % inhibition of the GroEL/ES machinery by the compounds IC_{50} values for the test compounds were obtained by plotting the % inhibition results in GraphPad Prism and analyzing by non-linear regression using the log(inhibitor) vs. response (variable slope) equation. Results presented represent the averages of IC_{50} values obtained from at least four replicates in the GroEL/ES-dMDH refolding assay.

Counter-screening compounds for inhibition of native MDH enzymatic activity

Reagent Preparations & Assay Protocol: This assay was performed as described above for the GroEL/ES-dMDH refolding assay; however, the assay protocol differed in the sequence of compound addition to the assay plates. The refolding reactions were allowed to proceed for 45 min at 37°C in the absence of test compounds (complete refolding of MDH occurs), then quenched with the EDTA stock. Compounds were then pin-transferred into the plates after the EDTA quenching step; thus, compound effects are only possible by inhibiting the fully-refolded MDH reporter substrate. Next, enzymatic activity of the refolded MDH was initiated by addition of 20 µL MDH enzymatic assay stock and followed by measuring the NADH absorbance in each well at 340 nm using a Molecular Devices SpectraMax Plus384 microplate reader (NADH absorbs at 340 nm, while NAD^+ does not). $A_{340\ nm}$ measurements were recorded

at 0.5 minutes (start point) and at successive time points until the amount of NADH consumed reached ~90% (end point, generally between 20-35 minutes). Compounds were tested in 8-point, 3-fold dilution series (62.5 µM to 29 nM during the reporter reaction) in clear, flat-bottom 384-well microtiter plates. IC_{50} values for the MDH reporter enzyme were determined as described above. Results presented represent the averages of IC_{50} values obtained from at least five replicates.

Evaluation of compounds in the GroEL/ES-mediated dMDH refolding assay and native MDH activity counter-screen in the presence of *E. coli* NfsB nitroreductase

These assays were performed nearly identically to those described above, but with a couple distinct modifications. For both assays, 10 µg/mL of the *E. coli* NfsB nitroreductase enzyme (Sigma product #N9284) was added to the initial GroEL/ES-dMDH solution. For the GroEL/ES-dMDH refolding assay, after stamping with compounds, 10 µL of a 2.4 mM NADH solution was added, followed by a 10 minute incubation period at 37°C to bioactivate the nitrofuran analogues. The remainder of the assay was conducted as above in the absence of the NfsB nitroreductase. With the extra 10 µL volume from the NADH addition, this made the compound concentrations during the refolding cycle part of the assay range from 83 µM to 38 nM (3-fold dilution series). For the native MDH activity counter-screen in the presence of *E. coli* NfsB nitroreductase, the assay was performed as described above for the GroEL/ES-dMDH refolding assay with NfsB; however, the compound addition to the assay plates was conducted after the EDTA quench step, followed by a 10 minute incubation period at 37°C to bioactivate the nitrofuran analogues. With the extra 10 µL volume from the NADH addition, this made the compound concentrations during the enzymatic reporter part of the assay range from 56 µM to 25 nM (3-fold dilution series). IC_{50} values for the test compounds were obtained by plotting the % inhibition results in GraphPad Prism

and analyzing by non-linear regression using the log(inhibitor) vs. response (variable slope) equation. Results presented represent the averages of IC_{50} values obtained from at least four replicates in each assay.

Evaluation of compounds for inhibition in the GroEL/ES-mediated dRho refolding assay

Reagent preparation: For this assay, five primary reagent stocks were prepared: 1) GroEL/ES-dRho binary complex stock; 2) ATP initiation stock; 3) thiocyanate enzymatic assay stock; 4) formaldehyde quench stock; 5) ferric nitrate reporter stock. Denatured rhodanese (dRho) was prepared by 3-fold dilution of rhodanese (Roche product #R1756, diluted to 10 mg/mL with H_2O) with denaturant buffer (12 M Urea, 50 mM Tris-HCl, pH 7.4, and 10 mM DTT). Rhodanese was completely denatured by incubating at room temperature for >45 min. The binary complex solution was prepared by slowly adding the dRho stock to a stirring stock of concentrated GroEL in modified folding buffer (50 mM Tris-HCl, pH 7.4, 50 mM KCl, 10 mM $MgCl_2$, 5 mM $Na_2S_2O_3$, and 1 mM DTT). The solution was centrifuged at 16,000 x g for 5 minutes, and the supernatant was collected and added to a solution of GroES in modified folding buffer to give final protein concentrations of 100 nM GroEL, 120 nM GroES, and 80 nM dRho. The binary complex stock was prepared immediately prior to use. For the ATP initiation stock, ATP solid was diluted into modified folding buffer to a final concentration of 2.0 mM. The thiocyanate enzymatic assay stock was prepared to contain 70 mM KH_2PO_4, 80 mM KCN, and 80 mM $Na_2S_2O_3$ in water. The formaldehyde quench solution contained 30% formaldehyde in water. The ferric nitrate reporter stock contained 8.5% w/v $Fe(NO_3)_3$ and 11.3% v/v HNO_3 in water.

Assay Protocol: First, 10 μL aliquots of the GroEL/ES-dRho complex stock were dispensed into clear, flat-bottom 384-well polystyrene plates. Next, 0.5 μL of the compound stocks (10 mM to 4.6 μM, 3-fold dilutions in DMSO) were added by pin-transfer. The chaperonin-mediated refolding cycle was initiated by addition of 10 μL of ATP stock (reagent concentrations during refolding cycle: 50 nM GroEL, 60 nM GroES, 40 nM dRho, 1 mM ATP, and compounds of 250 μM to 114 nM, 3-fold dilution series). After incubating for 40 minutes at 37°C for the refolding cycle, 30 μL of the thiocyanate enzymatic assay stock was added and incubated for 60 min at room temperature for the refolded rhodanese enzymatic reporter reaction. The reporter reaction was quenched by adding 10 μL of the formaldehyde quench stock, and then 40 μL of the ferric nitrate reporter stock was added to quantify the amount of thiocyanate produced during the enzymatic reporter reaction, which is proportional to the amount of dRho refolded by GroEL/ES. After incubating at room temperature for 15 min, the absorbance by $Fe(SCN)_3$ was measured at 460 nm using a Molecular Devices SpectraMax Plus384 microplate reader. A second set of baseline control plates were prepared analogously, but without GroEL/ES-dRho protein binary solution, to correct for possible interference from compound absorbance or turbidity. IC_{50} values for the test compounds were obtained by plotting the A_{460} results in GraphPad Prism and analyzing by non-linear regression using the log(inhibitor) vs. response (variable slope) equation. Results presented represent the averages of IC_{50} values obtained from at least four replicates.

Counter-screening compounds for inhibition of native rhodanese enzymatic activity

Reagent Preparations & Assay Protocol: Reagents were identical to those used in the GroEL/ES-dRho refolding assay described above; however, the assay protocol differed in the sequence of compound addition to the wells. Compounds were pin-

transferred after 50 minute incubation for the refolding cycle, but prior to the addition of the thiocyanate enzymatic assay stock. Thus, the refolding reactions were allowed to proceed for 50 min at 37°C in the absence of test compounds, but the enzymatic activity of the refolded rhodanese reporter enzyme was monitored in the presence of test compounds (inhibitor concentration range during the enzymatic reporter reaction is 100 µM to 46 nM – 3-fold dilutions). IC_{50} values for the rhodanese reporter enzyme were determined as described above. Results presented represent the averages of IC_{50} values obtained from at least four replicates.

Evaluation of compounds for inhibition in the GroEL-mediated ATPase assay

Reagent preparation: For this assay, four primary reagent solutions were prepared: 1) GroEL protein solution; 2) ATP initiation solution; 3) EDTA quench solution; 4) malachite green reporter solution. The GroEL protein solution consisted of 100 nM of GroEL in folding buffer (50 mM Tris-HCl, pH 7.4, 50 mM KCl, 10 mM $MgCl_2$, and 1 mM DTT), which was prepared immediately prior to dispensing into the assay plates. For the ATP initiation solution, ATP solid was diluted into folding buffer to a final concentration of 2 mM. Quench solution contained 300 mM EDTA (pH 8.0). The malachite green reporter solution contained 0.034% w/v malachite green, 1.04% w/v ammonium molybdate, 1% Tween-20, and 1 M HCl dissolved in H_2O.

Assay Protocol: First, 10 µL aliquots of the GroEL protein solution were dispensed into clear, flat-bottom 384-well polystyrene plates. Next, 0.5 µL of the compound stocks (10 mM to 4.6 µM, 3-fold dilutions in DMSO) were added by pin-transfer. GroEL-mediated ATPase activity was initiated by addition of 10 µL of ATP solution (compound concentrations during the assay ranged from 250 µM to 114 nM). After incubating for 45 minutes at 37°C, 10 µL of the EDTA quench solution was added

to quench the reaction cycle. Then, 60 µL of the malachite green reporter solution was added and the plates were incubated at room temperature for 10 min. The absorbance of the malachite green-phosphate complex was measured at 600 nm using a Molecular Devices SpectraMax Plus384 microplate reader. A second set of baseline control plates were prepared analogously, but without GroEL protein solution, to correct for possible interference from compound absorbance or turbidity. IC_{50} values for the test compounds were obtained by plotting the A_{600} results in GraphPad Prism and analyzing by non-linear regression using the log(inhibitor) vs. response (variable slope) equation. Results presented represent the averages of IC_{50} values obtained from at least four replicates.

Evaluation of compounds for inhibition of bacterial cell proliferation

Bacterial Strains: NEB 5-alpha *Escherichia coli* (a derivative of DH5α *E. coli*, New England Biolabs #C2987H); *Enterococcus faecium* - (Orla-Jensen) Schleifer and Kilpper-Balz strain NCTC 7171 (ATCC #19434); *Staphylococcus aureus* - Rosenbranch strain Seattle 1945 (ATCC #25923); *Klebsiella pneumoniae* - (Schroeter) Trevisan strain NCTC 9633 (ATCC #13883); *Acinetobacter baumannii* - Bouvet and Grimont strain 2208 (ATCC 19606); *Pseudomonas aeruginosa* - (Schroeter) Migula strain NCTC 10332 (ATCC #10145); *Enterobacter cloacae* - *E. cloacae*, subsp. cloacae (Jordan) Hormaeche and Edwards strain CDC 442-68 (ATCC #13047).

Growth Media: *E. coli* were grown with LB medium and all *ESKAPE* bacteria were grown in Brain Heart Infusion (BHI) medium (Becton, Dickinson and Company), with all liquid cultures supplemented with 25 mg/L Ca^{2+} and 12.5 mg/L Mg^{2+} to mimic physiological free concentrations of these cations.[32] A 10 mg/mL Ca^{2+} stock solution was prepared by dissolving 1.84 g of $CaCl_2 \cdot 2H_2O$ in 50 mL of deionized water, and a 10

mg/mL Mg^{2+} stock solution was prepared by dissolving 4.18 g of $MgCl_2 \cdot 6H_2O$ in 50 mL deionized water – filter sterilized using 0.2 µm cellulose-acetate filters. 2.5 mL of the sterile 10 mg/mL Ca^{2+} stock and 1.25 mL of the sterile 10 mg/mL Mg^{2+} stock solutions were added per 1 L of autoclaved LB or BHI media to obtain 25 mg/L Ca^{2+} and 12.5 mg/L Mg^{2+} ions, respectively.

General Assay Protocol: Stock bacterial cultures were streaked onto LB or BHI agar plates and grown overnight at 37°C. Fresh aliquots of cation supplemented media were inoculated with single bacterial colonies and the cultures were grown overnight at 37°C with shaking (240 rpm). The following morning, cultures were diluted 10-fold into fresh media and grown at 37°C until bacteria had reached mid-log phase growth (OD_{600} ~ 0.4-0.6). The cultures were then diluted into fresh media to achieve final OD_{600} readings of 0.017. Aliquots of these diluted cultures (30 µL) were added to clear, flat-bottom 384-well polystyrene plates that were previously stamped with 0.5 µL of test compounds in 20 µL of media (yielding initial OD_{600} = 0.01 bacterial cultures). All compounds were tested in dose-response with concentration ranges during the proliferation assays from 100 µM to 46 nM (3-fold dilution series). A second set of baseline control plates were prepared analogously, but without any bacteria added, to correct for possible compound absorbance and/or precipitation. Plates were sealed with "Breathe Easy" oxygen permeable membranes (Diversified Biotech) and left to incubate at 37°C without shaking (stagnant assay) until the bacteria had reached mid-log phase growth. Plates were then read at 600 nm using a Molecular Devices SpectraMax Plus384 microplate reader. EC_{50} values for the test compounds were obtained by plotting the OD_{600} results in GraphPad Prism and analyzing by non-linear regression

using the log(inhibitor) vs. response (variable slope) equation. Results presented represent the averages of EC_{50} values obtained from at least four replicates.

Evaluating compounds for effects on the viability of healthy human colon (FHC) and small intestine (FHs 74 Int) cells

Evaluation of compound cytotoxicities to FHC colon and FHs 74 Int small intestine cells were performed using Alamar Blue-based viability assays. FHC cells were maintained in Hyclone DMEM:F12 1:1 medium containing L-glutamine and supplemented with 10 mM HEPES, 10 ng/mL cholera toxin, 0.005 mg/mL insulin, 0.005 mg/mL transferrin, 100 ng/mL hydrocortisone, and 10% FBS (Midwest Scientific, USDAFBS). FHs 74 Int cells were maintained in Hybri-care medium (ATCC 46-X) supplemented with 30 ng/mL recombinant epidermal growth factor (EGF) and 10% FBS (Midwest Scientific, USDAFBS). All assays were carried out in 384-well plates (BRAND cell culture grade plates, 781980). Cells at 90% confluence were harvested and diluted in growth medium, then 45 µL of the FHC cells (1,500 cells/well) or FHs 74 Int cells (1,500 cells/well) were dispensed per well. Plates were sealed with "Breathe Easy" oxygen permeable membranes (Diversified Biotech) and incubated at 37°C, 5% CO_2, for 24 h. The following day, 1 µL of the compound stocks (10 mM to 4.6 µM, 3-fold dilutions in DMSO) were pre-diluted by pin-transfer into 25 µL of the respective growth media, then 15 µL aliquots of these solutions were added to the cell assay plates to give inhibitor concentration ranges of 100 µM to 46 nM during the assay (final DMSO concentration of 1% was maintained during the assay). Plates were sealed with "Breathe Easy" oxygen permeable membranes and incubated for an additional 48 h at 37°C and 5% CO_2. The Alamar Blue reporter reagents were then added to a final concentration of 10%, and the plates incubated at 37°C and 5% CO_2 while the reporter

reagents developed. Sample fluorescence (535 nm excitation, 590 nm emission) was read over time using a Molecular Devices FlexStation II 384-well plate reader (readings taken between 4-24 h of incubation so as to achieve signals in the 30-60% range for conversion of resazurin to resorufin). Cell viability was calculated as per vendor instructions (Thermo Fisher - Alamar Blue cell viability assay manual). Cytotoxicity CC_{50} values for the test compounds were obtained by plotting the % resazurin reduction results in GraphPad Prism and analyzing by non-linear regression using the log(inhibitor) vs. response (variable slope) equation. Results presented represent the averages of CC_{50} values obtained from at least four replicates for each of the FHC and FHs 74 Int cell lines.

Evaluation of *E. coli* resistance generation against lead inhibitors

To identify potential resistance toward **17**, nifuroxazide, and nitrofurantoin, a liquid culture, 12-day serial passage assay was employed (each compound was tested in duplicate). NEB 5-alpha *E. coli* bacteria were streaked onto an LB agar plate and grown overnight at 37°C. Two fresh aliquots of LB media (supplemented with 25 mg/L Ca^{2+} and 12.5 mg/L Mg^{2+}) were inoculated with separate bacterial colonies and the cultures were grown overnight at 37°C, with shaking (240 rpm). The overnight cultures were then sub-cultured (10x dilution) into fresh media solutions and grown at 37°C to mid-log phase, then diluted into fresh media to achieve two separate cultures with final OD_{600} readings of 0.01. Aliquots of the diluted cultures (200 µL) were dispensed into a clear, 96-well polystyrene plate (one culture was used for replicate 1 for each compound, and the other culture was used for replicate 2 for each compound), followed by the addition of 2 µL of nifuroxazide, nitrofurantoin, and compound **17** in DMSO. Test compounds were evaluated in duplicate with concentration ranges during the resistance assay from 100 µM to 48.8 nM, 2-fold dilution series. Plates were sealed with "Breathe

Easy" oxygen permeable membranes (Diversified Biotech) and left to incubate at 37°C without shaking (stagnant assay). OD_{600} readings were taken at the 24 h time point to monitor for bacterial growth. A second baseline control plate was prepared analogously, without any bacteria added, to correct for possible compound absorbance and/or precipitation. For inoculations on subsequent days, bacteria from the wells with the highest test compound concentration where the OD_{600} was >0.2, were sub-cultured in 5 mL of fresh media at 37°C until mid-log phase growth was reached. Separate cultures were maintained from this point forward for each of the compound replicates – i.e. 6 cultures continually propagated. The bacteria were then diluted into fresh media to OD_{600} of 0.01 and the bacteria were propagated again as described above. This procedure was repeated each day, for a total of 12 days, to observe changes in inhibitor EC_{50} values over each passage (aliquots of each of these daily cultures were flash frozen in liquid nitrogen and stored at -80°C for future use). Inhibitor EC_{50} values were obtained by plotting the OD_{600} results from each passage in GraphPad Prism and analyzing by non-linear regression using the log(inhibitor) vs. response (variable slope) equation.

Control compounds, calculation of IC_{50} / EC_{50} / CC_{50} values, and statistical considerations

For all assays, DMSO was used as negative control and a panel of previously discovered and reported chaperonin inhibitors were used as positive controls: e.g. compounds **8**, **9**, and **18** from Johnson *et. al* 2014 and Abdeen *et. al* 2016;[28,33] suramin and compound **2h-*p*** from Abdeen *et. al* 2016;[28] compounds **20R**, **20L**, and **28R** from Abdeen *et. al* 2018;[31] and closantel and rafoxanide from Kunkle *et. al* 2018.[32] Bacterial proliferation assays also included antibiotic controls such as vancomycin, daptomycin, and rifampicin. All IC_{50} / EC_{50} / CC_{50} results reported are averages of values determined

from individual dose-response curves in assay replicates as follows: 1) individual $I/E/CC_{50}$ values from assay replicates were first log-transformed and the average $\log(I/E/CC_{50})$ values and standard deviations (SD) calculated; 2) replicate $\log(I/E/CC_{50})$ values were evaluated for outliers using the ROUT method in GraphPad Prism (Q of 10%); and 3) average $I/E/CC_{50}$ values were then back-calculated from the average $\log(I/E/CC_{50})$ values. For compounds where $\log(I/E/CC_{50})$ values were greater than the maximum compound concentrations tested (i.e. >1.75, >1.80, >1.92, >2.00, and >2.40 – or >56, >63, >83, >100, and >250 µM, respectively), results were represented as 0.1 log units higher than the maximum concentrations tested (i.e. 1.85, 1.90, 2.02, 2.10, and 2.50 – or 71, 79, 105, 126, and 316 µM, respectively) so as not to overly bias results because of the unavailability of definitive values for inactive compounds.

APPENDIX - SUPPLEMENTAL TABLES

Table 2A - Bacterial proliferation EC_{50} (μM) Compilation of EC_{50} results for compounds tested in the various bacterial proliferation assays.

		Bacterial Proliferation EC_{50} (μM)							
		Compound # / Name	*E. faecium*	*S. aureus*	*K. pneumoniae*	*A. baumannii*	*P. aeruginosa*	*E. cloacae*	*E. coli*
Compound Substituents		Nitroxoline	18	9.5	2.8	2.5	99	6.6	4.0
		Nifuroxazide	8.1	16	37	>100	>100	54	0.97
R^1	R^2	Nitrofurantoin	38	27	40	>100	>100	36	0.74
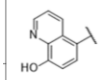		**2**	>100	37	>100	>100	>100	>100	80
		**3**	>100	63	99	74	>100	92	77
	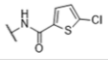	**4**	70	84	>100	>100	>100	>100	>100
		**5**	>100	69	82	56	>100	80	63
		**6**	>100	>100	>100	>100	>100	>100	79
	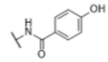	**7**	>100	48	87	71	>100	97	46
	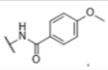	**1**	>100	87	85	>100	95	100	>100
	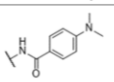	**8**	>100	99	>100	>100	>100	>100	93
		**9**	>100	56	>100	>100	>100	>100	>100
		**10**	>100	>100	>100	>100	81	>100	>100
	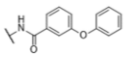	**11**	>100	>100	>100	>100	>100	>100	>100
	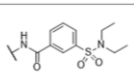	**12**	>100	>100	>100	>100	85	>100	99
	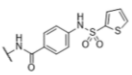	**13**	>100	>100	>100	>100	>100	>100	>100
	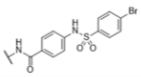	**14**	>100	>100	>100	84	>100	>100	100
	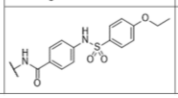	**15**	>100	>100	>100	>100	>100	>100	>100

		Bacterial Proliferation EC_{50} (μM)							
		Compound # / Name	*E. faecium*	*S. aureus*	*K. pneumoniae*	*A. baumannii*	*P. aeruginosa*	*E. cloacae*	*E. coli*
Compound Substituents		Nitroxoline	18	9.5	2.8	2.5	99	6.6	4.0
		Nifuroxazide	8.1	16	37	>100	>100	54	0.97
R^1	R^2	Nitrofurantoin	38	27	40	>100	>100	36	0.74
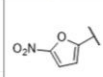	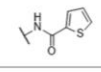	**16**	24	7.1	16	82	>100	40	0.42
	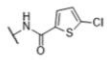	**17**	12	3	19	72	>100	49	0.53
		**18**	31	10	36	>100	>100	>100	2.1
		**19**	13	9.5	42	54	>100	73	2.4
	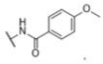	**20**	22	8.1	>100	>100	>100	>100	1.9
	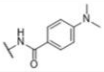	**21**	>100	34	>100	>100	>100	>100	10
	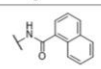	**22**	16	6	>100	>100	>100	>100	41
	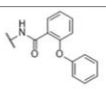	**23**	11	5.2	>100	>100	>100	>100	>100
	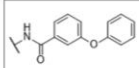	**24**	11	3.5	>100	>100	>100	>100	>100
	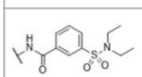	**25**	>100	9.6	>100	>100	>100	>100	>100
	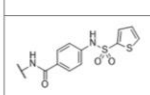	**26**	11	11	>100	>100	>100	>100	17
	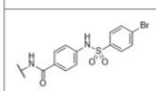	**27**	>100	>100	>100	>100	>100	>100	>100
	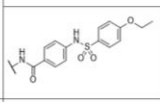	**28**	>100	>100	>100	>100	>100	>100	>100

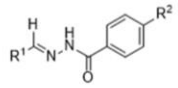		Bacterial Proliferation EC_{50} (μM)							
		Compound # / Name	*E. faecium*	*S. aureus*	*K. pneumoniae*	*A. baumannii*	*P. aeruginosa*	*E. cloacae*	*E. coli*
Compound Substituents		Nitroxoline	18	9.5	2.8	2.5	99	6.6	4.0
		Nifuroxazide	8.1	16	37	>100	>100	54	0.97
R^1	R^2	Nitrofurantoin	38	27	40	>100	>100	36	0.74
	OCH_3	**29**	>100	>100	>100	>100	>100	>100	>100
	H	**30**	>100	88	>100	>100	>100	>100	>100
	OCH_3	**31**	>100	>100	>100	>100	>100	>100	>100
	H	**32**	>100	>100	>100	>100	>100	>100	>100
	OCH_3	**33**	>100	>100	>100	>100	>100	>100	>100
	H	**34**	>100	>100	>100	>100	>100	>100	>100
	OCH_3	**35**	>100	>100	>100	>100	>100	>100	>100
	H	**36**	>100	>100	>100	>100	>100	>100	>100
	OCH_3	**37**	>100	>100	>100	>100	>100	>100	>100
	H	**38**	>100	>100	>100	>100	>100	>100	>100
	OCH_3	**39**	>100	>100	>100	>100	>100	>100	>100
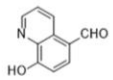		**40**	7.3	19	15	11	>100	24	14
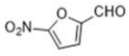		**41**	20	5.8	10	12	>100	13	9.5
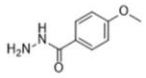		**42**	>100	>100	>100	>100	>100	>100	>100

Table 2B - Bacterial proliferation log(EC_{50}) (μM) Compilation of log(EC_{50}) results and standard deviations for compounds tested in the various bacterial proliferation assays.

		Bacterial Proliferation log(EC_{50}) (μM)							
		Compound # / Name	*E. faecium*	*S. aureus*	*K. pneumoniae*	*A. baumannii*	*P. aeruginosa*	*E. cloacae*	*E. coli*
Compound Substituents		Nitroxoline	1.26 ± 0.05	0.98 ± 0.23	0.45 ± 0.11	0.40 ± 0.11	2.00 ± 0.12	0.82 ± 0.15	0.60 ± 0.24
		Nifuroxazide	0.91 ± 0.08	1.20 ± 0.28	1.57 ± 0.08	>2	>2	1.73 ± 0.19	-0.01 ± 0.13
R^1	R^2	Nitrofurantoin	1.58 ± 0.05	1.43 ± 0.18	1.60 ± 0.15	>2	>2	1.56 ± 0.12	-0.13 ± 0.12
		**2**	>2	1.57 ± 0.18	>2	>2	>2	>2	1.90 ± 0.14
		**3**	>2	1.80 ± 0.20	2.00 ± 0.11	1.87 ± 0.15	>2	1.96 ± 0.09	1.89 ± 0.17
		**4**	1.85 ± 0.08	1.92 ± 0.24	>2	>2	>2	>2	>2
		**5**	>2	1.84 ± 0.16	1.91 ± 0.08	1.75 ± 0.13	>2	1.90 ± 0.10	1.80 ± 0.17
		**6**	>2	>2	>2	>2	>2	>2	1.90 ± 0.07
		**7**	>2	1.68 ± 0.21	1.94 ± 0.10	1.85 ± 0.11	>2	1.99 ± 0.01	1.66 ± 0.08
		**1**	>2	1.94 ± 0.13	1.93 ± 0.08	>2	1.98 ± 0.16	2.00 ± 0.09	>2
		**8**	>2	2.00 ± 0.11	>2	>2	>2	>2	1.97 ± 0.13
		**9**	>2	1.75 ± 0.45	>2	>2	>2	>2	>2
		**10**	>2	>2	>2	>2	1.91 ± 0.16	>2	>2
	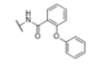	**11**	>2	>2	>2	>2	>2	>2	>2
	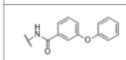	**12**	>2	>2	>2	>2	1.93 ± 0.17	>2	2.00 ± 0.12
	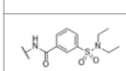	**13**	>2	>2	>2	>2	>2	>2	>2
	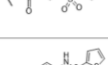	**14**	>2	>2	>2	1.92 ± 0.17	>2	>2	2.00 ± 0.08
	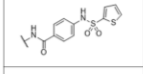	**15**	>2	>2	>2	>2	>2	>2	>2

		Bacterial Proliferation log(EC_{50}) (μM)							
		Compound # / Name	*E. faecium*	*S. aureus*	*K. pneumoniae*	*A. baumannii*	*P. aeruginosa*	*E. cloacae*	*E. coli*
Compound Substituents		Nitroxoline	1.26 ± 0.05	0.98 ± 0.23	0.45 ± 0.11	0.40 ± 0.11	2.00 ± 0.12	0.82 ± 0.15	0.60 ± 0.24
		Nifuroxazide	0.91 ± 0.08	1.20 ± 0.28	1.57 ± 0.08	>2	>2	1.73 ± 0.19	-0.01 ± 0.13
R^1	R^2	Nitrofurantoin	1.58 ± 0.05	1.43 ± 0.18	1.60 ± 0.15	>2	>2	1.56 ± 0.12	-0.13 ± 0.12
		16	1.38 ± 0.11	0.85 ± 0.29	1.20 ± 0.18	1.91 ± 0.22	>2	1.60 ± 0.21	-0.38± 0.12
		17	1.08 ± 0.10	0.48 ± 0.09	1.28 ± 0.19	1.86 ± 0.07	>2	1.69 ± 0.05	-0.28 ± 0.06
		18	1.49 ± 0.29	1.00 ± 0.08	1.56 ± 0.19	>2	>2	>2	0.32 ± 0.20
		19	1.11 ± 0.20	0.98 ± 0.27	1.62 ± 0.09	1.73 ± 0.16	>2	1.86 ± 0.13	0.38 ± 0.06
		20	1.34 ± 0.04	0.91 ± 0.22	>2	>2	>2	>2	0.28 ± 0.07
		21	>2	1.53 ± 0.37	>2	>2	>2	>2	1.00 ± 0.20
		22	1.20 ± 0.16	0.78 ± 0.14	>2	>2	>2	>2	1.61 ± 0.28
		23	1.04 ± 0.18	0.72 ± 0.27	>2	>2	>2	>2	>2
		24	1.04 ± 0.14	0.54 ± 0.22	>2	>2	>2	>2	>2
		25	>2	0.98 ± 0.29	>2	>2	>2	>2	>2
		26	1.04 ± 0.05	1.04 ± 0.18	>2	>2	>2	>2	1.23 ± 0.08
		27	>2	>2	>2	>2	>2	>2	>2
		28	>2	>2	>2	>2	>2	>2	>2

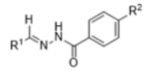		Bacterial Proliferation log(EC_{50})(μM)						
	Compound # / Name	*E. faecium*	*S. aureus*	*K. pneumoniae*	*A. baumannii*	*P. aeruginosa*	*E. cloacae*	*E. coli*
Compound Substituents	Nitroxoline	1.26 ± 0.05	0.98 ± 0.23	0.45 ± 0.11	0.40 ± 0.11	2.00 ± 0.12	0.82 ± 0.15	0.60 ± 0.24
	Nifuroxazide	0.91 ± 0.08	1.20 ± 0.28	1.57 ± 0.08	>2	>2	1.73 ± 0.19	-0.01 ± 0.13
R^1 / R^2	Nitrofurantoin	1.58 ± 0.05	1.43 ± 0.18	1.60 ± 0.15	>2	>2	1.56 ± 0.12	-0.13 ± 0.12
 / OCH_3	29	>2	>2	>2	>2	>2	>2	>2
/ H	30	>2	1.94 ± 0.16	>2	>2	>2	>2	>2
 / OCH_3	31	>2	>2	>2	>2	>2	>2	>2
/ H	32	>2	>2	>2	>2	>2	>2	>2
 / OCH_3	33	>2	>2	>2	>2	>2	>2	>2
/ H	34	>2	>2	>2	>2	>2	>2	>2
 / OCH_3	35	>2	>2	>2	>2	>2	>2	>2
/ H	36	>2	>2	>2	>2	>2	>2	>2
 / OCH_3	37	>2	>2	>2	>2	>2	>2	>2
/ H	38	>2	>2	>2	>2	>2	>2	>2
 / OCH_3	39	>2	>2	>2	>2	>2	>2	>2
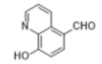	40	0.86 ± 0.08	1.28 ± 0.31	1.18 ± 0.03	1.04 ± 0.14	>2	1.38 ± 0.13	1.15 ± 0.24
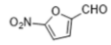	41	1.30 ± 0.24	0.76 ± 0.20	1.00 ± 0.15	1.08 ± 0.02	>2	1.11 ± 0.20	0.98 ± 0.17
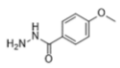	42	>2	>2	>2	>2	>2	>2	>2

Table 3A - Biochemical assay IC_{50} (μM) Compilation of IC_{50} results for compounds tested in the GroEL/ES-mediated dMDH and dRho refolding assays, native MDH and Rho reporter counter-screens, and GroEL-mediated ATPase assay.

		Biochemical Assay IC_{50} (μM)					
		Compound # / Name	GroEL ATPase	Native Rho	Native MDH	GroEL/ES-dRho Refolding	GroEL/ES-dMDH Refolding
Compound Substituents		Nitroxoline	>250	2.2	>63	5.9	50
		Nifuroxazide	>250	63	>63	99	>100
R^1	R^2	Nitrofurantoin	>250	>100	>63	>250	>100
		**2**	>250	>100	>63	76	>100
		**3**	>250	100	>63	15	65
		**4**	>250	14	>63	1.4	9.6
		**5**	>250	83	>63	52	>100
		**6**	>250	>100	>63	2.3	>100
	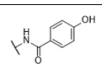	**7**	>250	83	>63	7.6	49
	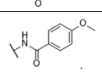	**1**	>250	96	>63	31	77
	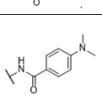	**8**	>250	72	>63	5	27
		**9**	>250	97	>63	1.9	13
		**10**	>250	88	>63	3.3	15
	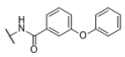	**11**	>250	80	>63	5.2	13
	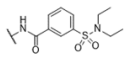	**12**	>250	96	>63	6.3	19
	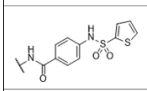	**13**	>250	>100	>63	0.7	3.2
	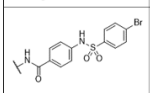	**14**	>250	>100	>63	1.7	12
	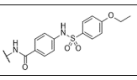	**15**	>250	>100	>63	1.4	6

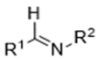		Biochemical Assay IC_{50} (μM)					
		Compound # / Name	GroEL ATPase	Native Rho	Native MDH	GroEL/ES-dRho Refolding	GroEL/ES-dMDH Refolding
Compound Substituents		Nitroxoline	>250	2.2	>63	5.9	50
		Nifuroxazide	>250	63	>63	99	>100
R^1	R^2	Nitrofurantoin	>250	>100	>63	>250	>100
		**16**	>250	>100	>63	222	>100
	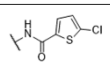	**17**	>250	56	>63	60	90
		**18**	>250	84	>63	100	>100
		**19**	>250	38	>63	64	>100
	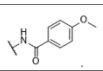	**20**	>250	>100	>63	89	69
	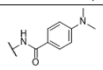	**21**	>250	>100	>63	26	20
		**22**	>250	45	>63	73	58
	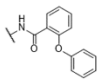	**23**	>250	43	>63	83	78
	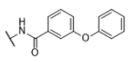	**24**	>250	65	>63	50	62
	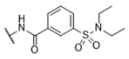	**25**	>250	>100	>63	100	>100
	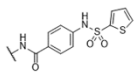	**26**	>250	40	>63	62	>100
	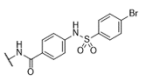	**27**	>250	41	>63	50	36
	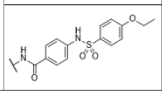	**28**	>250	45	>63	66	36

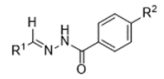		Biochemical Assay IC_{50} (μM)					
		Compound # / Name	GroEL ATPase	Native Rho	Native MDH	GroEL/ES-dRho Refolding	GroEL/ES-dMDH Refolding
Compound Substituents		Nitroxoline	>250	2.2	>63	5.9	50
		Nifuroxazide	>250	63	>63	99	>100
R^1	R^2	Nitrofurantoin	>250	>100	>63	>250	>100
	OCH_3	29	>250	82	>63	116	>100
	H	30	>250	>100	>63	209	>100
	OCH_3	31	>250	>100	>63	>250	>100
	H	32	>250	>100	>63	>250	>100
	OCH_3	33	>250	>100	>63	120	>100
	H	34	>250	>100	>63	183	>100
	OCH_3	35	>250	>100	>63	>250	>100
	H	36	>250	>100	>63	>250	>100
	OCH_3	37	>250	>100	>63	>250	>100
	H	38	>250	>100	>63	>250	>100
	OCH_3	39	>250	>100	>63	>250	>100
		40	>250	18	>63	20	>100
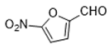		41	>250	30	>63	28	78
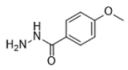		42	>250	>100	>63	>250	>100

Table 3B - Biochemical assay log(IC_{50}) (μM) Compilation of log(IC_{50}) results and standard deviations for compounds tested in the GroEL/ES-mediated dMDH and dRho refolding assays, native MDH and Rho reporter counter-screens, and GroEL-mediated ATPase assay.

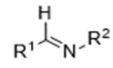		Biochemical Assay log(IC_{50}) (μM)					
		Compound # / Name	GroEL ATPase	Native Rho	Native MDH	GroEL/ES-dRho Refolding	GroEL/ES-dMDH Refolding
Compound Substituents		Nitroxoline	>2.40	0.34 ± 0.21	>1.80	0.77 ± 0.20	1.70 ± 0.39
		Nifuroxazide	>2.40	1.80 ± 0.20	>1.80	2.00 ± 0.11	>2
R^1	R^2	Nitrofurantoin	>2.40	>2	>1.80	>2.40	>2
		2	>2.40	>2	>1.80	1.88 ± 0.08	>2
		3	>2.40	2.00 ± 0.06	>1.80	1.18 ± 0.76	1.81 ± 0.20
		4	>2.40	1.15 ± 0.12	>1.80	0.15 ± 0.38	0.98 ± 0.48
		5	>2.40	1.92 ± 0.23	>1.80	1.72 ± 0.63	>2
		6	>2.40	>2	>1.80	0.36 ± 0.15	>2
		7	>2.40	1.92 ± 0.06	>1.80	0.88 ± 0.07	1.69 ± 0.13
		1	>2.40	1.98 ± 0.09	>1.80	1.49 ± 0.58	1.89 ± 0.15
		8	>2.40	1.86 ± 0.08	>1.80	0.70 ± 0.69	1.43 ± 0.21
		9	>2.40	1.99 ± 0.10	>1.80	0.28 ± 0.59	1.11 ± 0.57
		10	>2.40	1.94 ± 0.15	>1.80	0.52 ± 0.57	1.18 ± 0.25
	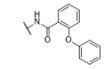	11	>2.40	1.90 ± 0.14	>1.80	0.72 ± 0.62	1.11 ± 0.26
	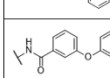	12	>2.40	1.98 ± 0.11	>1.80	0.80 ± 0.73	1.28 ± 0.14
	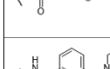	13	>2.40	>2	>1.80	-0.15 ± 0.40	0.51 ± 0.34
	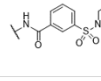	14	>2.40	>2	>1.80	0.23 ± 0.52	1.08 ± 0.47
	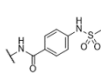	15	>2.40	>2	>1.80	0.15 ± 0.51	0.78 ± 0.43

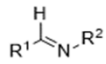		Biochemical Assay log(IC_{50}) (μM)					
		Compound # / Name	GroEL ATPase	Native Rho	Native MDH	GroEL/ES-dRho Refolding	GroEL/ES-dMDH Refolding
Compound Substituents		Nitroxoline	>2.40	0.34 ± 0.21	>1.80	0.77 ± 0.20	1.70 ± 0.39
		Nifuroxazide	>2.40	1.80 ± 0.20	>1.80	2.00 ± 0.11	>2
R^1	R^2	Nitrofurantoin	>2.40	>2	>1.80	>2.40	>2
		**16**	>2.40	>2	>1.80	2.35 ± 0.14	>2
		**17**	>2.40	1.75 ± 0.16	>1.80	1.78 ± 0.15	1.95 ± 0.12
		**18**	>2.40	1.92 ± 0.28	>1.80	2.00 ± 0.15	>2
		**19**	>2.40	1.58 ± 0.16	>1.80	1.81 ± 0.19	>2
		**20**	>2.40	>2	>1.80	1.95 ± 0.06	1.84 ± 0.04
		**21**	>2.40	>2	>1.80	1.41 ± 0.11	1.30 ± 0.12
		**22**	>2.40	1.65 ± 0.10	>1.80	1.86 ± 0.11	1.76 ± 0.15
		**23**	>2.40	1.63 ± 0.11	>1.80	1.92 ± 0.12	1.89 ± 0.12
	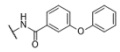	**24**	>2.40	1.81 ± 0.28	>1.80	1.70 ± 0.13	1.79 ± 0.12
	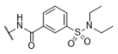	**25**	>2.40	>2	>1.80	2.00 ± 0.17	>2
	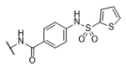	**26**	>2.40	1.60 ± 0.03	>1.80	1.79 ± 0.07	>2
	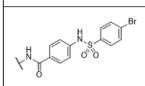	**27**	>2.40	1.61 ± 0.15	>1.80	1.70 ± 0.14	1.56 ± 0.16
	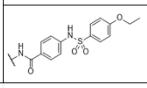	**28**	>2.40	1.65 ± 0.22	>1.80	1.82 ± 0.19	1.56 ± 0.13

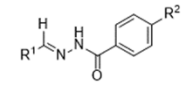		Biochemical Assay log(IC_{50}) (μM)					
		Compound # / Name	GroEL ATPase	Native Rho	Native MDH	GroEL/ES-dRho Refolding	GroEL/ES-dMDH Refolding
Compound Substituents		Nitroxoline	>2.40	0.34 ± 0.21	>1.80	0.77 ± 0.20	1.70 ± 0.39
		Nifuroxazide	>2.40	1.80 ± 0.20	>1.80	2.00 ± 0.11	>2
R^1	R^2	Nitrofurantoin	>2.40	>2	>1.80	>2.40	>2
	OCH_3	29	>2.40	1.91 ± 0.14	>1.80	2.06 ± 0.11	>2
	H	30	>2.40	>2	>1.80	2.32 ± 0.19	>2
	OCH_3	31	>2.40	>2	>1.80	>2.40	>2
	H	32	>2.40	>2	>1.80	>2.40	>2
	OCH_3	33	>2.40	>2	>1.80	2.08 ± 0.14	>2
	H	34	>2.40	>2	>1.80	2.26 ± 0.11	>2
	OCH_3	35	>2.40	>2	>1.80	>2.40	>2
	H	36	>2.40	>2	>1.80	>2.40	>2
	OCH_3	37	>2.40	>2	>1.80	>2.40	>2
	H	38	>2.40	>2	>1.80	>2.40	>2
	OCH_3	39	>2.40	>2	>1.80	>2.40	>2
		40	>2.40	1.26 ± 0.23	>1.80	1.30 ± 0.36	>2
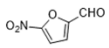		41	>2.40	1.48 ± 0.07	>1.80	1.45 ± 0.04	1.89 ± 0.13
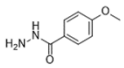		42	>2.40	>2	>1.80	>2.40	>2

Table 4A - Biochemical assay IC_{50} (μM) with and without nitroreductase Compilation of IC_{50} results for compounds tested in the GroEL/ES-mediated dMDH assay and native MDH counter-screen, in the presence and absence of *E. coli* NfsB nitroreductase (NR).

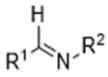		Biochemical Assay IC_{50} (μM)				
		Compound # / Name	Native MDH	Native MDH w/ NR	GroEL/ES-dMDH Refolding	GroEL/ES-dMDH Refolding w/ NR
Compound Substituents		Nitroxoline	>63	>56	50	26
		Nifuroxazide	>63	>56	>100	26
R^1	R^2	Nitrofurantoin	>63	>56	>100	86
		**2**	>63	>56	>100	>83
		**3**	>63	>56	65	29
	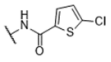	**4**	>63	>56	9.6	4
		**5**	>63	>56	>100	>83
		**6**	>63	>56	>100	>83
	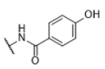	**7**	>63	>56	49	23
	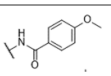	**1**	>63	>56	77	66
	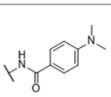	**8**	>63	>56	27	25
	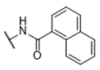	**9**	>63	>56	13	7.7
	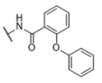	**10**	>63	>56	15	15
	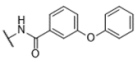	**11**	>63	>56	13	21
	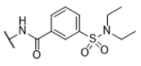	**12**	>63	>56	19	21
	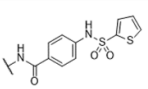	**13**	>63	>56	3.2	1.9
	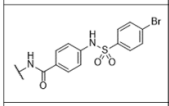	**14**	>63	>56	12	3.6
	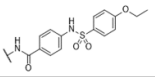	**15**	>63	>56	6	3.1

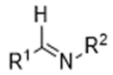		Biochemical Assay IC_{50} (μM)				
		Compound # / Name	**Native MDH**	**Native MDH w/ NR**	**GroEL/ES-dMDH Refolding**	**GroEL/ES-dMDH Refolding w/ NR**
Compound Substituents		**Nitroxoline**	>63	>56	50	26
		Nifuroxazide	>63	>56	>100	26
R^1	**R^2**	**Nitrofurantoin**	>63	>56	>100	86
		**16**	>63	>56	>100	8.6
	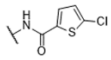	**17**	>63	>56	90	3.5
		**18**	>63	>56	>100	12
		**19**	>63	>56	>100	27
	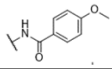	**20**	>63	>56	69	10
	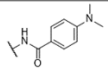	**21**	>63	>56	20	10
	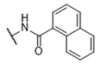	**22**	>63	>56	58	5.4
	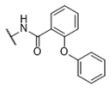	**23**	>63	>56	78	8.5
	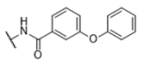	**24**	>63	>56	62	2.6
	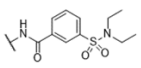	**25**	>63	>56	>100	5.7
	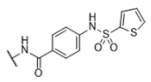	**26**	>63	>56	>100	6
	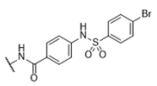	**27**	>63	>56	36	2
	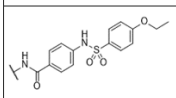	**28**	>63	>56	36	3.9

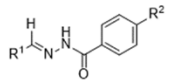		Biochemical Assay IC_{50} (μM)				
		Compound # / Name	Native MDH	Native MDH w/ NR	GroEL/ES-dMDH Refolding	GroEL/ES-dMDH Refolding w/ NR
Compound Substituents		Nitroxoline	>63	>56	50	26
		Nifuroxazide	>63	>56	>100	26
R^1	R^2	Nitrofurantoin	>63	>56	>100	>83
	OCH_3	29	>63	>56	>100	>83
	H	30	>63	>56	>100	>83
	OCH_3	31	>63	>56	>100	>83
	H	32	>63	>56	>100	>83
	OCH_3	33	>63	>56	>100	>83
	H	34	>63	>56	>100	>83
	OCH_3	35	>63	>56	>100	>83
	H	36	>63	>56	>100	>83
	OCH_3	37	>63	>56	>100	>83
	H	38	>63	>56	>100	>83
	OCH_3	39	>63	>56	>100	>83
		40	>63	>56	>100	>83
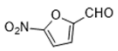		41	>63	>56	78	>83
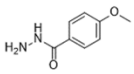		42	>63	>56	>100	>83

Table 4B - Biochemical assay log(IC_{50}) (μM) with and without nitroreductase Compilation of log(IC_{50}) results and standard deviations for compounds tested in the GroEL/ES-mediated dMDH assay and native MDH counter-screen, in the presence and absence of *E. coli* NfsB nitroreductase (NR).

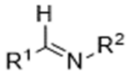		Biochemical Assay log(IC_{50}) (μM)				
		Compound # / Name	Native MDH	Native MDH w/ NR	GroEL/ES-dMDH Refolding	GroEL/ES-dMDH Refolding w/ NR
Compound Substituents		Nitroxoline	>1.80	>1.75	1.70 ± 0.39	1.41 ± 0.71
		Nifuroxazide	>1.80	>1.75	>2	1.42 ± 0.48
R^1	R^2	Nitrofurantoin	>1.80	>1.75	>2	>1.92
		**2**	>1.80	>1.75	>2	>1.92
		**3**	>1.80	>1.75	1.81 ± 0.20	1.46 ± 0.19
	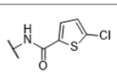	**4**	>1.80	>1.75	0.98 ± 0.48	0.60 ± 0.22
		**5**	>1.80	>1.75	>2	>1.92
		**6**	>1.80	>1.75	>2	>1.92
	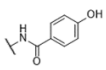	**7**	>1.80	>1.75	1.69 ± 0.13	1.36 ± 0.31
	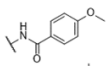	**1**	>1.80	>1.75	1.89 ± 0.15	1.82 ± 0.13
	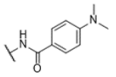	**8**	>1.80	>1.75	1.43 ± 0.21	1.40 ± 0.39
	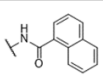	**9**	>1.80	>1.75	1.11 ± 0.57	0.89 ± 0.24
	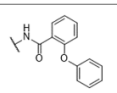	**10**	>1.80	>1.75	1.18 ± 0.25	1.18 ± 0.32
	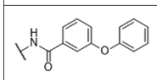	**11**	>1.80	>1.75	1.11 ± 0.26	1.32 ± 0.25
	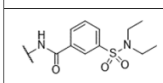	**12**	>1.80	>1.75	1.28 ± 0.14	1.32 ± 0.25
	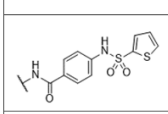	**13**	>1.80	>1.75	0.51 ± 0.34	0.28 ± 0.20
	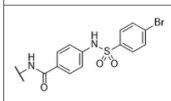	**14**	>1.80	>1.75	0.78 ± 0.47	0.56 ± 0.21
	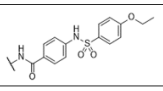	**15**	>1.80	>1.75	0.78 ± 0.43	0.49 ± 0.32

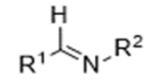		Biochemical Assay log(IC_{50}) (μM)				
		Compound # / Name	**Native MDH**	**Native MDH w/ NR**	**GroEL/ES-dMDH Refolding**	**GroEL/ES-dMDH Refolding w/ NR**
Compound Substituents		**Nitroxoline**	>1.80	>1.75	1.70 ± 0.39	1.41 ± 0.71
		Nifuroxazide	>1.80	>1.75	>2	1.42 ± 0.48
R^1	**R^2**	**Nitrofurantoin**	>1.80	>1.75	>2	>1.92
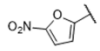		**16**	>1.80	>1.75	>2	0.93 ± 0.07
	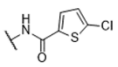	**17**	>1.80	>1.75	1.95 ± 0.12	0.54 ± 0.08
		**18**	>1.80	>1.75	>2	1.08 ± 0.10
		**19**	>1.80	>1.75	>2	1.43 ± 0.09
	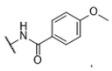	**20**	>1.80	>1.75	1.84 ± 0.04	1.00 ± 0.18
	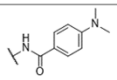	**21**	>1.80	>1.75	1.30 ± 0.12	1.00 ± 0.19
	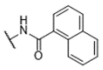	**22**	>1.80	>1.75	1.76 ± 0.15	0.73 ± 0.09
	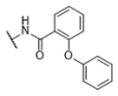	**23**	>1.80	>1.75	1.89 ± 0.12	0.93 ± 0.15
	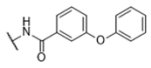	**24**	>1.80	>1.75	1.79 ± 0.12	0.41 ± 0.08
	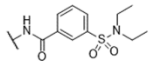	**25**	>1.80	>1.75	>2	0.76 ± 0.10
	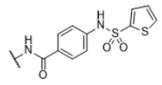	**26**	>1.80	>1.75	>2	0.78 ± 0.13
	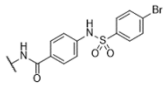	**27**	>1.80	>1.75	1.56 ± 0.16	0.30 ± 0.11
	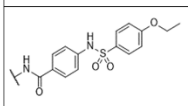	**28**	>1.80	>1.75	1.56 ± 0.13	0.59 ± 0.25

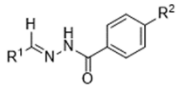		Biochemical Assay log(IC_{50}) (μM)				
		Compound # / Name	Native MDH	Native MDH w/ NR	GroEL/ES-dMDH Refolding	GroEL/ES-dMDH Refolding w/ NR
Compound Substituents		Nitroxoline	>1.80	>1.75	1.70 ± 0.39	1.41 ± 0.71
		Nifuroxazide	>1.80	>1.75	>2	1.42 ± 0.48
R^1	R^2	Nitrofurantoin	>1.80	>1.75	>2	>1.92
	OCH_3	29	>1.80	>1.75	>2	>1.92
	H	30	>1.80	>1.75	>2	>1.92
	OCH_3	31	>1.80	>1.75	>2	>1.92
	H	32	>1.80	>1.75	>2	>1.92
	OCH_3	33	>1.80	>1.75	>2	>1.92
	H	34	>1.80	>1.75	>2	>1.92
	OCH_3	35	>1.80	>1.75	>2	>1.92
	H	36	>1.80	>1.75	>2	>1.92
	OCH_3	37	>1.80	>1.75	>2	>1.92
	H	38	>1.80	>1.75	>2	>1.92
	OCH_3	39	>1.80	>1.75	>2	>1.92
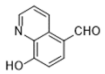		40	>1.80	>1.75	>2	>1.92
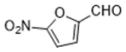		41	>1.80	>1.75	1.89 ± 0.13	>1.92
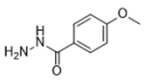		42	>1.80	>1.75	>2	>1.92

Table 5A - Human cell viability CC_{50} (μM) Compilation of CC_{50} results for compounds tested in the human FHC colon and FHs 74 Int intestine cell viability assays.

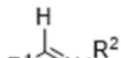		Human Cell Viability CC_{50} (μM)		
		Compound # / Name	FHC (Colon)	FHs 74 Int (Small intestine)
Compound Substituents		Nitroxoline	28	45
		Nifuroxazide	61	94
R^1	R^2	Nitrofurantoin	>100	>100
	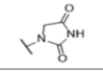	**2**	>100	>100
	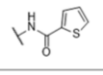	**3**	85	95
	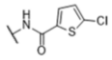	**4**	25	42
		**5**	74	53
		**6**	>100	>100
	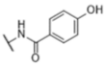	**7**	>100	94
	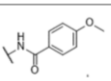	**1**	29	63
	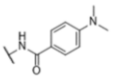	**8**	35	91
		**9**	46	58
		**10**	71	98
	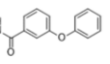	**11**	41	24
	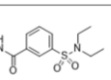	**12**	34	68
	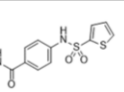	**13**	24	16
	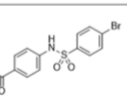	**14**	59	>100
	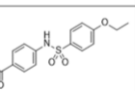	**15**	52	40

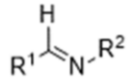		Human Cell Viability CC_{50} (μM)		
		Compound # / Name	FHC (Colon)	FHs 74 Int (Small intestine)
Compound Substituents		Nitroxoline	28	45
		Nifuroxazide	61	94
R^1	R^2	Nitrofurantoin	>100	>100
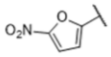	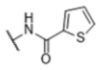	**16**	94	>100
	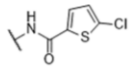	**17**	57	85
	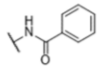	**18**	>100	94
	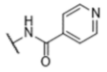	**19**	64	90
	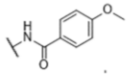	**20**	>100	>100
	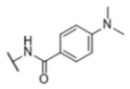	**21**	>100	93
	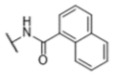	**22**	66	87
	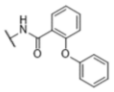	**23**	46	80
	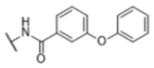	**24**	55	72
	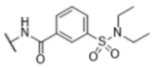	**25**	>100	>100
	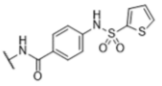	**26**	>100	61
	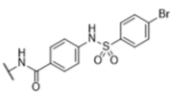	**27**	90	>100
	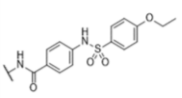	**28**	85	>100

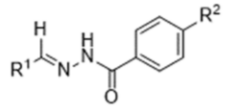		Human Cell Viability CC_{50} (µM)		
		Compound # / Name	FHC (Colon)	FHs 74 Int (Small intestine)
Compound Substituents		Nitroxoline	28	45
		Nifuroxazide	61	94
R^1	R^2	Nitrofurantoin	>100	>100
	OCH_3	29	>100	>100
	H	30	>100	>100
	OCH_3	31	>100	>100
	H	32	>100	>100
	OCH_3	33	>100	>100
	H	34	100	>100
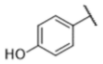	OCH_3	35	>100	>100
	H	36	>100	>100
	OCH_3	37	>100	>100
	H	38	>100	>100
	OCH_3	39	>100	>100
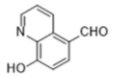		40	4.4	15
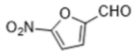		41	53	66
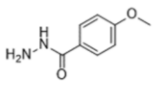		42	>100	64

Table 5B - Human cell viability log(CC_{50}) (μM) Compilation of log(CC_{50}) results and standard deviations for compounds tested in the human FHC colon and FHs 74 Int intestine cell viability assays.

		Human Cell Viability log(CC_{50}) (μM)		
		Compound # / Name	FHC (Colon)	FHs-74 int. (Small intestine)
Compound Substituents		Nitroxoline	1.45 ± 0.19	1.65 ± 0.26
		Nifuroxazide	1.79 ± 0.20	1.97 ± 0.11
R^1	R^2	Nitrofurantoin	>2	>2
		**2**	>2	>2
		**3**	1.93 ± 0.27	1.98 ± 0.12
	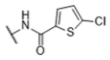	**4**	1.40 ± 0.22	1.62 ± 0.22
		**5**	1.87 ± 0.21	1.72 ± 0.35
		**6**	>2	>2
	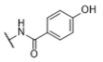	**7**	>2	1.97 ± 0.18
	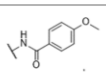	**1**	1.46 ± 0.32	1.80 ± 0.18
	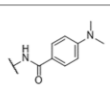	**8**	1.54 ± 0.38	1.96 ± 0.16
		**9**	1.66 ± 0.34	1.76 ± 0.14
	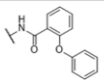	**10**	1.85 ± 0.30	1.99 ± 0.08
	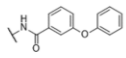	**11**	1.61 ± 0.42	1.38 ± 0.24
	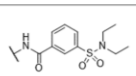	**12**	1.53 ± 0.40	1.83 ± 0.19
	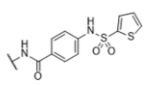	**13**	1.38 ± 0.30	1.20 ± 0.31
	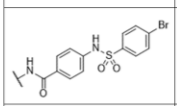	**14**	1.77 ± 0.31	>2
	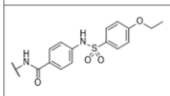	**15**	1.72 ± 0.30	1.60 ± 0.41

		Human Cell Viability log(CC_{50}) (μM)		
		Compound # / Name	FHC (Colon)	FHs-74 int. (Small intestine)
Compound Substituents		Nitroxoline	1.45 ± 0.19	1.65 ± 0.26
		Nifuroxazide	1.79 ± 0.20	1.97 ± 0.11
R^1	R^2	Nitrofurantoin	>2	>2
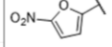	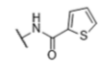	**16**	1.97 ± 0.15	>2
	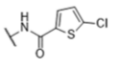	**17**	1.76 ± 0.24	1.93 ± 0.16
		**18**	>2	1.97 ± 0.21
		**19**	1.81 ± 0.22	1.95 ± 0.08
	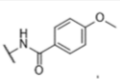	**20**	>2	>2
	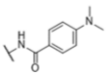	**21**	>2	1.97 ± 0.18
		**22**	1.82 ± 0.30	1.94 ± 0.22
	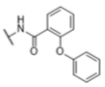	**23**	1.66 ± 0.25	1.90 ± 0.17
	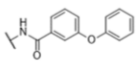	**24**	1.74 ± 0.18	1.86 ± 0.18
	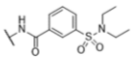	**25**	>2	>2
	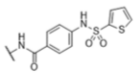	**26**	>2	1.79 ± 0.37
	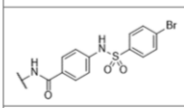	**27**	1.95 ± 0.13	>2
	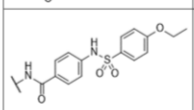	**28**	1.93 ± 0.20	>2

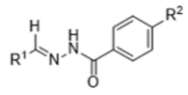		Human Cell Viability log(CC_{50}) (μM)		
		Compound # / Name	FHC (Colon)	FHs-74 int. (Small intestine)
Compound Substituents		Nitroxoline	1.45 ± 0.19	1.65 ± 0.26
		Nifuroxazide	1.79 ± 0.20	1.97 ± 0.11
R^1	R^2	Nitrofurantoin	>2	>2
	OCH_3	29	>2	>2
	H	30	>2	>2
	OCH_3	31	>2	>2
	H	32	>2	>2
	OCH_3	33	>2	>2
	H	34	2.00 ± 0.08	>2
	OCH_3	35	>2	>2
	H	36	>2	>2
	OCH_3	37	>2	>2
	H	38	>2	>2
	OCH_3	39	>2	>2
		40	0.64 ± 0.42	1.18 ± 0.35
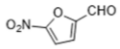		41	1.72 ± 0.23	1.82 ± 0.14
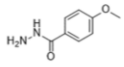		42	>2	1.81 ± 0.46

REFERENCES

1. Centers for Disease Control and Prevention. *Antibiotic resistance threats in the United States, 2019.* Centers for Disease Control and Prevention: Atlanta, Georgia, USA, 2019; p. 65-100.
2. Adedeji, W. A., The Treasure Called Antibiotics. *Ann Ib Postgrad Med* **2016,** *14* (2), 56-57.
3. Centers for Disease Control and Prevention. *Shiga Toxin-producing Escherichia coli (STEC) 2018 Case Definition.* Centers for Disease Control and Prevention: Atlanta, Georgia, USA, 2018.
4. Mead, P.S.; Slutsker, L.; Dietz, V.; McCaig, L.F.; Bresee, J.S.; Shapiro, C.; Griffin, P.M.; Tauxe, R.V., Food-related illness and death in the United States. *Emerg Infect Dis* **1999,** *5* (5), 607-25.
5. National World War II Museum. *Fact Sheet: The Challenge of Mass Production Discovery.* National World War II Museum: New Orleans, Louisiana, USA, 2017.
6. Davies, J.; Davies, D., Origins and evolution of antibiotic resistance. *Microbiol Mol Biol Rev* **2010,** *74* (3), 417-33.
7. Chopra, I.; Roberts, M., Tetracycline antibiotics: mode of action, applications, molecular biology, and epidemiology of bacterial resistance. *Microbiol Mol Biol Rev* **2001,** *65* (2), 232-60 ; second page, table of contents.
8. Leclercq, R.; Courvalin, P., Resistance to macrolides and related antibiotics in Streptococcus pneumoniae. *Antimicrob Agents Chemother* **2002,** *46* (9), 2727-34.
9. Dalhoff, A., Global fluoroquinolone resistance epidemiology and implications for clinical use. *Interdiscip Perspect Infect Dis* **2012,** *2012,* 976273.
10. Doctor Alerts. *Tetracyclines (Broad Spectrum Antibiotics): Classification, Uses, and Side Effects.* Doctor Alerts: 2017.
11. The Community College of Baltimore County. *Blocking Translation During Bacterial Protein Synthesis.* The Community College of Baltimore County: Catonsville, Maryland, USA.
12. Verchere, A; Picard, M.; Broutin, I., Functional investigation of the efflux pump MexA-MexB-OprM of *Pseudomonas aeruginosa*. *Biophys J* **2013,** *104* (2), 286a.
13. Santajit, S.; Indrawattana, N., Mechanisms of Antimicrobial Resistance in ESKAPE Pathogens. *Biomed Res Int* **2016,** *2016*, 2475067.
14. Munita, J. M.; Arias, C. A., Mechanisms of Antibiotic Resistance. *Microbiol Spectr* **2016,** *4* (2).
15. Triboulet, S.; Dubee, V.; Lecoq, L.; Bougault, C.; Mainardi, J. L.; Rice, L. B.; Etheve-Quelquejeu, M.; Gutmann, L.; Marie, A.; Dubost, L.; Hugonnet, J. E.; Simorre, J. P.; Arthur, M., Kinetic features of L,D-transpeptidase inactivation critical for beta-lactam antibacterial activity. *PLoS One* **2013,** *8* (7), e67831.
16. Macheboeuf, P.; Contreras-Martel, C.; Job, V.; Dideberg, O.; Dessen, A., Penicillin binding proteins: key players in bacterial cell cycle and drug resistance processes. *FEMS Microbiol Rev* **2006,** *30* (5), 673-91.
17. Lavollay, M.; Arthur, M.; Fourgeaud, M.; Dubost, L.; Marie, A.; Veziris, N.; Blanot, D.; Gutmann, L.; Mainardi, J. L., The peptidoglycan of stationary-phase Mycobacterium tuberculosis predominantly contains cross-links generated by L,D-transpeptidation. *J Bacteriol* **2008,** *190* (12), 4360-6.
18. Brandeis University. *Breaking Research: A method by which invading bacteria avoid detection could also be our key to defeating them.* Brandeis University: Waltham, Massachusetts, USA, 2014.
19. Salton, M.R.J.; Kim, K.S., Structure. In *Medical Microbiology,* th; Baron, S., Eds. Galveston (TX), 1996.

20. Adams, P. G.; Lamoureux, L.; Swingle, K. L.; Mukundan, H.; Montano, G. A., Lipopolysaccharide-induced dynamic lipid membrane reorganization: tubules, perforations, and stacks. *Biophys J* **2014,** *106* (11), 2395-407.
21. Ventola, C. L., The antibiotic resistance crisis: part 1: causes and threats. *P T* **2015,** *40* (4), 277-83.
22. Horwich, A. L.; Weber-Ban, E. U.; Finley, D., Chaperone rings in protein folding and degradation. *Proc Natl Acad Sci U S A* **1999,** *96* (20), 11033-40.
23. Georgescauld, F.; Popova, K.; Gupta, A. J.; Bracher, A.; Engen, J. R.; Hayer-Hartl, M.; Hartl, F. U., GroEL/ES chaperonin modulates the mechanism and accelerates the rate of TIM-barrel domain folding. *Cell* **2014,** *157* (4), 922-934.
24. Parsons, L. M.; Limberger, R. J.; Shayegani, M., Alterations in levels of DnaK and GroEL result in diminished survival and adherence of stressed Haemophilus ducreyi. *Infect Immun* **1997,** *65* (6), 2413-9.
25. Techtmann, S.M.; Robb, F.T., Archael-like chaperonins in bacteria. *Proc Natl Acad Sci U S A* **2010,** *107* (47), 20269-74.
26. Marchenkov, V.V.; Semisotnov, G.V., GroEL-assisted protein folding: does it occur within the chaperonin inner cavity? *Int J Mol Sci* **2009,** *10* (5), 2066-83.
27. Max Planck Society. *Mechanism of the E. coli Chaperonin System, GroEL-GroES.* Max Planck Institute of Biochemistry: Martinsried, Germany, USA.
28. Abdeen, S.; Salim, N.; Mammadova, N.; Summers, C.M.; Frankson, R.; Ambrose, A.J.; Anderson, G.G.; Schultz, P.G.; Horwich, A.L.; Chapman, E.; Johnson, S.M., GroEL/ES inhibitors as potential antibiotics. *Bioorg Med Chem Lett* **2016,** *26* (13), 3127-3134.
29. Stevens, M.; Abdeen, S.; Salim, N.; Ray, A. M.; Washburn, A.; Chitre, S.; Sivinski, J.; Park, Y.; Hoang, Q. Q.; Chapman, E.; Johnson, S. M., HSP60/10 chaperonin systems are inhibited by a variety of approved drugs, natural products, and known bioactive molecules. *Bioorg Med Chem Lett* **2019,** *29* (9), 1106-1112.
30. Washburn, A.; Abdeen, S.; Ovechkina, Y.; Ray, A.M.; Stevens, M.; Chitre, S.; Sivinski, J.; Park, Y.; Johnson, J.; Hoang, Q.Q.; Chapman, E.; Parish, T.; Johnson, S.M., Dual-targeting GroEL/ES chaperonin and protein tyrosine phosphatase B (PtpB) inhibitors: A polypharmacology strategy for treating Mycobacterium tuberculosis infections. *Bioorg Med Chem Lett* **2019,** *29* (13), 1665-1672.
31. Abdeen, S.; Kunkle, T.; Salim, N.; Ray, A.M.; Mammadova, N.; Summers, C.; Stevens, M.; Ambrose, A.J.; Park, Y.; Schultz, P.G.; Horwich, A.L.; Hoang, Q.Q.; Chapman, E.; Johnson, S.M., Sulfonamido-2-arylbenzoxazole GroEL/ES Inhibitors as Potent Antibacterials against Methicillin-Resistant Staphylococcus aureus (MRSA). *J Med Chem* **2018,** *61* (16), 7345-7357.
32. Kunkle, T.; Abdeen, S.; Salim, N.; Ray, A.M.; Stevens, M.; Ambrose, A.J.; Victorino, J.; Park, Y.; Hoang, Q.Q.; Chapman, E.; Johnson, S.M., Hydroxybiophenylamide GroEL/ES Inhibitors Are Potent Antibacterials against Planktonic and Biofilm Forms of Staphylococcus aureus. *J Med Chem* **2018,** *61* (23), 10651-10664.
33. Johnson, S. M.; Sharif, O.; Mak, P. A.; Wang, H. T.; Engels, I. H.; Brinker, A.; Schultz, P. G.; Horwich, A. L.; Chapman, E., A biochemical screen for GroEL/GroES inhibitors. *Bioorg Med Chem Lett* **2014,** *24* (3), 786-9.
34. Abouelhassan, Y.; Yang, Q.; Yousaf, H.; Nguyen, M. T.; Rolfe, M.; Schultz, G. S.; Huigens, R. W., 3rd, Nitroxoline: a broad-spectrum biofilm-eradicating agent against pathogenic bacteria. *Int J Antimicrob Agents* **2017,** *49* (2), 247-251.
35. Jawetz, E.; Hopper, J., Jr.; Smith, D. R., Nitrofurantoin in chronic urinary tract infection. *AMA Arch Intern Med* **1957,** *100* (4), 549-57.

36. Lopes, A.B.; Miguez, E.; Kummerle, A.E.; Rumjanek, V.M.; Fraga, C.A.; Barreiro, E.J., Characterization of amide bond conformers for a novel heterocyclic template of N-acylhydrazone derivatives. *Molecules* **2013,** *18* (10), 11683-704.
37. Miethke, M.; Marahiel, M. A., Siderophore-based iron acquisition and pathogen control. *Microbiol Mol Biol Rev* **2007,** *71* (3), 413-51.
38. Roldan, M. D.; Perez-Reinado, E.; Castillo, F.; Moreno-Vivian, C., Reduction of polynitroaromatic compounds: the bacterial nitroreductases. *FEMS Microbiol Rev* **2008,** *32* (3), 474-500.
39. Hall, B. S.; Wu, X.; Hu, L.; Wilkinson, S. R., Exploiting the drug-activating properties of a novel trypanosomal nitroreductase. *Antimicrob Agents Chemother* **2010,** *54* (3), 1193-9.
40. Spain, J. C., Biodegradation of nitroaromatic compounds. *Annu Rev Microbiol* **1995,** *49*, 523-55.
41. Hall, B. S.; Bot, C.; Wilkinson, S. R., Nifurtimox activation by trypanosomal type I nitroreductases generates cytotoxic nitrile metabolites. *J Biol Chem* **2011,** *286* (15), 13088-95.
42. Martin, J., Role of the GroEL chaperonin intermediate domain in coupling ATP hydrolysis to polypeptide release. *J Biol Chem* **1998,** *273* (13), 7351-7.
43. Skipper, P.L.; Kim, M.Y.; Sun, H.L.P.; Wogan, G.N.; Tannenbaum, S.R., Monocyclic aromatic amines as potential human carcinogens: old is new again. *Carcinogenesis* **2010,** *31* (1), 50-8.
44. Streeter, A. J.; Hoener, B. A., Evidence for the involvement of a nitrenium ion in the covalent binding of nitrofurazone to DNA. *Pharm Res* **1988,** *5* (7), 434-6.
45. Patterson, S.; Wyllie, S., Nitro drugs for the treatment of trypanosomatid diseases: past, present, and future prospects. *Trends Parasitol* **2014,** *30* (6), 289-98.
46. Wyllie, S.; Roberts, A. J.; Norval, S.; Patterson, S.; Foth, B. J.; Berriman, M.; Read, K. D.; Fairlamb, A. H., Activation of Bicyclic Nitro-drugs by a Novel Nitroreductase (NTR2) in Leishmania. *PLoS Pathog* **2016,** *12* (11), e1005971.
47. Race, P. R.; Lovering, A. L.; Green, R. M.; Ossor, A.; White, S. A.; Searle, P. F.; Wrighton, C. J.; Hyde, E. I., Structural and mechanistic studies of Escherichia coli nitroreductase with the antibiotic nitrofurazone. Reversed binding orientations in different redox states of the enzyme. *J Biol Chem* **2005,** *280* (14), 13256-64.
48. Abdeen, S.; Salim, N.; Mammadova, N.; Summers, C.M.; Goldsmith-Pestana, K.; McMahon-Pratt, D.; Schultz, P.G.; Horwich, A.L.; Chapman, E.; Johnson, S.M., Targeting the HSP60/10 chaperonin systems of Trypanasoma brucei as a strategy for treating African sleeping sickness. *Bioorg Med Chem Lett* **2016,** *26* (21), 5247-5253.
49. Whiteway, J.; Koziarz, P.; Veall, J.; Sandhu, N.; Kumar, P.; Hoecher, B.; Lambert, I. B., Oxygen-insensitive nitroreductases: analysis of the roles of nfsA and nfsB in development of resistance to 5-nitrofuran derivatives in Escherichia coli. *J Bacteriol* **1998,** *180* (21), 5529-39.
50. Kim, S.; Lieberman, T. D.; Kishony, R., Alternating antibiotic treatments constrain evolutionary paths to multidrug resistance. *Proc Natl Acad Sci U S A* **2014,** *111* (40), 14494-9.
51. Fleeman, R.; LaVoi, T. M.; Santos, R. G.; Morales, A.; Nefzi, A.; Welmaker, G. S.; Medina-Franco, J. L.; Giulianotti, M. A.; Houghten, R. A.; Shaw, L. N., Combinatorial Libraries As a Tool for the Discovery of Novel, Broad-Spectrum Antibacterial Agents Targeting the ESKAPE Pathogens. *J Med Chem* **2015,** *58* (8), 3340-55.

CURRICULUM VITAE

Christopher Ryan Howe

Education:

2018-2020 – **Indiana University, Indianapolis, Indiana, USA**.

- Completed MS. degree through the Department of Biochemistry and Molecular Biology
- Thesis: *Analogues of Nitrofuran Antibiotics are Potent GroEL/ES Pro-Drug Inhibitors with Efficacy Against Enterococcus faecium, Staphylococcus aureus, and Escherichia coli*

2014-2018 – **Purdue University, West Lafayette, Indiana, USA**.

- Completed BS. degree in Chemistry (ACS) with Biochemistry minor, Honors distinction

Positions and Employment:

Indiana University School of Medicine, Department of Biochemistry and Molecular Biology, Indianapolis, Indiana, USA:

2018(October)-2020(February): Graduate Research Student

- Developing potential pharmacological antibiotics against the resistant *ESKAPE* and *E. coli* pathogens, with joint activity against the bacterial GroEL/ES chaperone complex

Elanco Animal Health/Lilly, Quality Control and TS-MS, Clinton, Indiana, USA:

2018(May)-2018(August): Chemist Intern

- Method development for extracting lipid components from API-containing bacteria (fermentation samples), purifying the lipids, converting them to forms suitable for GC analysis, and adjusting GC run conditions to maximize peak resolution
- Quantitation of excess lipids fed into fermenters during a given fermentation lifecycle, using this method

Mead Johnson Nutrition, Quality Control, Evansville, Indiana, USA:

2017(May)-2017(August): Quality Control Intern

- Validation and improvement on an ELISA method used to quantitate allergens in infant formula production samples

Purdue University-Low Laboratory, Drug Discovery, West Lafayette, Indiana, USA:

2016(January)-2018(May): Undergraduate Researcher

- Developing peptide-drug conjugates (using both solid- and solution-phase methods) to target the folate receptor in various forms of cancer

- Characterized developed compounds

Honors and Activities:

- Alex and Besie Oblad Academic Scholar, Purdue University
- John Leighty Academic Scholar, Purdue University
- Phi Theta Tau Hammer and Tongs Scholar, Purdue University
- Alpha Lambda Delta/Phi Eta Sigma Honor Society, Purdue Chapter
- Zeta Beta Tau fraternity, Purdue Chapter
- Independent Calculus Tutor

Research Presentations:

- Elanco Animal Health Intern Presentation, Greenfield, Indiana: PowerPoint presentation of method development summer project
- Mead Johnson Nutrition, Evansville, Indiana: PowerPoint presentation of method validation for ELISA method

Technical Skills:

- FPLC with anion exchange, cation exchange, nickel-chelation, and size exclusion columns
- ELISA assays
- Gas chromatography
- High-pressure liquid chromatography
- IR spectroscopy
- Liquid chromatography mass spectrometry
- Protein expression and purification
- SDS-PAGE
- Solid-phase synthesis
- Solution-phase synthesis
- Tissue culture
- Thin-layer chromatography
- Ultra-performance liquid chromatography

Software Knowledge:

- Auto-Dock molecular docking
- BLAST
- ChemDraw
- Discovery Studio Visualizer
- Empower
- GraphPad Prism
- MS Office- Microsoft Word, Excel, PowerPoint, Publisher
- SciFinder